Zentrum für Entwicklungsforschung

Integrated desertification assessment in Southern Mongolia

Inaugural-Dissertation
zur
Erlangung des Grades
Doktor der Agrarwissenschaften
(Dr. agr.)

der Hohen Landwirtschaftlichen Fakultät
der
Rheinischen Friedrich-Wilhelms-Universität
zu Bonn

vorgelegt am 11. Juni 2007

von
Shurentuya Begzsuren
aus
Umnugobi, Mongolei

1. Referent: Prof. Dr. Paul L.G. Vlek

2. Referent. Prof. Dr. Armin Skowronek

Tag der Promotion: 6. August 2007

Erscheinungsjahr: 2007

Diese Dissertation ist auf dem Hochschulschriftenserver der ULB Bonn
http://hss.ulb.uni-bonn.de/diss_online elektronisch publiziert

ABSTRACT

The Bulgan soum in southern Mongolia is a part of the Gobi Three Beauty National Park. The territory is composed of arid and semi-arid desert, encompassing 720 000 ha. A desertification threat, which was virtually unknown for many years, has become a serious environmental problem in the last 20 years. Climatic variations, low variable rainfall, and dust storms overlaid by unsustainable human land-use practices, primarily poorly managed livestock grazing, are contributing to accelerated desertification.

The primary objective of this study is to assess desertification based on soil, vegetation, climate and socio-economic indicators including modified soil adjusted vegetation index (MSAVI), topsoil grain size index (GSI), shrinkage of groundwater sources, and extent of sand movement. Those were directly derived from Landsat MSS, TM, and ETM remote sensing images for the growing season months for the years of 1973, 1990, 1991, 2002 and 2005. The results show that the MSAVI is highly correlated to aboveground plant biomass and indicates a general decrease in vegetation biomass, while GSI manifests topsoil coarsening over the last 25 years.

In terms of climatic indicators, the historical climate records for the Bulgan soum show warming of approximately 0.7°C over the period 1970 to 2002. Drought occurs once every 2-3 years according to the SPI and Pedi indices (with 50% probability). The frequency of dust storms in the 1987-2002 period was about twice that during the period 1970-1986. There was however, no dust haze after 1994. Plant biomass was largely controlled by low variable rainfall, by dust storms, and temperature. Climate change scenarios, based on results from time series forecasting, indicate future warming by 0.05°C per year (with 37% probability) and by 0.4 dust storm frequencies per year (with 31% probability). It results in a decline of plant biomass of 2 kg ha^{-1} yr^{-1} (with 26% probability) that will likely to exacerbate desertification

In terms of the socio-economy of the herders, Chi-square tests show degradation classes to be associated with wealth groups, and the greater the livestock numbers, the greater the degradation. Large family size (triggers large stock numbers), older age, former herding households and decreased livestock moves were the causes of desertification. A time trend forecasting analysis projects an increase in livestock numbers (7000 standard stock units per year), particularly goats.

In general, land degradation in the study area increased from 1990 to 2005, and 94% of the area is considered to be degraded to varying degrees. The slightly degraded class covered 12%, the moderate class 44% and the severely degraded class 38% of the Bulgan soum in 2005. Sand encroachments occurred in 35% of the landscape, which have increased by 19% since 1973. 1.7% of total groundwater bodies in 1973 completely disappeared in 2005. Furthermore, the area affected by desertification has increased; the rate of desertification has also accelerated from 1% in the 1990s to 2% in 2005.

Integrierte Untersuchungen zur Desertifikation in der südlichen Mongolei

ZUSAMMENFASSUNG

Das Gebiet „Bulgan soum“ im Süden der Mongolei ist Teil des "Gobi Three Beauty National Park". Es besteht aus ariden und semi-ariden Wüstenbereichen mit einer Fläche von 720 000 ha. In den letzten 20 Jahren ist die Bedrohung durch Desertifikation, früher so gut wie unbekannt, zu einem ernsthaften Umweltproblem geworden. Klimaschwankungen, geringe und stark variierende Niederschläge sowie Staubstürme zusammen mit einer nicht nachhaltigen Landnutzung, hauptsächlich Überweidung, tragen zu der beschleunigten Desertifikation bei.

Das Hauptziel dieser Studie ist die Bewertung der Desertifikation auf der Grundlage von Boden-, Vegetations-, Klima- und sozioökonomischen Indikatoren einschließlich des "modified soil adjusted vegetation index (MSAVI), Korngrößenindex des Oberbodens (topsoil grain size index (GSI), Abnahme der Grundwasserressourcen und Ausmaß der Sandbewegung. Diese wurden aus Landsat MSS, TM und ETM Satellitenaufnahmen für die Vegetationsperioden der Jahre 1973, 1990, 1991, 2002 und 2005 entnommen. Die Ergebnisse zeigen, dass MSAVI mit der überirdischen Pflanzenbiomasse stark korreliert und auf eine allgemeine Abnahme der Biomasse hinweist, während der GSI eine Zunahme der gröberen Sandfraktionen während der letzten 25 Jahre deutlich macht.

Hinsichtlich klimatischer Indikatoren zeigen die historischen Klimaaufzeichnungen für den Bulgan soum eine Erwärmung von ca. 0.7°C zwischen 1970 und 2002. Die SPI- und Pedi-Indizes weisen auf eine Dürre alle 2 bis 3 Jahre hin (mit 50% Wahrscheinlichkeit). Staubstürme traten 1987 bis 2002 fast doppelt so häufig auf wie im Zeitraum 1970 bis 1986. Nach 1994 gab es jedoch keine Staubdunstereignisse. Pflanzenbiomasse wurde hauptsächlich durch niedrige und variierende Niederschläge, Staubstürme und Temperaturen beeinflusst. Klimawandelszenarien auf der Grundlage von Zeitreihenanalysen prognostizieren eine zukünftige Erwärmung um 0.05°C pro Jahr (mit 37% Wahrscheinlichkeit), sowie eine Zunahme der Staubstürme um 0.4 Sturm pro Jahr (mit 31% Wahrscheinlichkeit), werden zu einer Abnahme der Biomasse um 2 kg ha^{-1} $Jahr^{-1}$ (mit 26% Wahrscheinlichkeit) führen und damit voraussichtlich die Desertifikation beschleunigen.

Bezogen auf die sozioökonomische Situation der Hirten zeigen die Chi-square test, dass die Degradationsklassen mit Wohlstand korrelieren und, dass je größer die Herden, desto größer die Degradation. Große Familien (= große Herden), höheres Alter, ehemalige Nomaden-Haushalte und geringere Anzahl von Herdenbewegungen führten zu Desertifikation. Zeitreihenanalysen sagen eine Zunahme der Viehzahlen (7000 "standard stock units" pro Jahr), insbesondere von Ziegen, voraus.

Die Landdegradation im Untersuchungsraum nahm von 1990 bis 2005 zu, wobei 94% des Gebietes unterschiedlich stark degradiert ist. In 2005 nahmen gering degradierte Bereiche 12%, mäßig degradierte 44% und stark degradierte 38% des Bulgan soum ein. Starkes Vordringen von Sand konnte verzeichnet werden, der 35% der Landschaft bedeckt und um 19% seit 1973 zugenommen hatte. Eine Abnahme des Grundwassers um 1.7% der Grundwassermenge von 1973 wurde verzeichnet. Außerdem hat das durch Desertifikation betroffene Gebiet an Größe zugenommen und auch die Desertifikationsrate hat sich von 1% in den 1990er Jahren auf 2% in 2005 erhöht.

TABLE OF CONTENTS

LIST OF ABBREVIATIONS

Aimag	Administrative regional unit in Mongolia, larger than the soum
ARVI	Atmospheric resistant vegetation index
BI	Brightness index
BSI	Bare soil index
DSF	Dust storm frequency
GIS	Geographic Information System
GSI	Topsoil grain size index
MSAVI	Modified soil adjusted vegetation index
NDVI	Normalized difference vegetation index
NIR	Near infrared spectral band
MAP	Mean annual precipitation
MAT	Mean annual temperature
T	Temperature
TNDVI	T normalized difference vegetation index
R	Red spectral band
RI	Redness index
SAVI	Soil adjusted vegetation index
SARVI	Soil adjusted and atmospheric resistant vegetation index
SI	Soil index
Soum	Administrative regional unit in Mongolia, smaller than the aimag
SPI	Standard precipitation index
SSU	Standard stock unit
VI	Vegetation index

1 INTRODUCTION

1.1 Overview

1.1.1 Land degradation problems in Mongolia and the study area

Degradation of the rangelands of Mongolia has occurred on a wide scale. More than 40% of the area is affected, 400 rivers and lakes have dried out and degradation has increased by 8-10% over the last ten years (Adyasuren and Dash, 2001). It has been estimated that 78% of the total territory of Mongolia is at risk of desertification, of which nearly 60% is classed as highly vulnerable. Over 70% of pastures have been degraded through overgrazing. Vegetation biomass in the dry regions, notably desert steppe and steppe, has decreased by a factor of 6 (National desertification report, 2002). A significant portion of the land resources in Mongolia is degraded due not only to lack of rainfall, but also to dust storms, which are 4 times stronger than the 1960s (Batjargal, 2001). However, these figures are only estimates and the true extent and continuing nature of the problem have proved difficult to quantify. This is because the dry ecosystems show non-equilibrium behavior in which short term rainfall variability imposes changes in vegetation cover that mask any downward trend in conditions except in the most extreme cases (Behnke and Scoones, 1993; Ellis and Swift, 1988; Seligman and Leulen, 1989; Weins, 1984). The non-equilibrium behavior also makes it difficult to determine whether the land is continuing to degrade, remaining in a stable condition, or improving.

Bulgan soum (an administrative regional unit), Mongolia, is a case in point. Pastoral and rangeland ecosystems pose challenging management problems associated with increasing livestock populations, rangeland degradation and alteration of pastoral migration patterns (Ojima 2001; Sneath 1998). Rangeland degradation has been occurring mainly in the areas with high population density due to the increase in land-use pressure and inappropriate spatial management of livestock (Bedunah and Schmidt, 2000; Coughenour, 1991; Ingo et al., 1996). Livestock pastoralism (with cattle, camels, goats, sheep and horses) has been practiced for thousands of years under a nomadic movement pattern in the Bulgan soum, where it currently supports 411 000 SSU livestock (National report, 2002). The carrying capacity of pasture land is frequently exceeded in many places due to overgrazing, resulting in degradation of the plant cover,

productivity and composition of plant species (Batjargal, 2001; Chognii, 1990). Severe droughts and long-term shifts in the magnitude of precipitation are typical, and droughts occur as often as once every two or three years (Begzsuren et al., 2004). Therefore, the Bulgan soum is quite vulnerable to climate and human-induced changes and can easily shift from a persistent system to a degraded system particularly when overgrazing is combined with climate stress, namely droughts (Ellis et al., 2002; Ellis and Chuluun, 1993).

Furthermore, economic inflation made it increasingly interesting for herders to raise livestock (all lands of Mongolia are public). There are some concerns that "the tragedy of commons" may be occurring (Hardin, 1968). This theory implies that public use of land resources may lead to each individual herd owner taking maximum advantage of available resources to maximize his own herd. Thus, increasing herd growth will eventually lead to degradation through overgrazing.

Although many herders and government officials are aware of degraded lands in this semi-arid area, not a single study based on the Geographic Information System (GIS) and remote sensing technique has demonstrated that desertification is underway in the Bulgan soum. In addition, there is very little research on the true extent of the desertification process in this area, its causes and severity. Therefore, the aim of this study is to assess desertification severity degrees based on climatic and socio-economic factors, and satellite images that can be applicable for rangelands throughout Mongolia.

1.1.2 Research objectives and hypothesis

The main goal of this study is to assess desertification based on soil, vegetation, and socio-economic factors.

The specific objectives are as follows:

1. Determination of the temporal vegetation biomass and topsoil coarsening changes.
2. Analysis of the relationship between vegetation biomass and climatic factors.
3. Analysis of the relationship between vegetation biomass and soil factors.
4. Analysis of the relationship between vegetation biomass and land use by herders.
5. Integration of ecological and climatic factors to assess desertification.

The specific objectives are dealt with in individual chapters; overall the desertification assessment is conducted by combining all indicators.

The hypotheses corresponding to the respective objectives (and chapters) are the following:

3.1. Vegetation biomass within the Bulgan soum is significantly correlated to modified soil adjusted vegetation index (MSAVI), soil adjusted vegetation index (SAVI), Atmospheric resistant vegetation index (ARVI) and soil adjusted and atmospheric resistant vegetation index (SARVI) rather than normalized difference vegetation index (NDVI) and T normalized difference vegetation index (TNDVI) vegetation indices.

3.2. Vegetation biomass in the Bulgan soum has declined over the last 30 years.

4.1. Rainfall, precipitation and plant biomass have decreased, while droughts, temperatures and dust storms have increased over the last 30 years.

4.2. Plant biomass has decreased under the combined effects of decreased rainfall, increased temperatures and dust storms over the last 30 years.

5.1. Bulk density of soil has changed due to land degradation.

5.2. Primary production is higher on coarse-texture soils than on fine texture soils.

6.1. Desertification is accelerated in the grazing areas of large, rich households, and occurs more slowly in the grazing areas of small and poor families.

6.2. The gap between rich and poor herding households has been widening over the period 2000-2005.

1.1.3 Desertification indicators

Understanding the causes and extent of desertification is a complex task, involving aspects of climate, ecosystems, and land use strategies. Therefore, land degradation in the Bulgan soum was studied by utilizing remote sensing and field work to capture both natural and man-made indicators (Table 1.1).

Table. 1.1 Desertification indicators used in this study

	Indicator	Assumption	References
1	Changes in vegetation cover or biomass-vegetation indices	Land degradation processes, either natural or human induced, cause the vegetation cover to thin	Mouat et al., 1997
2	Changes in topsoil coarsening	Coarsening of topsoil grain size which has a positive correlation with fine sand content	Xiao et al., 2006
3	Sand drifts, dunes	Shifting sand dunes spread into grasslands	Mishra et al., 1994; Kharin et al., 1999;
5	Drought indices	Deviation of temperature and precipitation from the long-term pattern	Bayasgalan and Dash, 2002; Mouat et al., 1997
5	Mean annual rainfall, rainfall variability, temperature and dust storms	The lower the mean annual rainfall and higher the temperature, the more dust storms occur.	Mouat et al., 1997
6	Soil texture and bulk density	Primary production in arid and semi-arid regions is higher on coarse texture soils than on fine texture soils. Soil is more compacted under land degradation.	Noy-Meir, 1973
7	Socio-economic data	Wealth groups and household demography affect land capacity	

1.1.4 Outline and methods of the thesis

The thesis consists of eight chapters. Chapter 1 presents the main problems with regard to land degradation and desertification in Mongolia and the study site. Section 1 introduces the overall objectives, indicators of land degradation, methods, and outline of the thesis. Section 2 describes the basic concepts of land degradation, its indicators, causes, and a desertification assessment based on remote sensing and GIS results from previous studies.

Chapter 2 first provides an overview of the study site, its climate, soil and vegetation status, and particularly its land degradation features. Second, land degradation features such as sheet, gully, and wind erosion, which are prevalent at the study site. Third, the causes of desertification and the critical issues facing the rangelands of Bulgan soum are stressed.

In chapter 3, multiple vegetation indices such as NDVI, SAVI, MSAVI, ARVI, SARVI, BI and soil indices such as GSI, RI, BSI indices are calculated to manifest their ability to discriminate vegetation cover and biomass and topsoil

coarsening over the 40 km x 40 km area. The best suited index is determined by ground-truthing with vegetation and soil data. The output of this part of study serves as the core of change detection. When change detection is calibrated and verified using data or knowledge of a particular area, it highlights the degree of desertification. Numerous remote sensing image processing namely radiometric, geometric rectification, image enhancements, vegetation and soil indices calculation were used and results are represented explicitly using Erdas Imaging, and ENVI software. Within the GIS framework, ARC INFO, ARC VIEW, and occasionally ARC GIS, were used.

Chapter 4 deals with the relationship between vegetation biomass, climatic factors, and seasonal aspects (Objective 2) in order to provide insight into the causes of desertification. The long-term trend of climatic factors such as MAP, growing seasonal rainfall, temperature, drought indexes (SPI, and Pedi), dust storms and dust occurrence in relation to plant biomass are identified.

In chapter 5, the relationship between aboveground plant biomass, cover, soil types, and soil bulk density as a result of degradation threat and soil compaction is analyzed (Objective 3). Long-term climatic and vegetation data obtained from the Hydrometeorology Institute are processed into statistical linear and multiple regression analysis using SAS to highlight vegetation and climate interaction.

In chapter 6, the relationship between vegetation cover change and land use by herders, which can provide insight into the socio-economic causes and responses to desertification are analyzed (Objective 4). Socio–economic questionnaire survey results obtained from the households within the study area are integrated into remotely sensed data to delineate the association between degradation and socio-economy of herders using the Chi-square test.

In chapter 7, desertification is assessed in the Bulgan soum (Objective 5). A methodology for realistically assessing desertification and map desertification trends by taking into account natural indicators are used. The current status of land degradation using remote sensing and GIS is evaluated, and trends in land degradation hazard are highlighted. In addition, sand drift and water body change based on the change detection of remotely sensed data are presented. The significant indicators determined in the previous part of the study are integrated in a GIS framework in this last chapter (Figure 1.1).

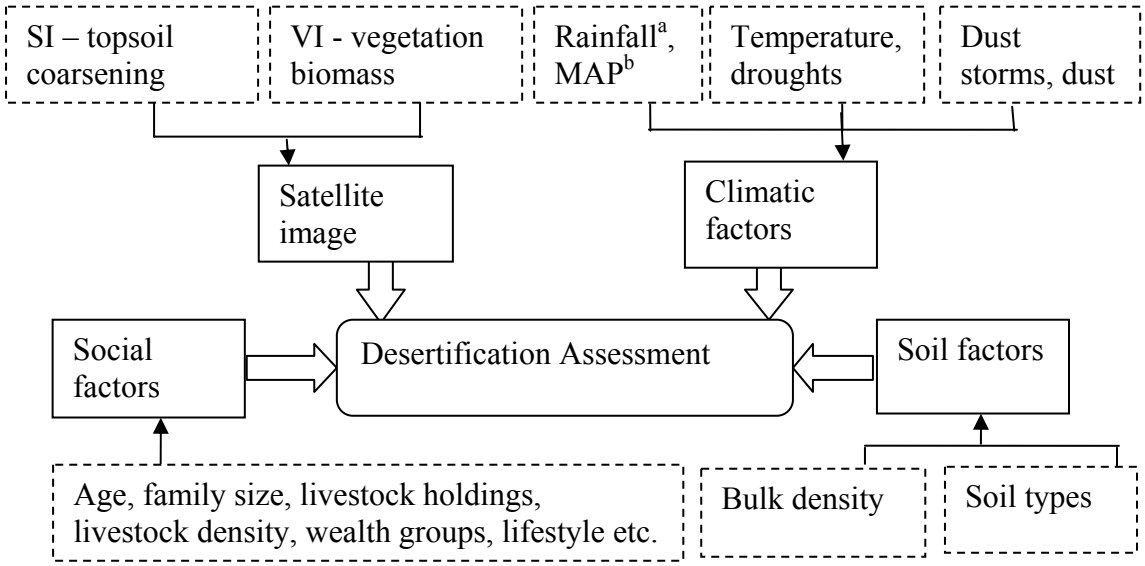

[a]– *growing season rainfall from April to September*
[b]- *mean annual precipitation – rainfall from January to December*

Figure 1.1 Flowchart of desertification assessment in this study

In chapter 8, summaries and conclusions are given.

1.2 State of the art

1.2.1 Definitions of desertification

UNEP in early 1990 defined desertification as 'land degradation in arid, semi-arid and dry humid areas resulting mainly from adverse human impact'- specified land degradation as desertification (Dregne et al. 1991). Land degradation is a process which implies a reduction of potential productivity of the land (Hill et al., 1995). In a broader sense, Conacher and Sala (1998) considered land degradation an "alteration to all aspects of the natural (or biophysical) environment by human actions to the detriment of vegetation, soils, landform, water (surface and sub-surface) and ecosystems". Land degradation in non-equilibrium rangelands may be defined in terms of loss of resilience (i.e., land's ability to recover from a disturbance) and is linked with lower economic productivity through reduction in forage consumption by stock. Land degradation is also considered to be a collective degradation of different components of the land such as water, biotic and soil resources (Hennemann, 2001a, b).

More recently, a report of the United Nations Conference on Environment and Development (UNCED) defined desertification as land degradation in arid, semi-arid

and dry sub-humid areas resulting from various factors, including climatic variation and human activities (UNCED, 1992). However, this definition does not distinguish between whether desertification is a process (a natural phenomenon marked by regular changes that lead to a particular result) and whether it is a condition (a state of being) created by land degradation (Katyal and Vlek, 2000). In addition, desertification appears when land degradation becomes irreversible or when loss of total productivity reaches 50% to 66% (Katyal and Vlek, 2000).

1.2.2 Causes of degradation

Land degradation entails two interrelated, complex systems: the natural ecosystem and the human social system. Natural forces include periodic stresses of extreme and persistent climatic events, aridity, and droughts. Aridity limits biological productivity and results in poor quality soil (Stewart et al., 1992). The fluctuating rainfall patterns, a coefficient of variation of annual precipitation exceeding 30%, and few rainy days are often associated with intensive dust storm events. Those features make dryland regions climatically unstable and susceptible to desertification (Katyal and Vlek, 2000).

Unsustainable human land use, is often cited as overgrazing, deforestation, over-cultivation, reclamation and abuse of sensitive vulnerable ecosystems act united, and creates feedback mechanisms which are not fully understood (Xiao et al., 2006).When pastures are overgrazed by too many animals, or unsuitable kinds of animals, edible plant species may be lost, allowing inedible species to invade (UNCCD, 2006). Causes of land degradation are not only biophysical, but also socio-economic (marketing, income, human health, institutional support, poverty), undermining food production and political stability (UNCCD, 2004; WMO, 2006).

1.2.3 Desertification indicators

Assessment of desertification severity relies, first and foremost, on the identification of pertinent indicators (Rubio and Bochet, 1998). Indicators of desertification include physical, biological and socio-economic phenomena. The FAO stressed the importance of indicators for monitoring desertification in 1980, and ascertained 22 indicators mostly suitable at local scale. Sharma (1998) proposed several indicators mostly related to hydrological processes and soil erosion such as reduced area of water bodies,

increased run-off, decreased infiltration, accelerated soil erosion and sedimentation, and deteriorated groundwater resources. Thus, the assessment of degradation severity is meaningful only when both natural and anthropogenic factors are taken into account. Land degradation assessment with indicators such as land cover, biomass, and proportion of unpalatable grass species derived directly from Landsat TM based vegetation indices was done in China (Liu, 2004). Aharoni and Ward (1997) identified areas of potential desertification using biotic and abiotic variables including mean annual precipitation, potential evapotranspiration, soil data converted to low, medium and high water holding capacity, animal masses, human and livestock population density, and vegetation cover. Soil erosion, salinization, soil chemistry, changes in species diversity and above-ground biomass, and changes in land-use and settlement patterns are potential indicators (Schlesinger et al., 1990).

Desertification indicators for Asian regions, including India, China, Thailand, and Kazakhstan, are shown in Table 1.2 (Tsunekawa, 2000).

Table 1.2 Desertification indicators for Asia

Climate	Vegetation	Soil and water	Human activities
Aridity Climatologic region Monthly temperature Monthly precipitation Windstorms (days) Climate change: in the past 100 years recent drought drought index (rainfall variability)	Outline of vegetation: vegetation map vegetation type biomass, plant coverage, dominant species, stratification Vegetation degradation: change in species composition, change in biomass Vegetation change: in the past 100 years Human impact on vegetation	Outline of soil: soil map soil type Physical properties: soil texture (grain size) water permeability pF Chemical properties: Fertility (C,N,Ca,Mg;K,P) EC pH CEC Ground water ground water level water quality (EC, pH) Status of water source in drought Soil degradation: sand shifting salinization water erosion wind erosion Human impact on soil	Land use: traditional land use recent land use, land tenure system land use change crop yield, livestock holdings Socio-economics: population population dynamics death ratio life expectancy cause of death migration average income mean income source staple food energy source number of villages average village population Influences of desertification and drought: outlook on human life yield in drought year number of migrants number of cases of malnutrition

1.2.4 Desertification assessment

Satellite remote sensing is the only available means for systematic measurements of surface parameters over large areas in a reproducible manner and at frequent rates. Therefore, it can serve as a tool allowing the monitoring of spatial and temporal desertification. In fact, remote sensing has long been recommended for its potential to detect, map and monitor degradation problems with spatial and spectral resolution and for the detection of degraded areas including their spread effects with time (De Jong, 1994; Raina et al., 1993; Sabins, 1987; Sommer et al., 1998; Sujatha et al., 2000).

Remote sensing is extensively used to view the extent of desertification in a given region through transformations in the vegetation index reflecting vegetation properties and physical vegetation parameters such as biomass, productivity, leaf area

index, or percent vegetation ground cover, total dry matter accumulation and annual net primary productivity (Tucker et al., 1985, 1986, 1991). Various vegetation indices such as Normalized Difference Vegetation Index (NDVI), and Soil Adjusted Vegetation Index (SAVI) and their time series data have been widely used to discriminate vegetation cover change (Hanan et al., 1991). In addition, remote sensing has the capability to detect and monitor specific surface characteristics and track sand movements. These characteristics can include parent material and soil substrates and biological and mineralogical crusting (Hill et al., 1995b).

In addition to the vegetation indices, multi-temporal remotely sensed data were successfully applied to the monitoring of desert expansion and to the assessment of factors that may cause desertification (Luk, 1983). Visual interpretation of Landsat Multi-Spectral Scanner (MSS) images and aerial photographs enabled Gad and Daels (1986) to identify landforms indicative of desertification and to assess desert encroachment along the Nile Valley. Temporal variation of eroded lands was investigated by Dwideti et al. (1997a,b) using Landsat MSS and Landsat TM and reported the increase in land degradation units both in spatial context and severity.

However, measurements from space can not replace local investigations on the ground to study the complex process of desertification such as the substitution of vegetation species by more resistant ones, the thinning out of the vegetation cover, the loss of biomass, the loss of soil by erosion, the increasing extent of the unsaturated zone in soils, demineralisation, salinisation and the related change of the soil-vegetation-atmosphere transfer of water and energy (Hill et al., 1995b). Therefore, field investigation is always combined with remote sensing data to interpret the data based on the ground features.

Furthermore, remote sensing can pick up indicators of the change of land-surface characteristics, which are related to parameters governing the desertification processes (Hill et al., 1995a) that are directly derived from satellite images in combination with GIS. The USA Desert Research Institute and U.S. Environmental Protection Agency (EPA) (Mouat et al., 1997) carried out a desertification assessment with a combination of five indicators with equal importance being attached to each indicator, as follows:

Desertification assessment = (E + PDSI + GP + WI + NDVI)

Where E is erosion potential; PDSI is Palmer Drought Severity Index; GP is grazing pressure; WI is weedy invasive species as a percent of total vegetation cover; and NDVI.

It was assumed that there was no interaction between indicators, and the products of each indicator layer were summed without weightings. At a regional scale, Grunblatt et al. (1992) used summation to give an equal representation to all indicators, and found that higher values for individual indicators resulted in higher overall index values. Desertification susceptibility analysis was carried out on the basis of four indicators using continental-scale remotely sensed data: vegetation cover from NDVI, rain-use efficiency, surface runoff and soil erosion (Symeokalis and Drake, 2004). Linear mixture modeling, based on the computation of vegetation, soil, and parent material abundances, has been successfully implemented in mapping land degradation in semiarid environments such as the Mediterranean regions of Europe (Hill et al. 1995a), and the eastern Andes of Bolivia (Metternicht, 1996).

In general, there are few models that integrate multiple desertification processes. These models are two types. Models of the first type, e.g. Mouat et al. (1997) and Grunblatt et al. (1992), assess the risk of desertification by considering multiple desertification processes over a wide land area. The other type, developed by Proctor (1999), assesses the balance between population and biological resources from the viewpoint of demand and supply by villagers, and takes into account over-grazing and over-cultivation processes.

However, a comprehensive model covering the whole process of desertification causes, results, and effects has not yet been developed (Tsunekawa, 2000). If the cause and effect relationship of desertification processes is taken into account, desertification has causal processes (including socio-economic factors such as poverty and population increase, climatologic factors such as global climate change), resultant physical desertification processes (such as water and wind erosion, salinization, and vegetation degradation) and effects caused by them (including occurrence of economic loss, refugees and poverty). This kind of model is still in the conceptual stage (Tsunekawa, 2000).

Remote sensing is also used in conjunction with Geographic Information Systems (GIS), opening additional pathways for the application of spatialized simulation models and the assessment of desertification that relate dynamic landscape processes to changes in spectral-spatial characteristics captured by remote sensing instruments (Hill, 1995a). Severity of desertification is assessed in the GIS by integrating all identified indicators or all data layers (Liu, 2004).

2 OVERVIEW OF STUDY AREA

2.1 Location of Bulgan soum

The research was carried out in the Bulgan soum, southern Mongolia, bounded by 43 ^{o} 45' N and 44 ^{o} 84' N latitude, and 102 ^{o} 87' E and 104 ^{o} 14' E longitude, and covering an area of 720 000 ha composed of semi-desert, steppe desert and mountain semi-desert zones (Figure 2.1).

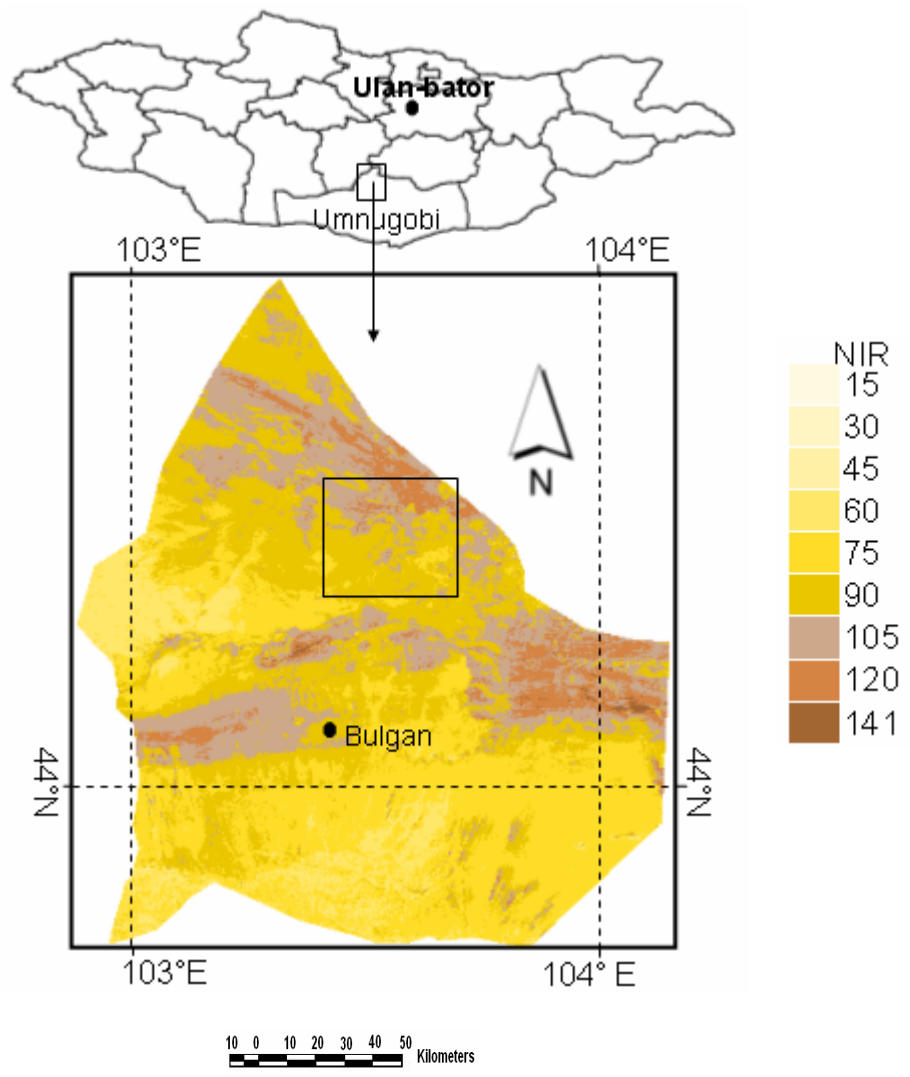

Figure 2.1 Location of the Bulgan soum and near infrared band 4 (NIR) of Landsat TM. The marked area indicates 40 km x 40 km study area. Southern Mongolia, July 2002

2.2 Climate

The climate in the Bulgan soum is strongly continental and arid, characterized by cold winters (temperatures as low as –41^{o} C), dry, windy springs, relatively hot summers (41 ^{o} C), and a short growing season of 158 days from April to September.

Precipitation is low, averaging 117 mm yr$^{-1;}$ 60-78% of the total annual precipitation falls from April through September. Precipitation during the last 51 years ranged from 60.4 mm to 261.5 mm, with 39% CV (coefficient of variation). This high CV of mean annual precipitation qualifies this region as one which display non-equilibrium dynamics (Ellis and Galvin, 1994). The mean annual precipitation (MAP) is subject to considerable interannual fluctuations, and an oscillation trend is visualized in the long run (Figure 2.2), with 119 mm of MAP for 1970-1980, 112 mm for 1980-1990, and 124 mm for 1990-2000.

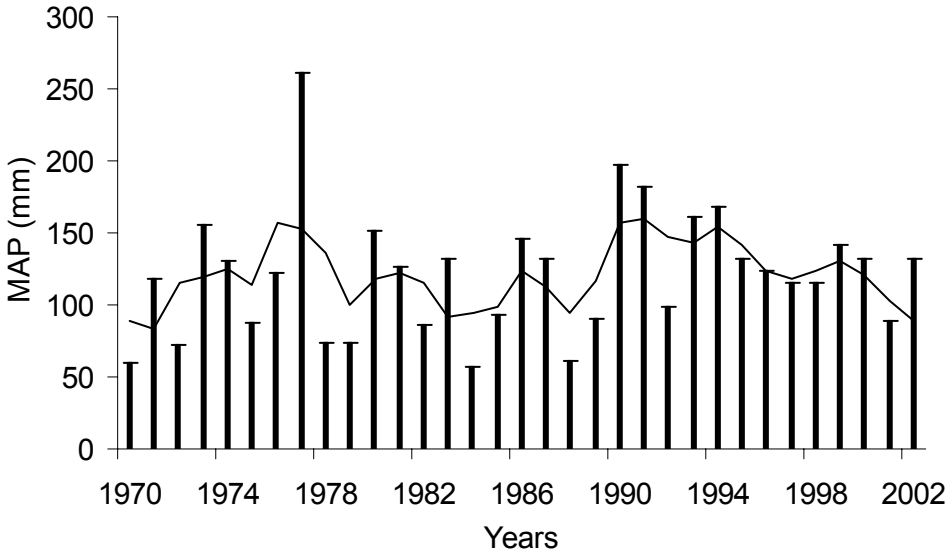

Figure 2.2 Mean annual precipitation (MAP) in the Bulgan soum, Mongolia, 1970-2002, compared with 3-year mean. The 3 year mean was calculated by the average of previous, present and next year's MAP

The Bulgan soum is with highest wind speeds in Mongolia. The monthly average wind speed is 5-7 m s^{-1} in summer, 8-10 m s^{-1} in winter. However, 48% of storms have wind speeds greater than 10 m s^{-1}. Wind speeds greater than 15m s^{-1} occur on 102-116 days. The dominant wind direction is west (40%), southwest (21.2%) and northwest (18%), and three-quarter of the year is windy.

2.3 Soils

Two broad groups of soils can be distinguished in the 720 000 ha study area. These include the typical brown desert-steppe soil with stones, constituting 24% of the area, and the typical brown steppe-desert soil with brown aeolian deposits covering 13% of the area. Those soils are non-productive, light-structured and sensitive to water and wind erosion (Figure 2.3). Of the total area, 42% are sandy, solanchak and bare soil, which is extremely sensitive to desertification.

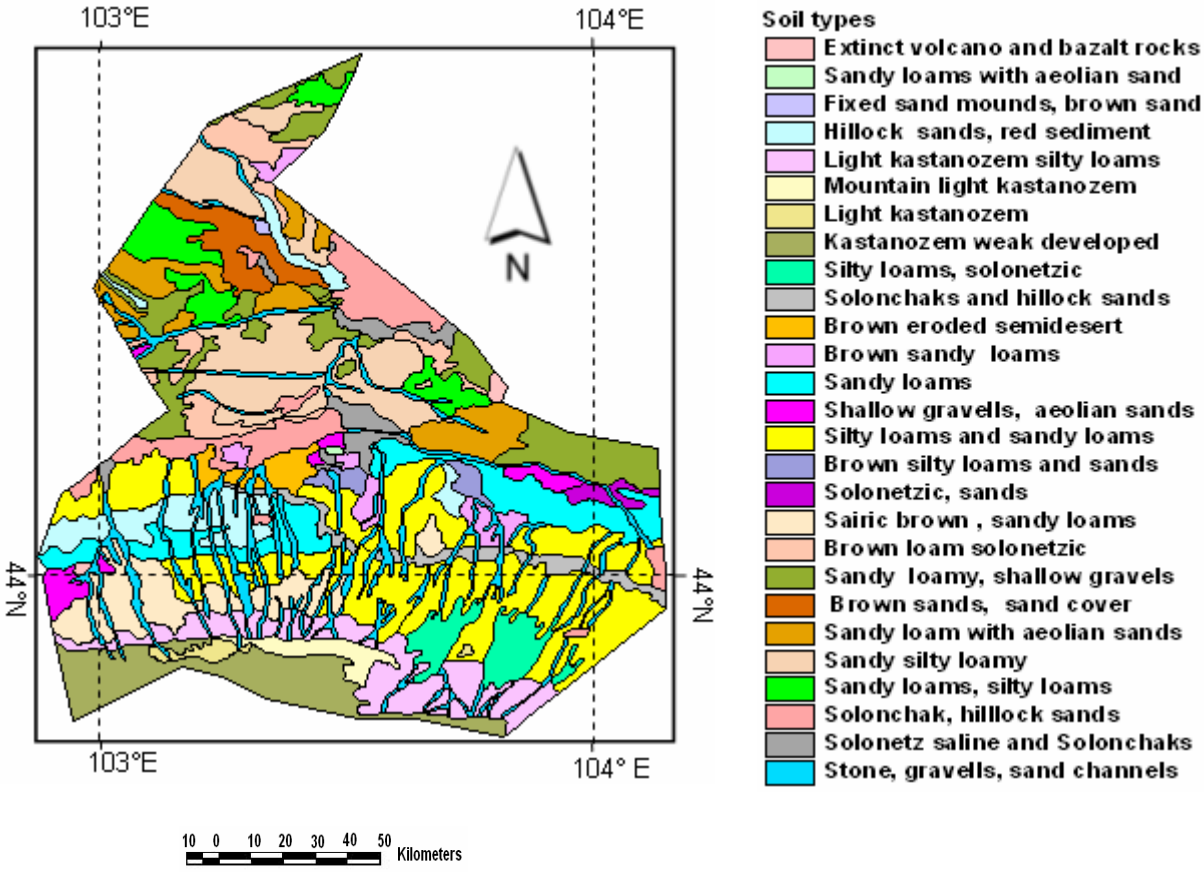

Figure 2.3 Soil map of Bulgan soum, Mongolia (Hydrometeorology Institute, 2005)

2.4 Vegetation

Vegetation is scarce, with a total of 192 species in 22 vascular plant families (Figure 2.4) (Dashnyam, 1986). Dominant vegetation classes are *Cleistogenes* (needle grass), *Caragana leucophloea* (21% or 157 500 ha) and needle grass-*Allium-Anabasis* (26.7% or 200 250 ha). Plant biomass increases slowly through the spring and reaches a maximum by mid summer. In terms of plant forms, 1 % is wood, 6.5% are shrubs, 54%

annuals and 24% perennials. There are large expanses of sand and active sand dunes providing habitats for the tree (saxaul) *Haloxylon ammodendron* (Figure 2.5).

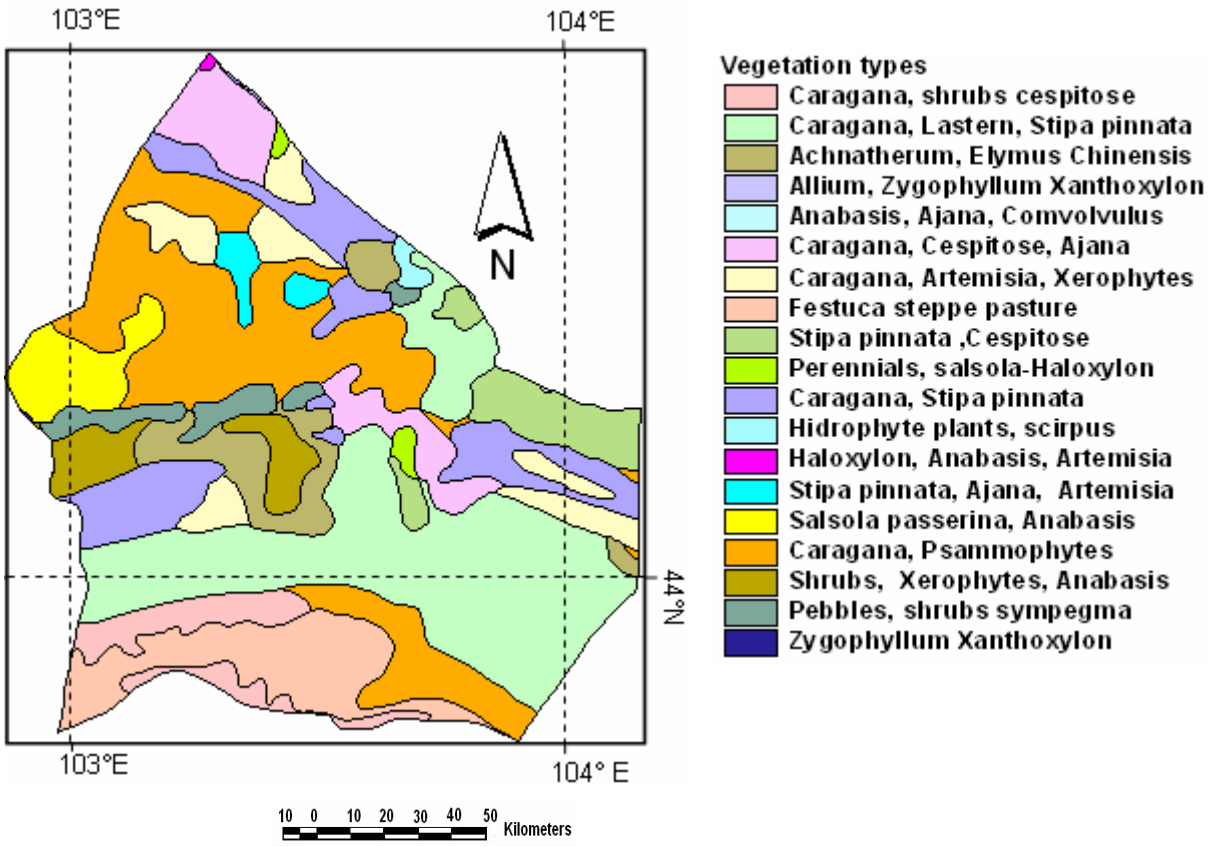

Figure 2.4 Vegetation map of Bulgan soum, Mongolia. (Hydrometeorology Institute, 2005)

Compared to the 1950 and 1970's, annuals have become abundant and cover large areas due to frequent droughts. The functions of annuals are manifolds including: rapid growth after small rainfall events, hibernation of seeds in winter, capability of dormant state of seeds up to 20 years, generation of seeds at the age of 1-2 months with 1 cm height and rapid distribution (Sanjid et al., 2004). The present abundance of annuals compared to some decades ago is attributed to droughts and land degradation, and its first succession stage growing on degraded soils (Sanjid et al., 2004). In addition, the annuals can easily adapt to newly modified environments associated with climate change. However, the annuals are in a senescence state in winter and fall, therefore livestock often suffer food shortage in cold winters (Sanjid et al., 2004). Droughts are frequent, once every 2-3 years, when *Rheum nanum* and *Ferula bungeania* turn

dormant, while some drought-resistant species such as *Stipa glareosa, Convolvulus ammanii,* and *Ptilotricum canescens* stay (Bedunah and Schmidt, 2000).

2.5 Herders and livestock

Nomadic pastoralism has been the main land-use form in the Bulgan soum for thousands of years, and requires a maximum amount of flexibility and movement of livestock (Coughenour, 1991). There have been large increases in the number of herding families and in livestock numbers since 1990 with current livestock numbers likely approaching 411 000 animals (in SSU) managed by 450 herding families in 2000 (Figure 2.5) (National report, 2002). Privatization of livestock in 1990-1992 due to communism collapse led to an increased livestock of 60-70 thousand SSU by 2000, causing growing disparities in household wellbeing between rich and poor herders (PALD, 1997).

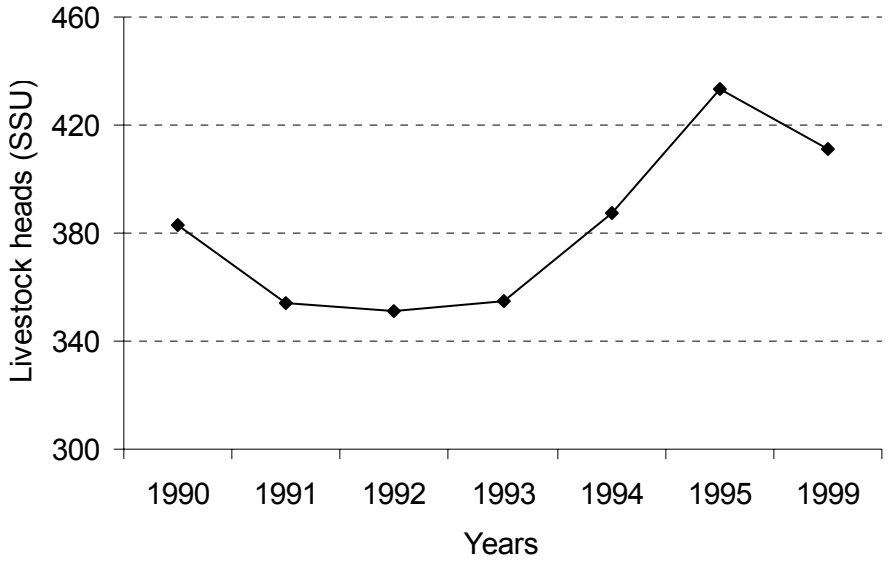

Figure 2.5 Increase in livestock heads in SSU. 1 Standard stock unit (SSU) is a Mongolian measure to express the feed requirement of one sheep per year. Accordingly, horses, cattle, camels and goats have been assigned as equivalent to 7, 6, 5 and 0.9 standard stock unit, respectively. Bulgan soum, Mongolia (National report, 2002)

As part of the livestock, horses, cows, sheep and goats have increased whereas the number of camels has decreased. Between 1990 and 2000, goats increased by the highest percentage (54%), horses by 76%, cows by 33% and sheep by 51%,

while camels decreased by 8.1% in relation to their numbers (Figure 2.6). The increase in the number of goats is directly related to the market requirements of cashmere. However, goats eat the widest range of food, thus endangering limited range rock plants. Goats with sharp hooves cut through the cryptobiotic crust of fungi and other lower plants holding together the exposed soil in areas of sparse vegetation, thus making the soil susceptible to wind erosion. It has been suggested that the recent severe spring dust storms might have been aggravated by the larger number of goats present across the Gobi region (UNDP, 1998).

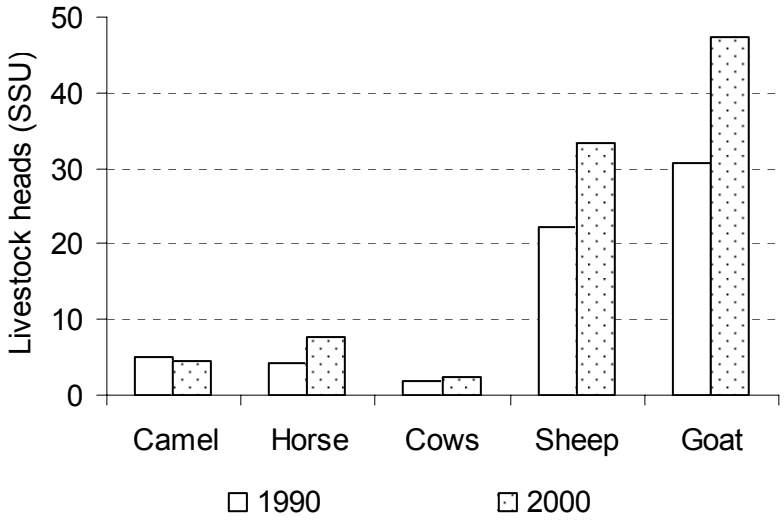

Figure 2.6 Number of livestock types in 1990 and 2000 (in thousand SSU) in the Bulgan soum, Mongolia. (National report, 2002)

2.6 Manifestations of desertification

Manifestations of desertification can be clearly seen and are widespread on the land surface of the Bulgan soum, including (1) accelerated soil erosion by wind and water and moving sand dunes, (2) increased salinization of soils and near-surface groundwater supplies, (3) augmented surface runoff or sheet and (4) gully erosion, and (5) dried surface water resources.

2.6.1 Wind erosion

Wind erosion is the detachment, transportation and redeposition of soil or sand particles by wind (Chrapko, 2001). It is commonly observed in the Bulgan soum, and occurs once vegetation has been lost and when soil particles are loosened. Early signs of wind

erosion include deposition of sand particles around plants and micro-ripples on the surface of exposed areas (Bettis, 1983). These are very common in the semi-desert and desert steppe in the northern and central part of the soum. The loss of topsoil as a result of wind erosion is frequently seen as rocky or gravelly knolls, or thin soils mixed with lighter colored subsoil. Hence wind erosion is most pervasive. Aridisols and entisols – the two other soil orders dominating- though porous, are prone to wind erosion due to the mostly dry surface and lack of stable structure.

The generally high temperatures (MAT = 5.4 °C) and low precipitation (MAP = 117 mm) lead to poor organic matter production and poor aggregation and thus a high potential for wind erosion. The area is subjected to rainfall events only during the growing season from April to September. In the case of a rainfall event, raindrops form structural crusts/seals on wind-eroded soil, which decrease infiltration, increase run-off and generate overland flow and erosion. Most rainfall generates overland flow, i.e. a huge yellow reddish water flow, as a manifestation of severe soil erosion.

Classic sand desert dune structures can be found in the north and many places in the semi-desert and desert steppe of the soum. Herders claimed that a small sand dune (*moltsog* in Mongolian) moved 2 m over the last 3 years.

2.6.2 Soil salinity

Salinized areas are commonly seen on dry bottoms of shrunken water bodies, such as lakes and rivers, namely Baasan river and Ulaan lake. However, these cover only a very small proportion of the area. There are signs that those salinized areas have changed the physical condition of the soil, reducing infiltration, increasing runoff and erosion, and impairing biological activity.

However, some areas have naturally high salt content in the soil, while saline seeps can occur when water moves through the soil, picking up salts, and then emerges at a seep or spring. On those areas, only annual salt-resistant plants, including *Iris bungei* grow.

2.6.3 Sheet erosion

Sheet erosion occurs when unprotected soil particles are loosened by trampling through wind erosion and by the impact of rainfall (NETC, 2005). The other definition is a

general lowering of the soil level, leaving raised pedestals where the root mass of the remaining vegetation protects it (Bettis, 1983). Sheet erosion by water is concentrated mostly on mountainous areas, while wind-forced sheet erosion is observed on semi desert and desert steppe, and the saxaul forest areas of the Bulgan soum. Saxaul trees keep the wind from distributing large amounts of sand and are therefore considered as the most efficient plants for stopping sand movement.

2.6.4 Gully erosion

Gully erosion is the most obvious demonstration of erosion, although in most areas actually less significant in terms of total land degradation (Bettis, 1983). Concentrated stream flow during the rains from the high mountains such as Gobi Three Beauty and Arts Bogd has resulted in several gullies with differing depths. They are mostly triggered by erosion along livestock tracks, road edges and seasonal water flow from the mountains. The process can start with "rills" and end up with gullies that range from 5 m to over 20 m in depth and from 30 m to 2 km in width.

2.7 Degradation related critical issues

Pastoral and wildlife ecosystems pose challenging management problems associated with increasing livestock populations, rangeland degradation and alteration of pastoral migration patterns (Sneath, 1998; Ojima, 2001). Grazing pressure is greatest near settlements and water sources (Batjargal, 2001). In addition, the area supports hundreds of large wild herbivores, including khulans, wild camels and gazelles.

With the area of sand increasing and new sand dunes appearing, the process of desertification is continuing. Since 1970, a total of 2 wells and 8 cattle pens have been sand drifted). There is shrinkage of the discharge from the ‘Ongi’ river and from 3 small rivers and streams flowing from the north to the south in the Gobi zone. The diversion of rivers for gold mining is the major reason for disappearance of lake ‘Ulaan’.

The water deficiency in the arid Gobi region has negative effects on the vegetation cover as seen by the lowering of plant biomass production and decrease in plant diversity (National desertification report, 2002). Over half of the pasture areas are exposed to erosion, and the grassland yield in 2000 is as low as the yield recorded in 1970 (Sanjid et al., 2004). The critical issue is how to preserve land resources while improving the livelihood of the herders. To preserve the land resources and thus combat

desertification, traditional livestock grazing methods such as rotational grazing need to be adopted by the herders. However due to economic and social constraints, the movements of the herders have been decreasing, causing overgrazing in winter settlements and near wells in many places (Batjargal, 2001).

Yet natural degradation of vegetation is typically gradual. A fragile degraded ecosystem triggered by the sandy eroded soil, strong frequent dust storms, less and variable rainfalls as well as detrimental human land use mainly caused by overgrazing and less rotation by herders are accelerating desertification in the Bulgan soum (Figure 2.7). Shrinkage of Ulaan and Ongi rivers due to gold mining activities, loss of many plant species and active sand dunes were the main concern of the herders during the field work. However, no guidance and information on combating desertification is available at the local level. There are some signs of herders becoming farmers and planting economically viable trees that can stop sand movement such as sea buckthorn. But only a small number of the herders are involved. Irrigation is currently from wells and springs at center of the soum, which causes high water consumption and water loss.

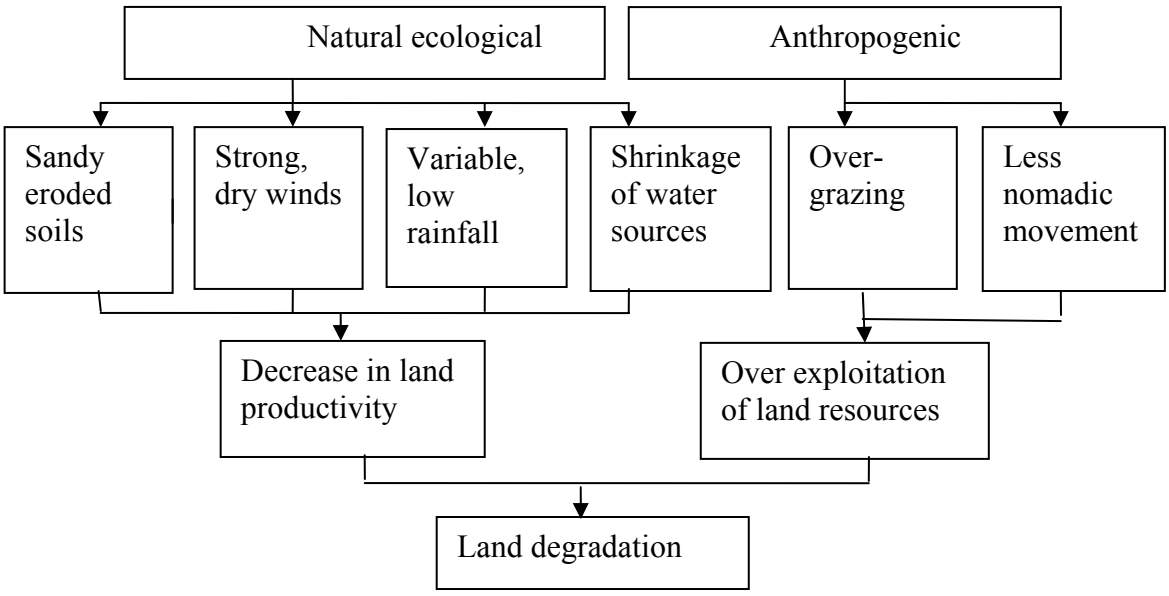

Figure 2.7 Causes of desertification in the Bulgan soum, Mongolia

3 DESERTIFICATION ASSESSMENT BY VEGETATION AND SOIL INDICES

3.1 Introduction

Land degradation in semi-arid ecosystems is defined as destruction of the biological potential of land and its ability to support populations (Mainguet, 1994). It refers to the resilience property of systems, meaning whether or not the system is persistent through time and space (Katyal and Vlek, 2000). Persistent reduction in productivity is an expression of desertification (land degradation eventually leads to desertification), and one means to investigate if land degradation processes are occurring (Prince et al., 2001). Land degradation processes, either naturally or human induced, cause the vegetation cover to become thin and the non-vegetated patches to increase in extent. Such changes can be measured and monitored using remotely sensed data, through the use of calculated vegetation indices (Deering and Haas, 1980).

Vegetation indices (VIs) are made by combining bands of satellite-derived data, and are based on the fact that plants reflect less in visible red (R) light, and more in near infrared radiation (NIR), compared with non-vegetated surfaces (Bannari et al., 1995; Karnieli et al., 2001). The most commonly used index, the normalized difference vegetation index (NDVI), successfully indicates vulnerable areas and assesses changes in a qualitative way (Bolle, 1994; Justice et al., 1985). However, interannual changes of vegetation cover in dry regions expressed by NDVI values can reflect rainfall fluctuations rather than desertification (Nicholson et al., 1998; Tucker et al., 1991; Williams, 2000). Also, background soil color affects NDVI, especially in semi-arid and arid environments where there is less than 30% plant cover (Major et al., 1990; Pech et al., 1986). To reduce the soil background effect, many vegetation indices, such as the weighted difference vegetation index (WDVI) by Clevers (1989), soil-adjusted vegetation index (SAVI) by Huete (1988), and MSAVI, the modified version of SAVI (Qi et al., 1994), were introduced. Both SAVI and MSAVI use soil adjustment factors, thus they are not functionally equivalent to NDVI, and contain different information on vegetation characteristics (Baret et al., 1989).

Kaufman and Tanre (1992) developed several VIs that directly correct the red-radiance aerosol effect in the atmosphere by incorporating the blue (B) band called

the atmospheric resistant vegetation index (ARVI) and the soil-adjusted atmospheric resistant vegetation index (SARVI). Later, they were updated by Huete et al. (1997). The ARVI adjusts for air interference and the SARVI corrects for both air and soil interference. Both, the SARVI in particular, derived from Landsat TM images, showed promise where the NDVI was unsuitable under South African conditions (Huete et al., 1984; 1997). Therefore, depending on local conditions, the best suitable vegetation indices should be utilized to depict the actual vegetation cover change. Research in Mongolia has shown the MSAVI to correlate reasonably well with vegetation biomass in desert steppe, while the enhanced vegetation index (EVI) was well suited in mountain steppe and plain steppe zones (Javzandulam, 2002).

In addition, bright soils have been shown to reduce values in vegetation indices such as NDVI (Heute et al., 1985). Therefore, Escadafal and Bacha (1996) developed a new brightness index (BI) well suited to arid areas where dominant vegetation types such as shrubs are often photosynthetically inactive, and where the vegetation cover affects only the brightness index (BI). A decrease in brightness index can be due either to the wetting of the soil surface after rainfall, to an increase in plant cover or in soil roughness, or to degraded soil (Escadafal and Bacha, 1996). Simple ground information and knowledge on land surface processes are necessary to interpret the BI in ecological terms (Escadafal and Bacha, 1996).

Soil related spectral indices (SI) such as the redness index (RI) detect soil surface color changes due to the presence of more reddish soil materials and hematite content (Escadefal et al., 1989; Ray et al., 2005). Escadefal and Bacha (1996) combined images of brightness index (BI), greenness or NDVI, and redness index (RI), which are linked to soil surface parameters such as brightness, green vegetation cover and soil color to evaluate desertification. A decrease in the RI generally corresponds to the thinning of the surficial sandy soil layer leading to a lowering of water intake and seedling emergence capabilities of the soil, which indicated ongoing desertification in Tunisia (Escadefal and Bacha, 1996). Both brightness and redness indicate soil degradation independent of the vegetation type and abundance (Escadafal and Bacha, 1996). However the authors noted that like BI, the RI should be interpreted carefully in different areas, because in some areas the higher RI values might be just opposite.

Another soil index, the bare soil index (BSI), is commonly used to evaluate desertification processes. It increases as bare soil exposure increases (Rikimary and Miyatake, 1997). However, the BSI, like NDVI, is strongly dependent on precipitation, which has large temporal and spatial variability and uncertainty in arid regions (Xiao et al, 2006). Even one rainfall event can make vegetation cover significantly increase, thus, these indices misinterpret the actual degree of desertification (Xiao et al, 2006). To overcome this problem, Xiao et al. (2006) proposed a new index, topsoil grain size index (GSI), which is associated with the mechanical composition of topsoil. It indicates the coarsening of topsoil grain size which has a positive correlation with fine sand content (this class of sand is dominated by the finer sizes of sand particle, and somewhat less coarse than either sand or coarse sand) of surface soil texture, as a manifestation of undergoing desertification. The more severe the desertification, the coarser the topsoil grain size composition (grain size refers to the mean or effective diameter of individual mineral grains or particles. Coarse particles having effective diameters greater than 2 mm, sand sized and larger) is found. Overgrazing is one of the causes of soil coarsening due to accelerating soil erosion by wind (Fu et al., 2002).

Desertification in and around southern Mongolia has been significant over the past decade, causing problems not only in neighboring countries but also in East Asia, affecting both natural forces and human activities. With ground truth data on vegetation and soil data in 2005, Bulgan soum the aim of this study was to obtain reliable desertification information from vegetation and soil index differencing of multitemporal Landsat data. The objective was to delineate the characteristics vegetation in terms of various VIs, such as NDVI, TNDVI, SAVI, MSAVI, ARVI, and SARVI to describe their ability to discriminate vegetation cover and biomass over a 40 km x 40 km area. The indices are grouped into three sets based on their features: the first set (NDVI and TNDVI) includes the vegetation indices that directly give the spectral response of chlorophyll by using the ratio between red and NIR bands. The second set (SAVI, MSAVI) was used to remove the soil noise by changing the slope value of red and NIR bands. The third set (ARVI, SARVI) was used to reduce aerosol atmosphere and soil noises by including the blue band. The following hypotheses regarding the relative strength of various vegetation indices made from Landsat (MSS, TM, ETM+) data were formulated and tested.

Hypothesis 3.1. Vegetation biomass within the Bulgan soum is significantly correlated to MSAVI, SAVI, ARVI and SARVI rather than NDVI and TNDVI.

Once one of the useful VIs was identified, images from years with similar rainfall were subtracted to define long-term vegetation biomass change. Any negative trend in vegetation biomass would support the assumption (Prince, 2001) that a persistent reduction of vegetation cover even during wetter periods is a sign of desertification.

Hypothesis 3.2. Vegetation biomass in the Bulgan soum has declined over the last 30 years based on VI differencing.

To reveal desertification degree of severity in association with soil properties and bare land exposure, multiple SIs were calculated and correlated with the sand percentage of soil, and the bare ground percentage. Soil indices included redness (RI), bare soil index (BSI) and topsoil grain size (GSI). The GSI were tested in combination with the VIs, with the assumption that increasing GSI indicates topsoil texture coarsening.

3.2 Methods

3.2.1 LANDSAT MSS, TM, and ETM data

Vegetation is the most dynamic element of the landscape from a remote sensing perspective. To avoid confusion of seasonal changes in vegetation cover with long term decreases or increases in cover, it is preferable to use images that are recorded at times when development of different vegetation is identical or at a very similar stage. For this reason, cloud-free remotely sensed orthorectified LANDSAT images from years with similar mean annual precipitation (MAP – rainfall from January to December) and growing seasonal rainfall (rainfall from April to September) between 1973 and 2005 were selected (Table 3.1). The obtained images except 2005 were the only free images available to this region.

Table 3.1 Database used for change analysis

Database	Date	Scene identification	Cloud coverage	MAP (mm)	Rainfall (mm)
MSS	1973/06/03	p142r29_1m19730603	0	155.2	76.9
TM	1990/09/17	p132r29_4t19900917	0	197.3	114.7
TM	1991/06/16	p132r29_5t19910616	0	182.6	94.1
TM	2002/07/24	p71132029_2920020724	0	132.6	68.7
ETM oft	2005/06/14	7132029000516550	0	158.7	76.2
GIS		boundary, DEM, soil			

[a] – rainfall from January to December, [b] – rainfall from April to September

The Landsat MSS and TM data by USDA ARS, University of Maryland, USA, and Landsat ETM + oft data by USGS were acquired. The MSS imagery covered four channels (2 visible, 2 near-infrared) at 79 m resolution. The TM features 7 spectral bands, bandwidths of 10 nm, and covers a continuous spectrum over 0.4 to 2.5 nm wavelength range (3 visible, 1 near-infrared, 2 mid-infrared, 1 thermal-infrared) at 28.5 m nominal ground resolution (Table 3.2) (Lillesand and Kiefer, 1994). ETM+ has all the attributes of TM, plus a panchromatic band. Due to a strip of image data missing from the 2005 (Landsat ETM+) image, the 2004 and 2003 images were used for gap filling by the provider (USGS).

Table 3.2 Landsat characteristics

Sensor	Band	Spectral (μm)	Range
PAN ETM +	8	0.52-0.90	15
TM, MSS	1 (blue)	0.45-0.52	30
	2 (green)	0.52-0.60	
	3 (red)	0.63-0.69	
	4 (nir)	0.76-0.90	
	5 (swir)	1.55-1.75	
	6 (fir)	10.40-12.50	60
	7 ($swir_2$)	2.08-2.35	30

Landsat MSS – Bands 1-4, Landsat TM – Bands 1-7, Landsat ETM+ - Bands 1-8

The remotely sensed TM, and ETM+ Landsat data (Path/Row 132-29), covered a region across the Bulgan soum, with seven bands (Table 3.3). The data used in this study were a sub-scene from the original dataset, with 1403 x 1403 pixels, or 40 km x 40 km, extracted. Geolocation information is as follows: Output Georeferenced Units, Projection Universal Transverse Mercator zone 48N; WGS 84. In Table 3.3, the full scene coordinates for four images are given.

Table 3.3 Coordinates of the images for the Bulgan soum, Mongolia in UTM projection

Location/Date	1973/06/03	1990/09/17	1991/06/16	2002/07/24	2005/06/14
Upper left X	324330	324232	324244	321081	318060
Upper left Y	5063025	5046531	5046751	5048091	5051055
Lower right X	568632	550868	550876	550278	567150
Lower right Y	4834113	4837580	4837590	4830237	4227900
Width	4887	7955	7958	8043	8741
Height	4017	7341	7340	7365	7831

3.2.2 Image pre-processing and enhancement

The radiometric and systematic geometric errors of Landsat data had to be removed prior to analyses of change. In addition, standardization of values from different satellites, with differences in illumination and atmospheric conditions had to be undertaken (Pickup and Chewings, 1988). The distortions in the images were corrected by using ground control points. Each of the images was geo-referenced with a nearest neighbor resampling algorithm trained using 4 ground control points (because the area contains very few buildings) obtained from the filed work in 2005 and a first-order polynomial fit. Image software allowed for easy zooming and on-the-fly contrast enhancement to assist in point selection.

For radiometric correction, noise (random or regular interfering effects in the data which degrade its information-bearing quality) and haze were (atmospheric scatter) removed for all images. Gaussian filtering was applied to remove the noise and modify the spatial and spectral features for enhancement. Haze was reduced using low 3 x 3 pass convolution kernel. Remotely sensed data processing, including pre-processing, vegetation index computation, etc., was carried out at the Center for the Remote Sensing, University of Bonn, Germany using ERDAS Imagine 8.6 and occasionally ENVI. Overall image pre-processing used to identify the severity of land degradation is illustrated in Figure 3.1.

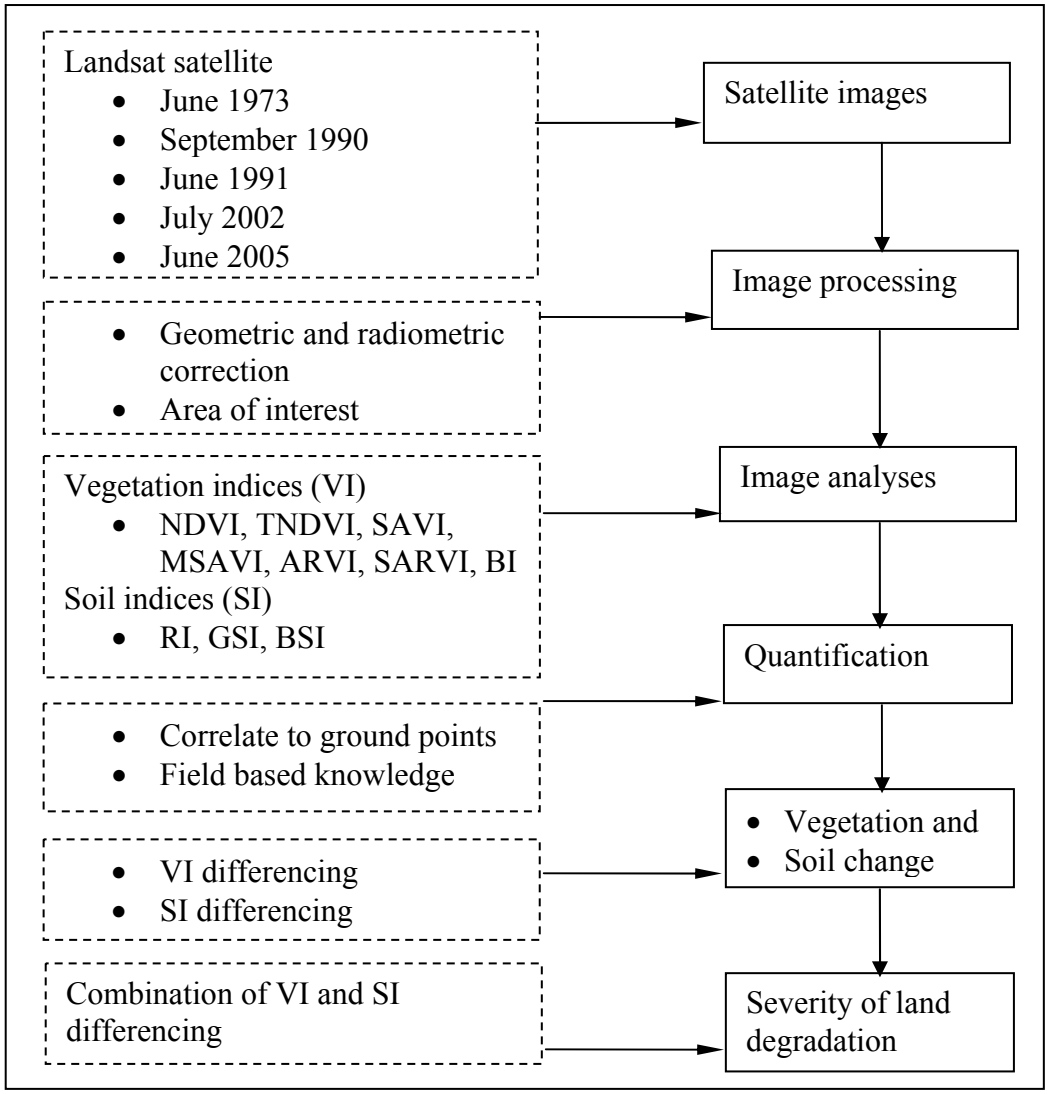

Figure 3.1 Satellite image pre-processing and land degradation assessment

3.2.3 Calculation of vegetation and soil indices

Multiple VIs have been developed using combinations of two or more spectral bands with an assumption that multiple bands provide more information than a single band (Fassnacht et al., 1997). All index equations (Table 3.4) were applied to the atmospherically and geometrically corrected scenes using ERDAS Imagine spatial modeling software. The geometrically rectified and radiometrically calibrated TM, ETM+ bands 1, 2, 3, 4 and 5 were used to derive the VIs. Satellite derived 'vegetation index images' were produced to portray surface changes (Escadafal and Bacha, 1996).

First, the commonly used NDVI images were generated for the image from 2005. NDVI is a measurement of the reflection in the near-infrared wavelength band

(0.73-1.10 μm) and the red wavelength band (0.58-0.68 μm). The red spectral response is inversely related to absorption by plant chlorophyll, while the near-infrared spectral response increases as leaf canopy layer increases. The normalization gives NDVI a potential range from between -1 and +1, and active green vegetation gives the index a positive value. The NDVI and the TNDVI are also influenced by sun angle changes and are affected by soil background to the point that they are as sensitive to soil darkening as to vegetation development (Huete et al., 1984; Huete, 1988)

The SAVI (soil adjusted vegetation index) computes the ratio between the red and near-infrared spectral region with some added terms to adjust for different brightness of background soil (Huete, 1988). L is a correction factor, which ranges from 0 for very high vegetation cover to 1 for very low vegetation cover. The typically used value is 0.5, which is for intermediate vegetation cover. The modified soil adjusted vegetation index (MSAVI) is designed to correct weaknesses in the SAVI, showing how vegetation responds as it moves from the soil line (observed linear relationship between red (R) and near-infrared (NIR) reflectance or image intensity of bare soil (Fox et al., 2003; Qi et al., 1994). The MSAVI has the same conceptual basis as the SAVI, but is improved. It is accordingly believed to be more accurate in reflecting how vegetation spectral responses actually behave. Because of this improvement over the SAVI, the MSAVI is expected to perform better than the SAVI in this work.

Kaufman and Tanre (1992) developed several VIs that directly correct for the red radiance from the aerosol effect by incorporating the blue (B) band. These are the atmospheric resistant vegetation index (ARVI) and the soil adjusted and atmospheric resistant vegetation index (SARVI), where the value L, is expected to be similar to the L used in calculating SAVI. The brightness index (BI) can be obtained by linear combination of measurements in the spectral domains of the bands green (G), R and NIR (Escadafal and Bacha, 1996).

The soil related spectral indices (SI) include the RI, BSI and GSI. The redness index (RI) calculates the ratio of three bands R, G and B. It reflects the hematite content of soil, crusts and sand dunes formation (Escadafal and Bacha, 1996; Ray et al., 2005).

Topsoil grain size index (GSI) computes the ratio of three bands R, B, and G (Xiao et al., 2006). The GSI correlates positively with fine sand percentage of topsoil when desertification is underway. The bare soil index (BSI) is expressed by four bands

(SWIR; R, NIR, and B), and increases along the gradient of bare soil exposure. This index was successfully used in combination with the NDVI to determine forest canopy density by Rikimaru and Miyatake (1997).

Table 3.4 Definition and calculation of vegetation indices used in this study

Vegetation index	Abbr	Formula	Reference
Normalized difference vegetation index	NDVI	$\frac{NIR-R}{NIR+R}$	Rouse et al., 1973 Tucker, 1979
T normalized difference vegetation index	TNDVI	$\sqrt{\frac{NIR-R}{NIR+R}}$	Deering et al., 1975
Soil adjusted vegetation index	SAVI	$\frac{NIR-R}{NIR+R+L}*(1+L)$	Huete, 1988
Modified soil adjusted vegetation index	MSAVI	$\frac{NIR+1-\sqrt{(2NIR+1)^2-8(NIR-R)}}{2}$	Qi et al., 1994
Atmospheric resistant vegetation index	ARVI	$\frac{NIR-RB}{NIR+RB}$ $RB = R-\gamma(B-R)$	Kaufman and Tanre, 1992
Soil adjusted and atmospheric resistant vegetation index	SARVI	$\frac{NIR-RB}{NIR+RB+L}*(1+L)$ $RB = R-\gamma(B-R)$	Huete et al., 1997
Brightness index	BI	$\frac{\sqrt{G^2+R^2+NIR^2}}{3}$	Escadafal and Bacha, 1996
Redness index	RI	$\frac{R^2}{(B*G)}$	Escadafal and Huete, 1991; Ray et al., 2005
Topsoil grain size index	GSI	$\frac{(R-B)}{(R+B+G)}$	Xiao et al., 2006
Bare soil index	BSI	$\frac{(SWIR+R)-(NIR+B)}{(SWIR+R)+(NIR+B)}*100+10$ 0	Rikimary and Miyatake, 1997

NIR – near infrared wavelength, ETM+ Band4, R – red wavelength, ETM + Band 3, L –a value of 0.5, γ–a value of 1, G – green wavelength, ETM + Band 2, B – blue wavelength, ETM + Band 1, SWIR – swir wavelength, ETM + Band 5

3.2.4 Sample area survey and data collection

Field sampling was carried out during the growing season of 2005 during the month that followed the acquisition of the satellite images used in the study. Based on the preliminary change detection of NDVI analysis before the field work, 41 sampling sites were selected. The field sampling area encompassed 40 km x 40 km in the semi-desert

and desert-steppe zones. In the field, the locations of some sampling sites were altered due to difficulties accessing the selected sites.

Aboveground herbaceous biomass was determined by clipping 1 m^{-2} (1 m x 1 m) plots located in a random manner within 40 m x 120 m plots at sample sites. On each site, plant cover was estimated; three 1 m^2 plots were clipped to ground level (Newbould, 1967). At the time of clipping, live species, aboveground dead, and litter materials were separated. Litter was collected by hand from the harvested plots. After being dried to a constant mass at 45 ^oC, aboveground plant biomass (g m^{-2}) and standing dead parts (g m^{-2}) were estimated.

Plant cover was measured by laying out 1 m x 1 m quadrants with 10 cm x 10 cm sub-squared grid on a low herbaceous cover, each within a 10 m^2 area in the 40 m x 120 m plot. The cross points of the string grid were used to determine whether or not the point intercepted plant species, litter, bare ground, or rock (Cummings and Smith, 2001).

In each plant sampling plot (total of 41 sample plots), six soil samples were taken depths of 0-10 cm, 10-20 cm and 20-30 cm. Their textures were determined by the Hydrometer method and particle size analysis.

Elevations and geographic positions of the 41 sample sites were recorded using a Garmin global positioning system (GPS) receiver set into ARC 1960 at zone 48 UTM and later transferred to GIS and projected to the datum used for the satellite images.

3.2.5 Data analysis

An important factor when estimating vegetation biomass through remote sensing is the capacity to precisely locate the sampling points in the image (Mumby et al., 1997). Therefore, the ‘getting grid values’ extension on ArcView was applied to relate point locations to the corresponding vegetation indices. After the pixels at positions corresponding to the ground sampling plots were retrieved, mean and standard deviation were computed from each index, which improved the procedure for evaluating degradation. The relationships of the VIs and ground measurements of vegetation variables were evaluated using Pearson’s correlation coefficients.

The relationships of the soil indices (SI) and ground measurements of vegetation variables, bare ground percentage (opposite of the vegetation cover on the field), and sand percentage of soil (determined from the soil texture analysis) were evaluated using Pearson's correlation coefficients. The coefficient of determination (r^2) was used as an indicator to determine the robustness of a correlation, and the p-value was considered significant when < 0.05. This correlation analysis served as field based knowledge to interpret the vegetation and soil indices within the context of local land surface processes.

3.2.6 Change detection and desertification assessment

To estimate the change in vegetation, pair wise differences were calculated by subtracting one image from another on a pixel-by-pixel basis using the VI and SI images found most appropriate based on comparisons with field data (Singh, 1989; Jano et al., 1998). This meant subtracting the VI image 1973 (before image) from the corresponding 1990, 2000, 2002 and 2005 images (after image), and the image for 1990 from that of 2002 to detect interannual vegetation biomass and topsoil coarsening changes. Differencing was calculated as:

$$Index\ Differencing = VI\ (t_1) - VI\ (t_2) \quad (3.1)$$

Where t_1 is before image and t_2 is after image.

The resulting difference images of the VI and the SI were combined to indicate degradation severity. The image was subdivided into four degradation categories: intact, slight, moderate and severe. Positive values indicate 'intact' class, and minus values were classified into three severity classes**:** slight, moderate and severe. A productivity loss of 10% to 15% is considered a slight degradation (Sehgal and Abrol, 1994). Moderate degradation corresponds to a potential productivity loss of 10% to 25% or 33 % (Dregne and Chou, 1992; Sehgal and Abrol, 1994). Severe land degradation starts when the productivity loss reaches 50% to 66% (Dregne and Chou, 1992; Sehgal and Abrol, 1994). The threshold for each rank of a given indicator is giving Table 3.5

Table 3.5 Indicators and corresponding change values in the assessment of land degradation severity classes

Indicator	Severity class		
	Intact	Moderate	Severe
Vegetation biomass change (%)	<15	15–35	35-100
Soil coarsening (%)	<15	15–35	35-100

3.3 Results

3.3.1 Ground data

Fieldwork was carried out from June to September 2005 on sites predefined based on the NDVI maps depicting change between 1990 and 2002. A total of 41 sampling plots were selected on which vegetation sampling was done with the help of an expert of the Academy of Science, Mongolia. Aboveground plant biomass varied from 4.6 g m^{-2} to 49.5 g m^{-2} with a mean of 31.6 g m^{-2}, while the aboveground plant cover ranged between 4% and 29%, with a mean of 11% and a standard deviation of 8.1% (see also Chapter 5).

3.3.2 Effectiveness of vegetation indices

To decide which VI is the most suitable for studying grassland degradation in this semi-arid area, the VIs (Table 3.4) were calculated and correlated to vegetation characteristics collected in the field (Appendix 1). Two vegetation characteristics, percent grass covers and gram per square meter biomass were used as degradation indicators.

The values for multiple VIs differ. As the near infrared (NIR) value was lower than the red (R) reflectance value (Table 3.6), in general, negative VI values occurred in most of the calculations. The NDVI and TNDVI showed no significant standard deviations. Both the ARVI and SARVI showed some degree of standard deviation. The NDVI, SAVI and MSAVI showed negative values in most of the areas, reflecting low vegetation biomass in the study area. In terms of SIs, the BSI showed the highest values, while the VI values ranged between -1 and 1.

Table 3.6 Vegetation and soil indices for Bulgan soum, Mongolia, 2005

Index	Mean	Max	Min	St. Dev
R	120	179	79	14
NIR	92	141	51	12
NDVI	-0.134	0.109	-0.333	0.011
TNDVI	0.605	0.78	0.408	0.009
SAVI	-0.19	0.31	-0.42	0.016
MSAVI	-0.052	0.59	-0.53	0.305
ARVI	0.028	0.189	-0.138	0.032
SARVI	0.041	0.283	0.207	0.048
RI	0.15	0.22	-0.022	0.018
BI	61	69	55.7	3.8
GSI	0.022	0.22	0	0.05
BSI	70	123	82	3.7

The VIs show natural vegetation coverage as brighter areas. The NDVI and TNDVI show similar bright areas, suggesting the same sensitivity to the vegetation biomass. The MSAVI shows slightly darker areas than the NDVI. In all cases, the vegetation indices using the same ratio of spectral bands showed similar sensitivity to vegetation biomass.

In general, the use of soil adjustments produced more reliable results for the desert grassland (Table 3.7). Grass cover percentages on the sample plots did not bear any definite relationship with the values of their corresponding pixels on the VI images derived from NIR, and R. In terms of vegetation biomass, all r^2 values were similar to one another if the same number of spectral bands was used to derive the index. The TNDVI, ARVI and SARVI showed positive r^2 values in all cases (r^2=0.29-0.36). The TNDVI and NDVI showed slightly higher r^2 and significant relationships compared to the other VIs (r^2 values of 0.39-0.40). The two indices ARVI and SARVI had lower but significant correlations (r^2 values of 0.29-0.34). The highest correlation coefficients were found with plant biomass and the SAVI and MSAVI, with r^2 values between 0.40-0.41. Overall, plant biomass was correlated with all the VIs except the SARVI. Among the six indices, MSAVI was selected for use in further analyses, because it was the most highly correlated with plant biomass at r^2=0.41. None of the soil indices (GSI, RI, and BSI) were correlated with plant biomass and plant cover of the ground plots.

Table 3.7 Pearson's correlation coefficient matrix of the vegetation and soil indices from 41 sample plots, Bulgan soum, Mongolia, 2005

Index	Plant biomass	Plant cover
NDVI	0.40*	-0.14
TNDVI	0.39*	-0.14
SAVI	0.40*	-0.14
MSAVI	0.41*	-0.14
ARVI	0.34*	-0.07
SARVI	0.29	-0.08
BI	0.41*	0.03
GSI	0.09	-0.01
BSI	0.06	-0.01
RI	0.05	0.04

** - p value < 0.05; ** - p value < 0.005*

To quantify land degradation, the soil indices BSI, RI, and GSI were used along with the VIs. RI relates to the hematite content on the ground or crusts and sand dune formation. GSI depicts the coarsening of topsoil that directly relates to fine sand content. As expected, the VIs did not correlate with the soil texture (Table 3.8). Xiao et al. (2006) found that in Inner Mongolia, the GSI correlated with fine sand content of soil. However, the data in the present study provided only sand content including fine and coarse sand, therefore no significant correlation was found. The GSI showed a reasonable correlation of $r^2 = 0.28$, but this was not statistically significant. In any case, it showed the highest correlation among other soil indices. This discrepancy might be due to the fact that the above-mentioned authors used the reflectance value to calculate GSI based on experiments both in the field and laboratory, whereas the index was computed directly from Landsat reflectance values. In addition, as mentioned earlier, data on fine sand content soil were not available, but only on sand percentage including fine and coarse sand. The soil indices BSI and RI also showed no significant correlation with soil texture.

Table 3.8 Pearson's correlation coefficient between vegetation and soil indices and soil texture from 41 sample plots, Bulgan soum, Mongolia, 2005

Indices	Sand	Clay	Silt	Clay and silt
ARVI	-0.30	0.14	0.15	0.15
SARVI	-0.29	0.14	0.16	0.15
TNDVI	-0.31	0.39	0.41	0.26
NDVI	-0.26	0.33	0.48	0.43
SAVI	-0.27	0.23	0.38	0.33
MSAVI	-0.27	0.23	0.38	0.33
GSI	0.28	0.19	0.17	0.16
BSI	-0.18	-0.25	-0.22	-0.24
BI	-0.44*	0.17	0.24	0.22
RI	0.19	0.16	0.17	0.21

**- p value < 0.05; ** - p value < 0.005*

The BI correlated highly with plant biomass, like MSAVI (Table 3.7). To depict the BI trend line and GSI relation to soil sand percentage, linear regression was computed (Figure 3.3). The BI increases with an increase in soil sand percentage and plant biomass indicated by MSAVI. In this case, the high values of BI indicate both high plant biomass and sand percentage, resulting in mixed vegetation and soil features (Figure 3.2.a,b). The GSI showed the highest correlation coefficient at r^2= 0.28 (Table 3.7), indicating that GSI increased along the sand percentage gradient or coarsening of topsoil (Figure 3.2.c). The correlation is not high, but it does mean that the soil degradation and soil coarsening on the ground can be indicated better by this index than other SIs used. The GSI was selected for further analysis to indicate soil degradation in combination with the MSAVI.

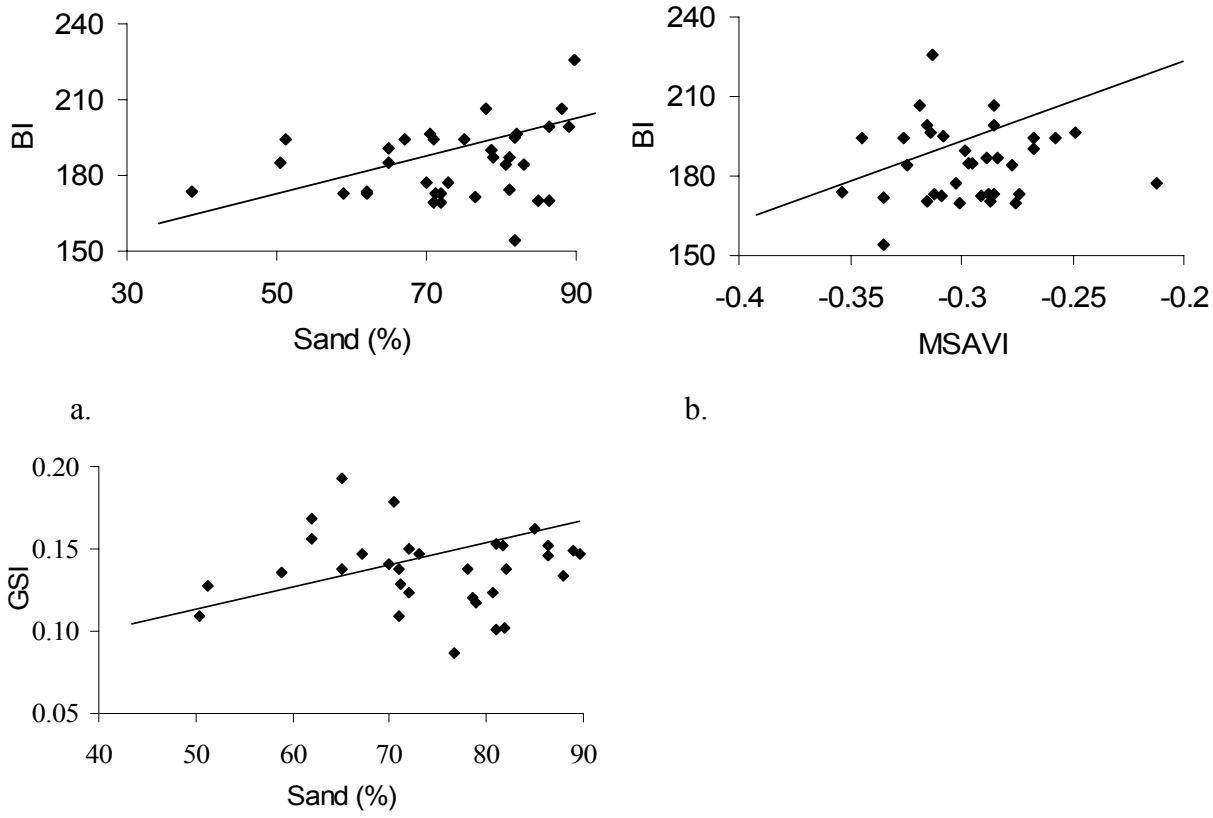

Figure 3.2 Linear regressions of significant VI and SIs: a) Brightness index (BI) and sand percentage of soil; b). BI and MSAVI; c) Topsoil grain size index (GSI) and sand percentage of soil. Bulgan soum, Mongolia, 2005

Since Hypothesis 3.2 was to test the vegetation decrease for the last 30 years based on VI differencing, the MSAVI vegetation index was considered best for the change detection analysis. The fact is it showed the highest correlation with the ground spot's plant biomass (Table 3.7). To use the MSAVI values to predict plant biomass over the entire Bulgan soum, a linear regression was conducted using the following formula (Figure 3.3):

$$Plant\ biomass = 90.3 + 213.7 * MSAVI$$

$$n = 41,\ r^2 = 0.41,\ \text{p-value} = 0.05$$

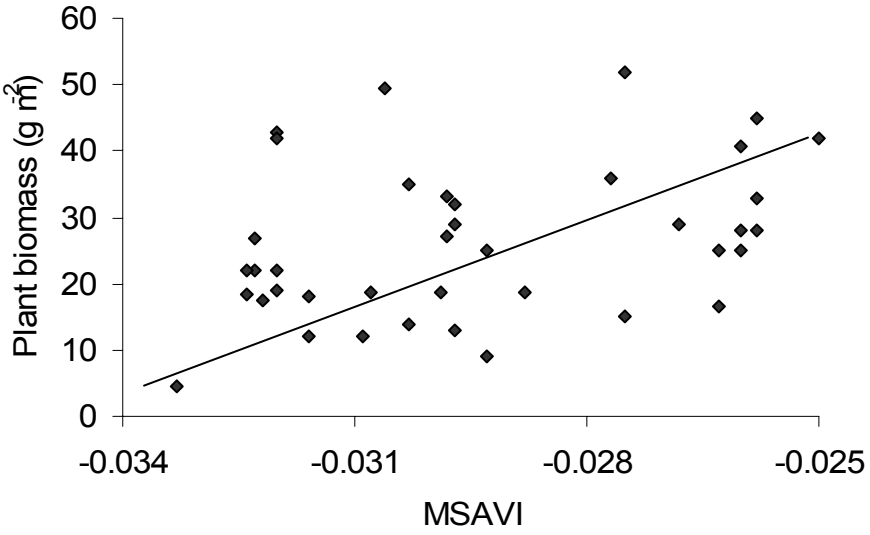

Figure 3.3 Linear regression of plant biomass g m^{-2} and MSAVI. Bulgan soum, Mongolia, 2005

To compare the performance of the vegetation indices for the estimate of vegetation cover, a second order polynomial regression was used. Statistically significant second order polynomial regressions of plant cover to NDVI and TNDVI were found, while no regression were found with other vegetation indices (Table 3.9). Plant cover increases with first order NDVI and decreases with second order NDVI, while increases with first order TNDVI and decreases with second order TNDVI.

Table 3.9 Second order polynomial regression of plant cover and NDVI and TNDVI, Bulgan soum, Mongolia

Plant cover (%)	r^2	p-value
-82-148* NDVI -1547 * $NDVI^2$	0.18	0.05
-35+116*TNDVI – 46* $TNDVI^2$	0.26	0.05

Decreasing MSAVI values along time indicate land degradation, and increasing GSI values indicate soil degradation (Table 3.10, Figure 3.4). In general, low MSAVI and high GSI values were found in 2002 and 2005. Overall, the highest MSAVI values occurred in 1991, and the lowest minimum value occurred in 2005. The years 1973 and 2005 were relatively similar in terms of MSAVI. The mean values of MSAVI decreased through the time period. In contrast, the mean, maximum and minimum

values of GSI increased through the time period, indicating increased topsoil coarsening.

Table 3.10 Modified soil adjusted vegetation index (MSAVI) and topsoil grain size index (GSI) changes for four different years in Bulgan soum, Mongolia, 2005

	MSAVI				GSI			
	Min	Max	Mean	SD	Min	Max	Mean	SD
1990	-1	0.81	-0.06	0.1	-0.6	0.5	-0.1	0.05
1991	-0.7	1	0.02	0.07	-0.6	0.1	-0.06	0.06
2002	-0.4	0.6	-0.16	0.14	-0.1	0.24	0.1	0.04
2005	-1	0.9	-0.17	0.1	-1	0.76	0.1	0.03

To make Table 3.10 visually interpretable, MSAVI images for different years are shown in Figure 3.4. In 1990 and 1991, plant production was much higher compared to the latest years, 2002 and 2005. Particularly, 1991 showed the highest plant biomass, and 55% of the areas had plant biomass classified as high (green in Figure 3.4). The years 2002 and 2005 showed low vegetation biomass. Negative MSAVI values correspond to yellow and brown colors. In general, a decreasing pattern of vegetation biomass is seen through time.

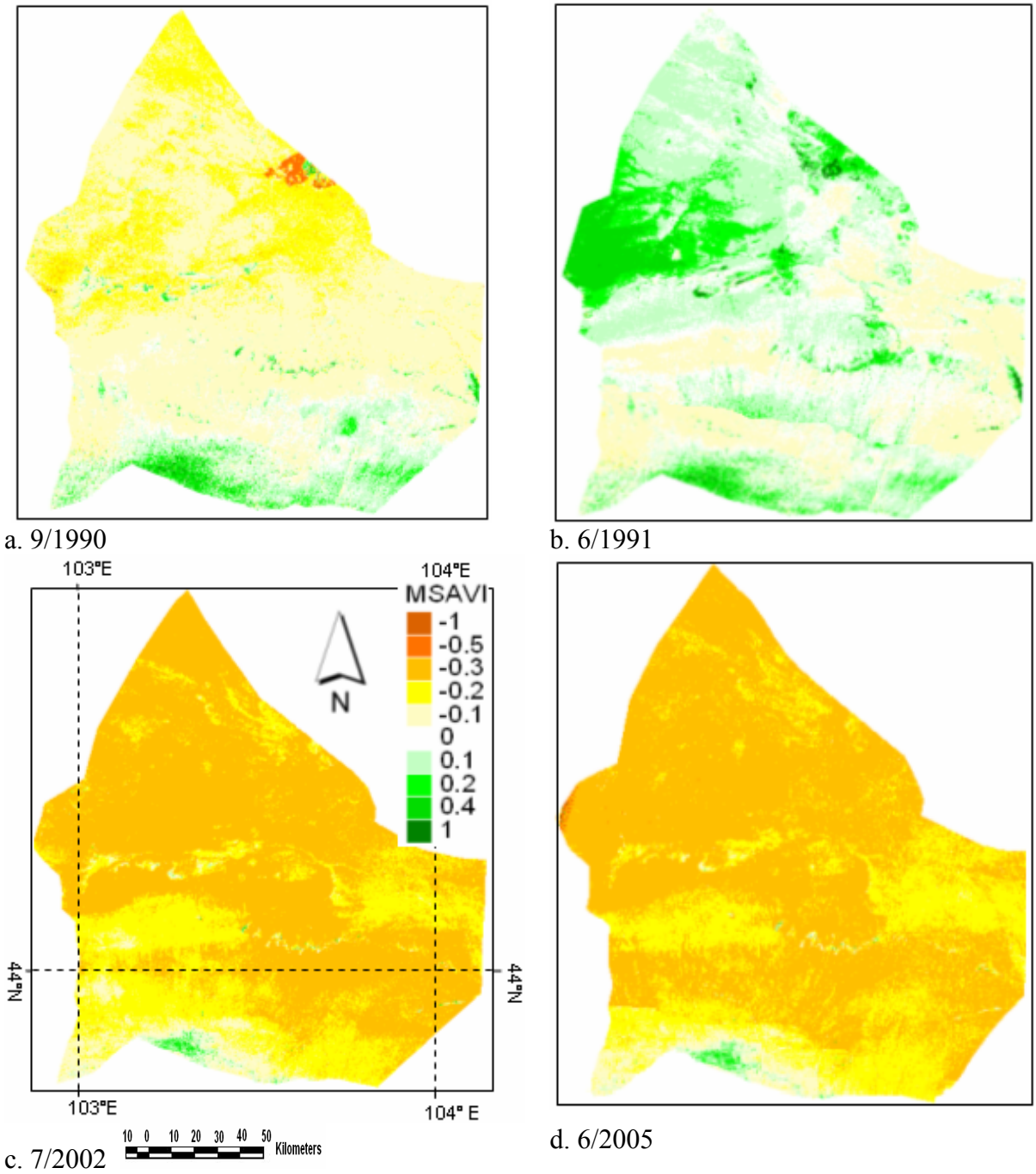

Figure 3.4 Modified soil adjusted vegetation index (MSAVI) in four different years in Bulgan soum, Mongolia. Positive values indicate vegetated areas, negative values indicate little vegetation to non-vegetated areas

Forage production in semi-arid regions is largely dependent on the rainfall pattern. Therefore, the monthly rainfall pattern for the year of images should be taken into consideration (Figure 3.5). The fact is that forage production should be different even if MAP is similar. The image of 1990 acquired in September corresponded to the

highest rainfall (80 mm) in July. The highest vegetation biomass in 1991 corresponded to the highest rainfall (80 mm) in June. The June 1973 image was obtained during the largest rainfall (60 mm) of June. Monthly rainfall data for 2000 and 2002 were not available.

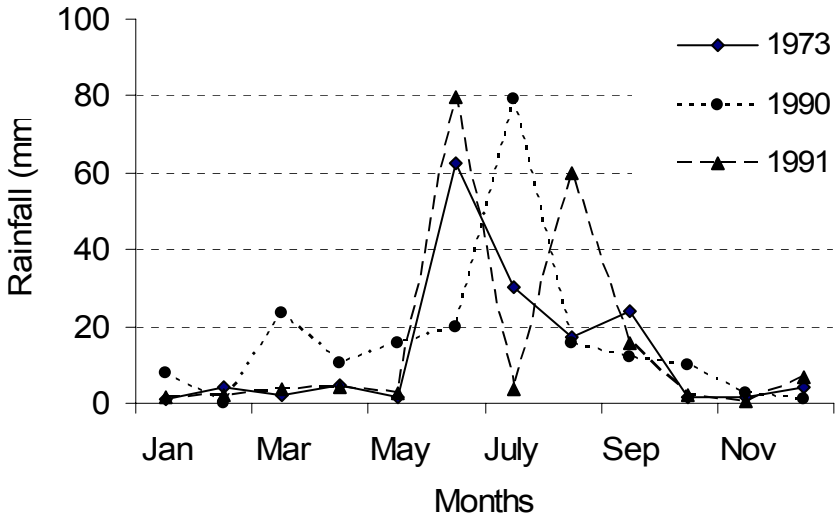

Figure 3.5 Monthly rainfall pattern for the year of satellite image (June 1973, September 1990 and June 1991). Bulgan soum, Mongolia (Hydrometeorology Institute, 2005)

Figure 3.6 depicts topsoil grain size index values (GSI) for different years. As could be expected, based on MSAVI responses, topsoil coarsening increased in the early 2000s compared to the early 1990s. A GSI below -1 and close to 0 indicates vegetated area, and positive values indicate topsoil coarsening (Xiao et al., 2006). The dominant green color representing non-degraded land was prevalent in the early 1990s, but the last two years showed strong topsoil coarsening and soil degradation. The light yellow color corresponding to topsoil coarsening even appears in the highest rainfall year of 1991. It appears that GSI is able to show degradation better than MSAVI. MSAVI responses are highly dependent on rainfall, while GSI is independent of rainfall (Xiao et al., 2006).

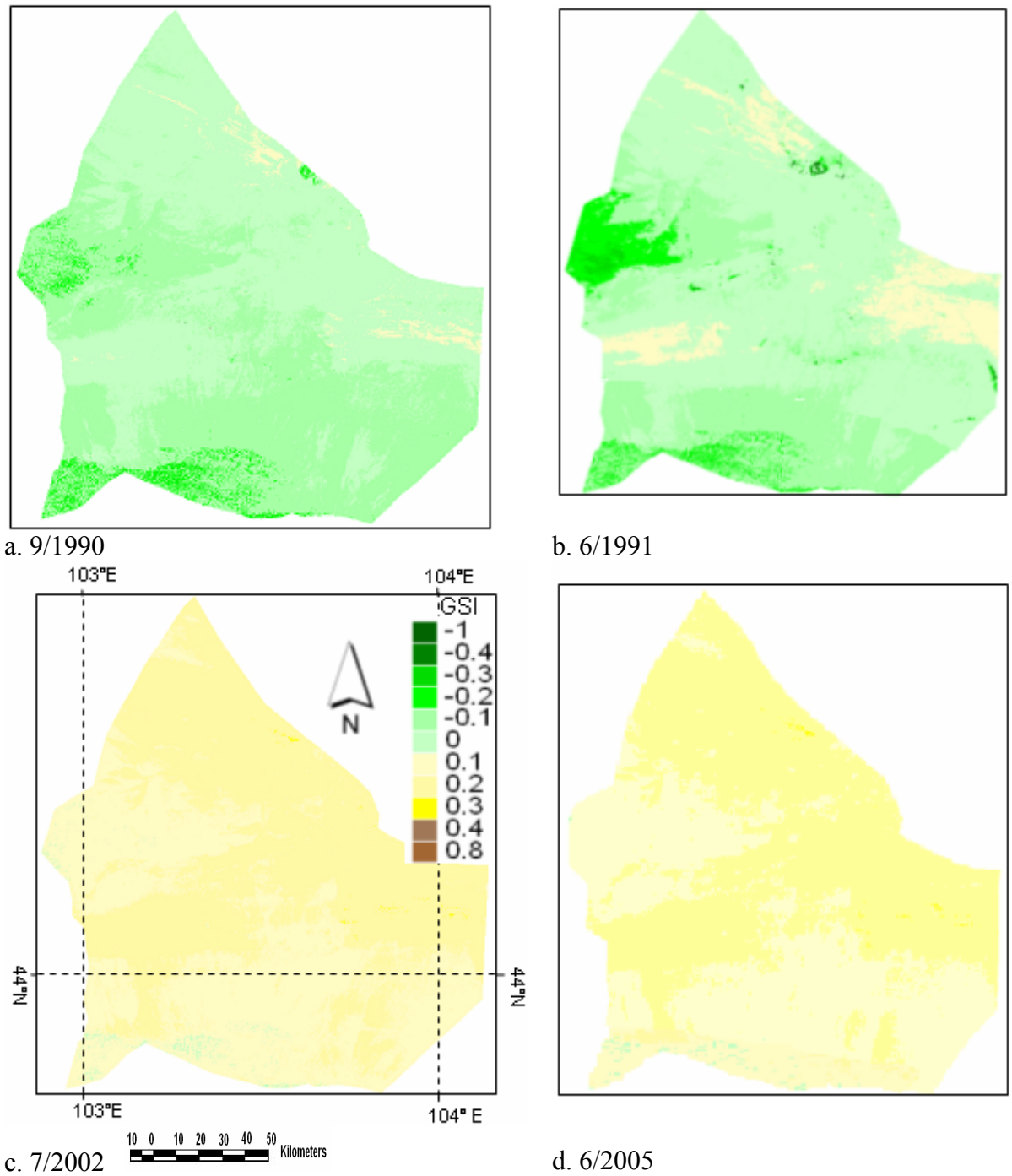

Figure 3.6 Topsoil grain size index (GSI) for four different years in Bulgan soum, Mongolia. Positive values indicate bare ground and topsoil coarsening, negative values and close to 0 indicate vegetated areas

3.3.3 Degraded area change

Vegetation index differencing was used on a 5-year difference of the MSAVI. In this case, the extent of changes was specified using a 5% threshold defining notable change.

Table 3.11 depicts change detection MSAVI values after VI differencing, where (-) values denote a negative change, and (+) a positive change. Overall, the highest negative change appeared between the 1990–2002 and 1991-2005 maps, as expected.

Table 3.11 Change detection for MSAVI differencing images. Bulgan soum, Mongolia

Years	1973-1991	1991-2002	1990-2002	1973-2005	1991-2005	2002-2005
Mean	0.205	-0.181	-0.107	0.020	-0.185	0.005
Max	0.25	0.647	0.8	0.75	0.9	0.9
Min	-1	-0.	-1	-1	-1	-0.95
St. Dev	0.228	0.188	0.128	0.113	0.194	0.071

To depict overall degradation, the combined change image obtained by the MSAVI and GSI differencing over the 1990-2005 periods was created (Figure 3.7). Overall, the red color representing the severely degraded classes accounts for the largest proportion of the area.

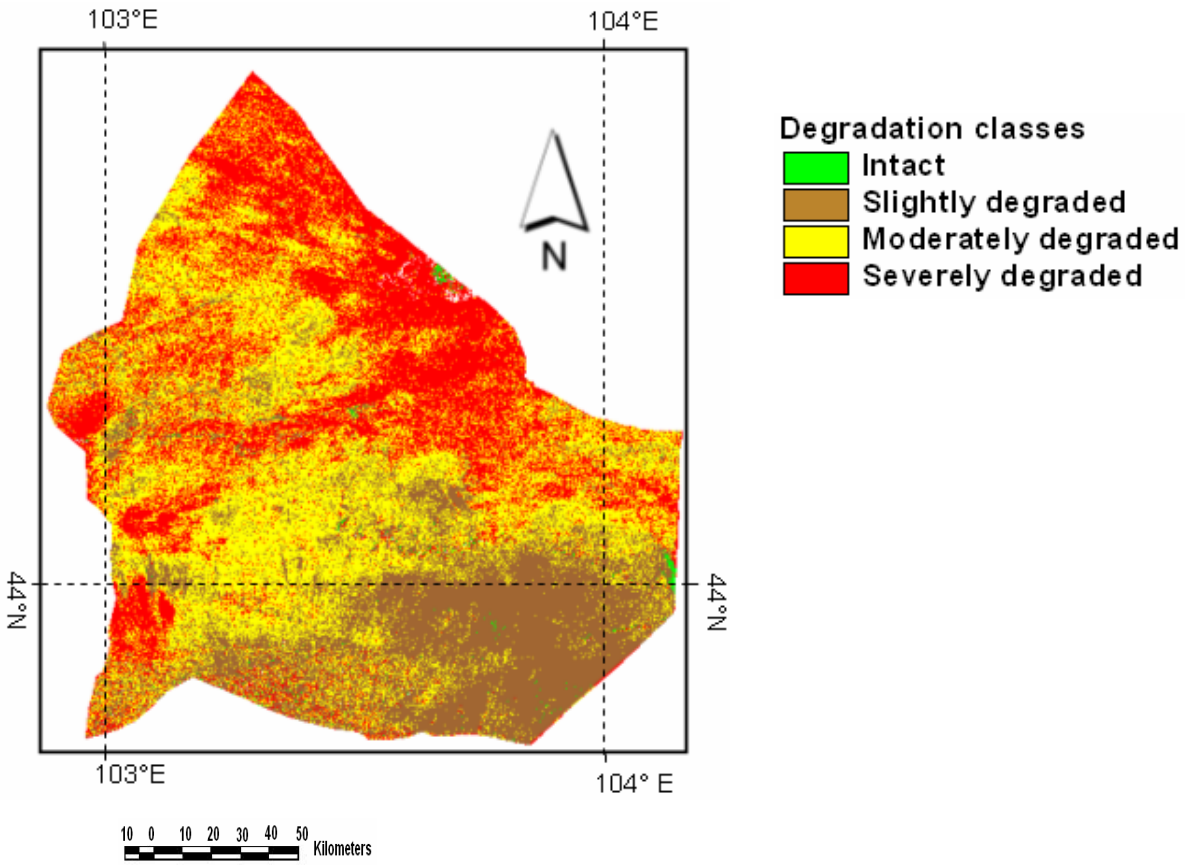

Figure 3.7 Degradation severity degree based on MSAVI and GSI difference between: 1990-2005. Bulgan soum, Mongolia

The result of computing degraded areas based on the MSAVI and GSI changes over time is presented in Table 3.12. The year 1990 was subtracted from 2002, while the 1991 subtracted from 2005 pixel to pixel basis to detect change. Finally those subtracted change images were combined together to highlight the final change over 1990-2005. These data indicate vegetation biomass declines and topsoil coarsening. It is clear that the degraded area has been increasing, although the mean value of indices in 1991 only increased slightly compared to the base year. It can be seen that 33% of the area was intact between the 1990 and 2002, and 31% between 1991 and 2005. In 1990-2005 severely degraded area increased by 23%, whereas moderately degraded decreased by 9%, and slightly degraded increased by 9% (Table 3.12). Here, areas of change were believed to be pastures and grasslands. The image differences between MSAVI and GSI show that the main changes were occurred along the north border of the Bulgan soum, close to dried Ulaan Lake areas. The overall trend is negative in all image-year combinations except for 1991.

Table 3.12 Changes in degradation classes based on MSAVI and GSI differencing 1990-2005, Landsat TM and ETM+ images. Bulgan soum, Mongolia. The last column indicates the change of area percentage for degradation severity degrees

Desertification degree	1990-2002 Area (%)	1991-2005 Area (%)	1990-2005 Area (%)	1990-2005 Areal change (%)
Intact	33	31	10	-23
Slightly degraded	12	14	21	9
Moderately degraded	32	31	23	9
Severely degraded	23	24	46	23

3.4 Discussion

Desertification assessment by vegetation and soil indices through detecting the variations of the green vegetation biomass and soil coarsening was the main objective of this chapter. Satellite images and derived vegetation indices were extensively utilized; however, some vegetation indices are distorted by soil reflectance. For this reason, several VIs such as NDVI, TNDVI, MSAVI, SAVI, ARVI and SARVI were tested for their correspondence to the ground vegetation biomass and cover properties (Hypothesis 3.1). In general, the use of soil background adjustments resulted in more reliable results. From the multiple calculated indices, the NDVI, TNDVI, SAVI, and MSAVI

were more closely correlated with ground plant biomass than the other VIs (Table 3.7).

No relationship between grass cover and the values of their corresponding pixels on the TM, ETM bands-derived VI images were found. The absence of such a correlation is attributed to atmospheric effects, even though the satellite image had been radiometrically rectified. Perhaps that correction did not eliminate atmospheric effects completely. Tasselled cap transformation to detect vegetation in the first transformed band, and soil background in the second transformed band did not significantly improve r^2 values (i.e., < 0.02 in most cases). Another reason might be that the vegetation in the Gobi desert of Mongolia is dominated by photosynthetically inactive shrubs, resulting in low reflectance in NIR (Escadefal and Huete, 1991). Moreover, the plants from the steppe are short woody shrubs with short leaves, which make them difficult to detect with these indices. Certain types of arid soils cause noise in the vegetation indices (Escadafal and Bacha, 1996). Another point is that the sampling size of roughly 1 m^2 adopted in this study is much smaller than the sampling size of 30 m by 30 m on the TM image.

Even vegetation cover was not linearly correlated with ground plant cover, like Purevdorj et al., 1998, percent vegetation cover could have estimated by NDVI index using second order polynomial regression (Table 3.9). He suggested that NDVI is the best for estimating a wide range of grass densities, while SAVI suits well at very low densities of grass cover. However, grass cover was estimated by NDVI and TNDVI in this research, but not by SAVI. The reason for the poor estimate vegetation cover is concluded to be due to the absence of spectral reflectance estimation on the field. No correction between spectral reflectance on the field and raw spectral band reflectance of LANDSAT images was made, therefore, poor correlations of vegetation cover and vegetation indices were found. In favor of Hypothesis 3.1 (*vegetation biomass within the Bulgan soum is significantly correlated to MSAVI, SAVI, ARVI and SARVI rather than to NDVI and TNDVI*), all vegetation indices except SARI were correlated to the ground vegetation biomass, so the hypothesis was rejected.

According to the correlation analysis (Table 3.7), the modified soil adjusted vegetation index (MSAVI) showed the highest correlation and linear regression (Figure 3.3) to the ground plant biomass, and was thus selected as an indicator of plant biomass. Overall, high MSAVI indices were observed in the 1991s, and declined in the early

2000s (Table 3.10). Change detection analysis showed vegetation biomass has declined in the last 30 years, which supports Hypothesis 3.2 (Table 3.11). The years 2002 and 2005 showed (by a factor of 1 and 2) lower plant production than the 1970s and 1990s respectively. Vegetation degradation as described by LeHouerou (1992) is essentially a 'long-term decrease in biomass and ground cover of perennial native vegetation, with respect to pristine or primeval condition under little or no anthropogenic impact'. When 1973, 1990 and 1991 Landsat MSS and TM images considered pristine and primeval condition, plant biomass decreased twice as fast in the last 15 years (1990-2005) than 20 years before (1973-1990).

It should be noted that plant growth in non-equilibrium environments is highly dependent on rainfall. The years 1990 and 1991 had the highest rainfall in a 32 year period (1970-2002) (Table 3.1), therefore the significant plant production decrease is biased. In addition, the monthly rainfall pattern for the years of the Landsat images (Figure 3.5) show that both dates of 1990 and 1991 images were acquired after the highest rainfall (80 mm). Nevertheless, plant biomass and plant cover changes are supported by the findings of the long-term Russian – Mongolian expedition research teams in the Gobi region (Gunin et. al., 2000; Sanjid, 2004). The findings of long term fenced plot's research by Russian –Mongolian expedition in the Bulgan soum showed a decreasing plant biomass over the last 30 years (Figure 3.8). It supports the finding by Erdenetuya (2000), suggested a general decrease of plant cover over the 1990-2000 using NDVI AVHRR. The overriding factors were climatic and anthropogenic – 'Nowadays, such changes are driving by intensive anthropogenic influences' (Gunin et al., 2000). Overgrazing was one of the human-induced factors (Chapter 5, Figure 5.6) (Gordeeva, 1978; Davaajamts, 1974; Sanjid 2004).

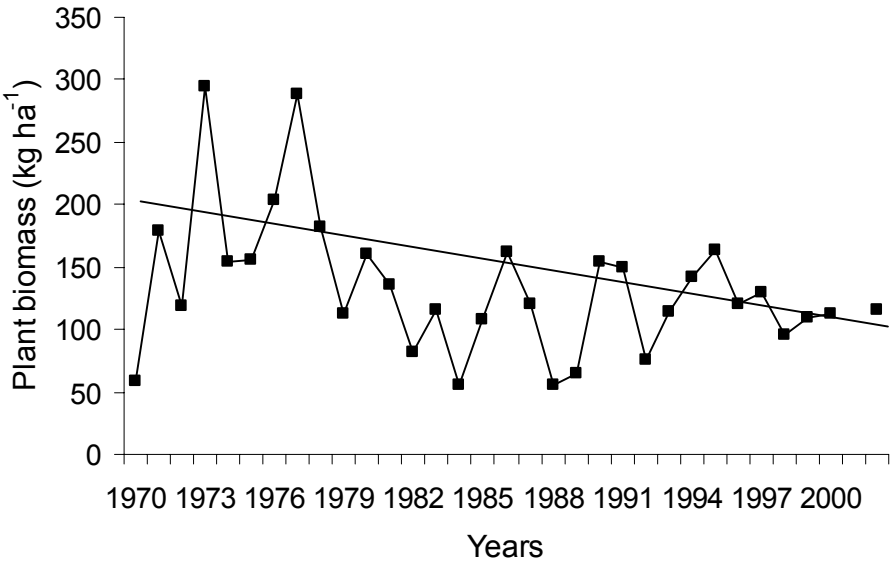

Figure 3.8 Long-term plant biomass, Bulgan research station, Mongolia (Gunin et. al., 2000; Sanjid, 2004)

The GSI, an indicator of soil degradation, shows more topsoil coarsening in 2005 than the early 1990s (Figure 3.6). The integrated desertification assessment made by combining both plant and soil satellite-derived indices shows a 41% difference in the desertified area between the three dates (1990, 1991 and 2005). In all, 90% of the area are subjected to land degradation (1990–2005), in which the severely degraded area has increased by 23%, the moderate decreased by 9%, and the slight increased by 9% compared to the period 1990-2002 (Table 3.12). Land degradation appeared mostly in pastures, grassland areas and dried water bodies. The annual rate of desertification degree (slight, moderate, severe) was 2% for 1990 - 2005.

The use of brightness indices in evaluating desertification was not helpful in this research, as it positively correlated with increasing vegetation biomass and sand content of the soil. Therefore, the combination of MSAVI and GSI was further employed to detect the desertification status. This combination made the desertification assessment more realistic by summarizing vegetation degradation and topsoil coarsening at the same time. The GSI was effective in detecting the degree of desertification; however, it is recommended both indices be used to evaluate desertification. In conclusion, the land cover in the Bulgan soum has degraded, as shown using a multi-temporal change detection analysis over 32 years. Furthermore, for

future research, the use of rain use efficiency (RUE) should be used as an indicator of desertification. In fact, RUE for the Sahel has steadily increased, suggesting that plant productivity had risen even the satellite record bolster desertification (Prince et al., 1998). It was further supported by Idso et al. (1999) that the ongoing rise in the air's CO_2 content enhanced plant water use efficiency.

4 CLIMATE AND VEGETATION DEGRADATION

4.1 Introduction

Vulnerability to desertification and the severity of its impact are governed by climate and human land use patterns, and from which climatic factors play an important role in semiarid regions. Climate, particularly recurrent feature of climate change might exacerbate desertification through alteration of spatial and temporal patterns in temperature, rainfall, droughts, dust storms and winds (IPCC, 2001). Plant productivity in semi arid region is low (Behnke and Scoones, 1993; Westoby et al., 1989), because it is largely controlled by low and highly variable rainfall (Goudie and Middleton, 1992; Tucker et al., 1986, 1985). Therefore, desertification increases when rainfall decreases but may improve during periods of increased rainfall (Burton, 2001; IPCC, 2001).

Dust storm is closely linked to desertification. Its frequency worldwide is at a peak in semi-arid areas where mean annual rainfall is between 100 and 200 mm (Goudie, 1983). Linacre and Geerts (2002) found a close relationship between rainfall and dust storms, and dust storms are probably a consequence of the long-term decline in rainfall (Tchayi et al., 1994).

Drought, i.e., a shortage of precipitation over an extended period, is a regular and recurrent feature of the Gobi desert climate in Mongolia (Baysgalan and Dash, 2002; NDMC, 2006). The resulting severe soil moisture deficits lead to devastate plant productivity and deteriorate quality of soils (Stewart et al., 1992; Thiam, 2002). Furthermore, drought impacts on society depend on both intensity and duration (NDMC, 2006). To monitor droughts, Hayes et al. (1999) used the standardized precipitation index (SPI; current precipitation deviation from long-term average). The SPI was used to detect the start of a drought, its spatial extension, and its temporal progression. In Mongolia, Bayasgalan and Dash (2002) used the Pedi index (current T and precipitation deviation from long-term average), since soil moisture measurements are not available throughout the country.

The Mongolian regions comprise of 21.8% arid and 19.5% semiarid areas, which have supported nomadic livestock pastoralism for thousands of years. Land degradation, which used to be virtually unknown, has become a serious environmental problem in the last 20 years. Many grazing areas have been abandoned by herders, as

these areas no longer provide sufficient plant production. Likewise, MAP (mean annual precipitation) and growing season rainfall decline have been suggested as major causes of desertification in Mongolia (Baysgalan and Dash, 2002). Mongolia is source of dust storms, and soil particles transported thousands of kilometers have a definite impact upon the countries of East Asia (UNEP, 2002). Intense wind storms in springtime in Southern Mongolia generate huge yellow clouds of suspended dust which, depending on the direction of the prevailing wind, even reaches the sea and the USA (Qu et al., 2006). Strong dust storms are called '*ugalz*' (simoom) by Mongolians in the Gobi region, where they occur on 30-60 days each year. They annually carry 4000 tons of sand and dust into the atmosphere per 1 km^{-2} in Southern Mongolia (UNEP, 2002).

The main objective of this chapter is to present the causes of land degradation caused by climatic factors as measured by plant biomass reduction. Climatic stress can be measured as a function of changes in the Standardized Precipitation Index-SPI (McKee, 1993) and Pedi index - by deviations of temperature (T) and precipitation from the long term pattern (Bayasgalan and Dash, 2002). Dust storms, dusts, changes in seasonal limits of rainfall (climate and water balance) and decline in plant productivity are measures of the impact of the climatic stress. Two specific objectives are proposed:

4.1. Identification of long-term trends and changes in climatic factors such as MAP, growing season rain, temperature (T), drought indices (SPI, and Pedi) as measures of climatic change. Dust storms and dust occurrence and aboveground plant biomass are indications of the impacts of the resulting stress.

4.2. If aboveground biomass has been declining for the last 30 years, which climatic factors can have caused this (Figure 4.1). To meet the objective, the assumption was that the lower the MAP and the higher the temperature, the more dust storms will occur.

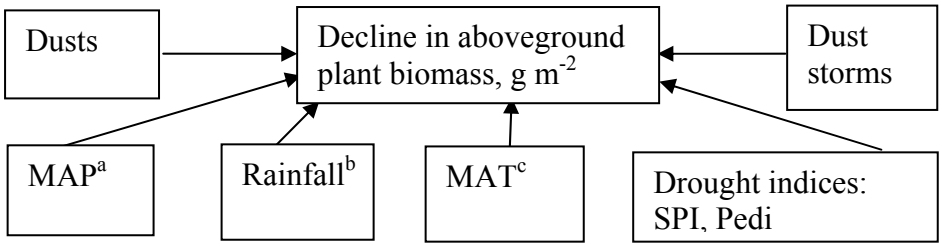

[a]- *mean annual precipitation (precipitation from January to December)*
[b] - *growing season rain from April to September*
[c] – *mean annual temperature*

Figure 4.1 Factors affecting in decline in aboveground biomass. Bulgan soum, Mongolia

Proposed hypotheses are:

4.1. Rainfall, precipitation and plant biomass have decreased, while droughts, temperatures and dust storms have increased over the last 30 years.

4.2. Plant biomass has decreased under the combined effects of decreased rainfall, increased temperatures and dust storms over the last 30 years.

4.2 Methods

Annual and seasonal precipitation, mean annual temperatures, monthly precipitation and temperature, and annual dust storms and dust frequency data were collected from the Bulgan meteorological station (Hydrometeorology Institute) for the period 1970–2002 (Appendix 2). This is the only station in the Bulgan soum. These data were used to explore the relationship between climatic factors, plant biomass and the trends.

Long term vegetation biomass data for 1970-2000 was obtained from the Bulgan research station. This station operated under a Russian–Mongolian research expedition team for the period 1970-1980. Data were collected from the fenced control plots (Gordeeva, 1978; Davaajamts, 1974; Sanjid, 2004). Since 1980, the control plots have been monitored by the Academy of Science of Mongolia, and the findings from several scientific publications in the Mongolian language were collected (Sanjid, 2004).

A dust storm is defined as an occasion when visibility is reduced below a specified level because of the presence of dust in the near-surface layers of the atmosphere. Dust storm frequency (DSF) means the number of days of dust weather and days of dust storms in a month or year. Thus, the frequency of dust storms is be determined by the proximity of the recording station to a source and the strength of that

source. The data set contains a record of the average number of days (based on daily observations) on which dust storms occurred across the recording time interval. A dust storm is defined as an event during which visibility is reduced to <1 km. In our case, annual DSF data were obtained. Dust is the occurrence of dust haze up to 2 m above the land surface. Dust frequency means the number of days of dust haze happen in one year.

The Pedi index, a drought index, is expressed as (Bayasgalan and Dash, 2002).

$$Pi = \Delta\tilde{T}/\sigma\tilde{T} - \Delta R/\sigma R \quad (4.1)$$

Where $\Delta R \Delta\tilde{T}$ is deviation of current temperature and precipitation current values from the long-term averages and σT, σR is standard deviation of temperature and precipitation.

-1 < Pi < 1. If Pi = -1, conditions are favorable (no drought), if Pi =1, severe drought occurs.

McKee (1993) developed the very simple drought index - Standardized Precipitation Index (SPI) to quantify precipitation deficits for different time scales. This index indicates advanced condition of drought when the values fall below -1 (Hayes et al., 1999). SPI is calculated as follows:

$$SPI = (X\,ij - X\,im)/\sigma \quad (4.2)$$

Where X ij is the seasonal precipitation at the ith rain-gauge station and jth observation, X im is the long-term seasonal mean, and σ is the standard deviation.

McKee et al. (1995) in the original classification scheme proposed ‘mild drought’ for SPI values less than 0.00 (Table 4.1). Due to scarce classification of Pedi index, the years classified into 3 major drought classes (Table 4.2).

Table 4.1 Standardized precipitation index (SPI) categories (McKee, 1993)

SPI Range	Climate classification	Theoretical occurrence (%)
+2.0 and above	Extreme wet	2.3
+1.5 to +1.99	Severe wet	4.4
+1.0 to +1.49	Moderate wet	9.1
0 to +0.99	Mild wet	33.9
0 to -0.99	Mild drought	33.9
-1.0 to –1.49	Moderate drought	9.1
-1.5 to–1.99	Severe drought	4.4
-2.00 and below	Extreme drought	2.3

Probability of drought occurrences was computed as following:

$$P(droughts) = \frac{Drought\ occurrences}{Number\ of\ observed\ years} \quad (4.3)$$

The graphics and comparisons for Hypothesis 4.1 are based on long-term climatic data and were generated for visual interpretation. To predict trends, time series forecasting based on linear or exponential smoothing analysis for all climatic factors and plant biomass was carried out in SAS. Time series model assume that there is some permanent deterministic pattern across time (SAS 8.1). The equation is $x_t = \beta_o + e_t$, where e_t is an independent, zero-mean, random error, and β_o is the true series mean. For the linear model, x_t values are generated according to the equation: $x_t = \beta_o + \beta_1 t + e_t$.

Exponential smoothing is a procedure for obtaining polynomial curve getting procedure with the idea that the estimates of the parameters of fit can be updated at each step when new information becomes available (SAS 8.1). It fits a time trend model using a smoothing scheme in which the weight decline geometrically as you goes backward in time. Forecasts from exponential smoothing are based mostly on the recent observations instead on all the observations equally. This analysis assesses how much the given factor fluctuates along the time range, and if so, how it will increase, decrease, or remain stagnant in the future. Damped trend exponential smoothing is $y_t = \mu_t + \beta_t t + e_t$. In each case, tendency, p value and r^2, were tested.

Probability of time series forecasting result (continues random variable) was computed using the following formula:

$$Z = \frac{y - \mu}{\sigma} \quad (4.4)$$

Where y is observed value, μ is mean, σ is standard deviation, and Z is score. The formula postulates the area under a normal curve distribution from the mean μ to a point z standard deviation σ to the right of μ.

To test Hypothesis 4.2, simple regression analyses were conducted to determine the relationship between plant biomass and climatic factors. The climatic factors were also regressed with each other to obtain correlations. If climatic factors affect each other, e.g., droughts accelerate dust storms while causing high temperatures and deficiency in rainfall, or dust storm lead to lower plant biomass, etc. Subsequently, vegetation was regressed against all climatic factors using a multiple regression model. The data are shown by graphics and linear and multiple regression analysis was computed with SAS 8.1.

4.3 Results

4.3.1 Climatic factors change

The mean annual precipitation (MAP) for Bulgan soum over the 32 years of data (1970-2002) was 117 mm. Variation was great ranging from 51.5 mm to 261 mm, CV = 39%, and SD = 45% (Figure 4.2). Below-average precipitation years occurred in 13 years. For the first 10-year period between 1970 and 1980, the Bulgan soum received a relatively large amount of rainfall, reaching 261mm in 1977. From 1981 onward, MAP never reached 200 mm.

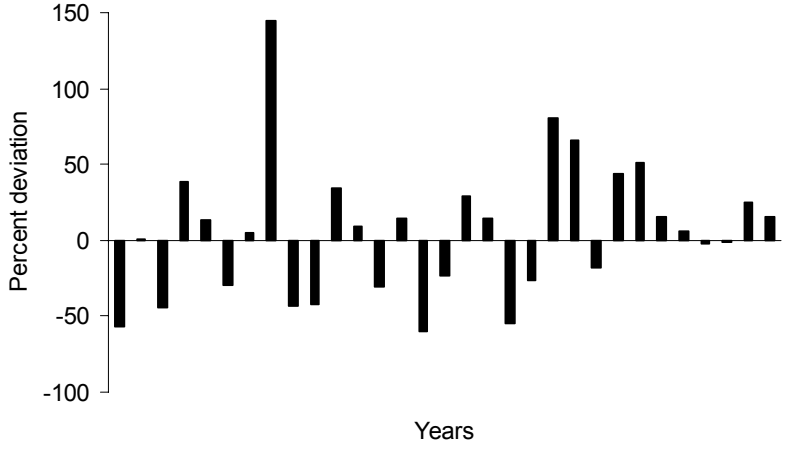

Figure 4.2 Percentage deviation from long-term means annual rainfall (117 mm) at Bulgan soum, Mongolia, for 1970-2002 (Hydrometeorology Institute, 2005)

Mean annual precipitation and growing season rainfall showed large interannual variability and was closely correlated (Figure 4.3). In the 1970s, the area received a large amount of rainfall, reaching as much as 261 mm of MAP. The pattern of oscillation of 10 year's shows high rainfall in the 1970s, low in the 1980s, and increasing in the 1990s. However, a general decrease was not found. This is contrast to the common claim of decreasing rainfall in Mongolia.

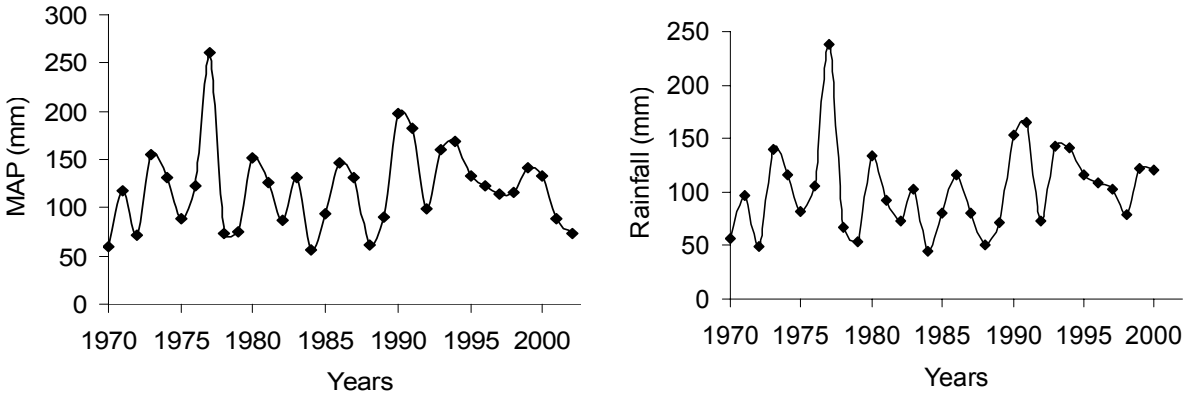

Figure 4.3 Mean annual precipitation (MAP) and growing season-rainfall, Bulgan soum, Mongolia, for 1970-2002 (Hydrometeorology Institute, 2005)

The comparison of monthly precipitation patterns over the periods 1970-1986 and 1987-2002 (The data is from 1970 to 2002. Then, the total 32 years was divided into two periods 1970-1986 and 1987-2002, with 16 year interval for comparison purpose) reveal an increase over the last 16 years, with a maximum in August, with an increase of 7 mm (Figure 4.4). Another increase in precipitation occurred in July and September, while snowfall increased in January, February and March. In regard to mean annual precipitation, a slight increase of 10 mm over the last 16 years was revealed.

The comparison of the monthly temperature pattern (Figure 4.4) shows hardly any difference over the periods 1970-1986 and 1987-2002, except a slight decrease in the winter months. Over the last 16 years, temperatures have dropped by -2.8°C in December, -1°C in January, and by -2.8°C in February. Nomadic herders have experienced reduced cold winter hazard. They however, have experienced increased snowfall in the winter months 1987-2002, which might have caused blizzards and led to livestock loss.

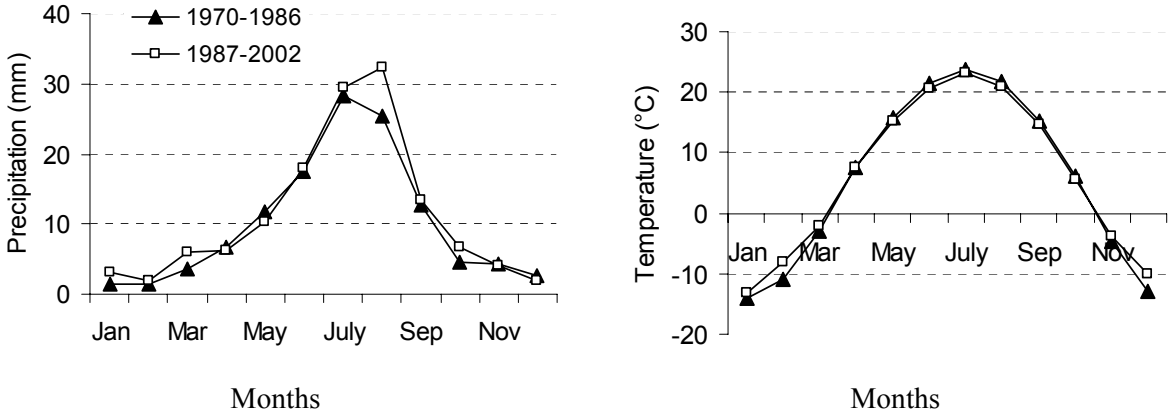

Figure 4.4 Monthly average precipitation. MAP was 120 mm for 1970-1986, and 130 mm for 1986-2002; Monthly average temperature pattern. MAT was 5.5°C for 1970-1985 and 5.9°C for 1986-2002, Bulgan soum, Mongolia. (Hydrometeorology Institute, 2005)

Over the last 32 years, the yearly average temperature increased by 0.5-2.5^{0}C in comparison with the long-term average, especially since 1990 (Figure 4.5). Temperatures increased around 20% since 1990, with a maximum increase of 7^{0}C in 1992 and 2002. A generally increasing trend was found in the 1980s and again since mid 1990s compared to the average MAT 5.5^{0}C of MAT. For the last 30 years, average MAT increased by 0.7°C.

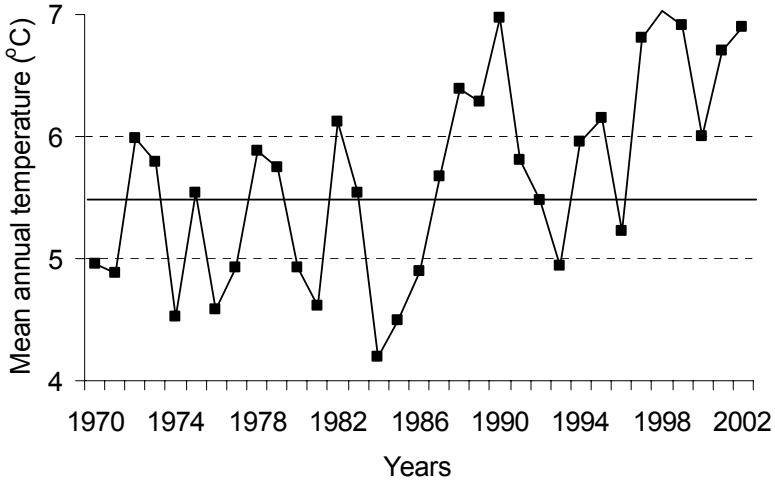

Figure 4.5 Changes in mean annual temperature (^{o}C) for 1970-2002, Bulgan soum, Mongolia (Hydrometeorology Institute, 2005)

The SPI and Pedi index for the period 1970 to 2002 were determined using the techniques developed by Hayes et al. (1999) and McKee (1993) (Figure 4.6; Table 4.2). A SPI of 2 or more was found for about 3% of the time and a normal index (SPI between 1 and -1) happened 70% of the time. SPI values lower than -1 reflect extreme droughts, occurred 6 times. An SPI of 0 to -1 is considered to be normal or slightly below normal, and was found in 9 out of 32 years (Table 4.2). Probability of drought occurrence (Eq 4.3) according to Pedi index was 56%, while 47% for SPI.

Table 4.2 Drought occurrence according to Pedi and SPI, Bulgan soum, Mongolia (Hydrometerology Institute, 2005)

	Range		SPI		Pedi	
	SPI	Pedi	Frequency	Relative frequency	Frequency	Relative frequency
No drought	+2-0	-1 - 0	17	53	14	44
Mild drought	0- -1	0-1	9	28	7	29
Severe drought	<-1	>1	6	19	11	34

The SPI relies on only rainfall, while the Pedi index is calculated with both rainfall and temperatures. Both indices identify drought conditions. Pedi index with -1 (good condition) or better was found 5 times, and a normal condition (Pedi between 1 and -1) 14 times or 45% of the time (Figure 4.6). A Pedi index of 1 and above (drought) was found 11 times or 30% of the time.

Comparing the SPI and Pedi indices related to drought conditions, a SPI of -1 and below was found only 6 times, whereas a Pedi of 1 or above occurred 11 times. Thus, the Pedi index is more suitable than the SPI in Mongolian conditions. The majority of years were considered as droughts by locals during the field work in 2005. The Pedi index is commonly used by Mongolian meteorologists.

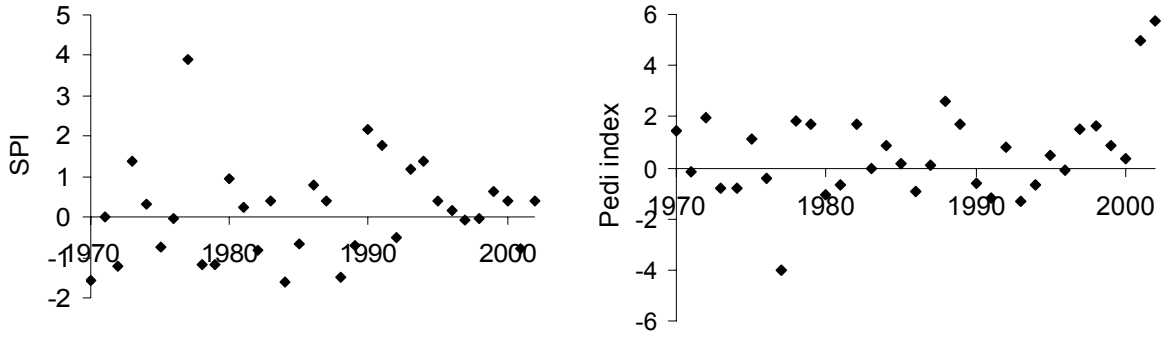

Figure 4.6 Standard precipitation index (SPI) and Pedi index for 1970-2002, Bulgan soum, Mongolia (Hydrometeorology Institute, 2005)

The number of dust storms showed a strong peak in the early spring, tapering off through the summer with a smaller peak in autumn (Figure 4.7). Similarly, dusts (2 m above the land surface) reached their maximum in April and May, then generally decrease during the growing season, and increase again from October. Dust storm frequency (DSF) was highest in April (6.2) and May (5.8), and increased again from October till January.

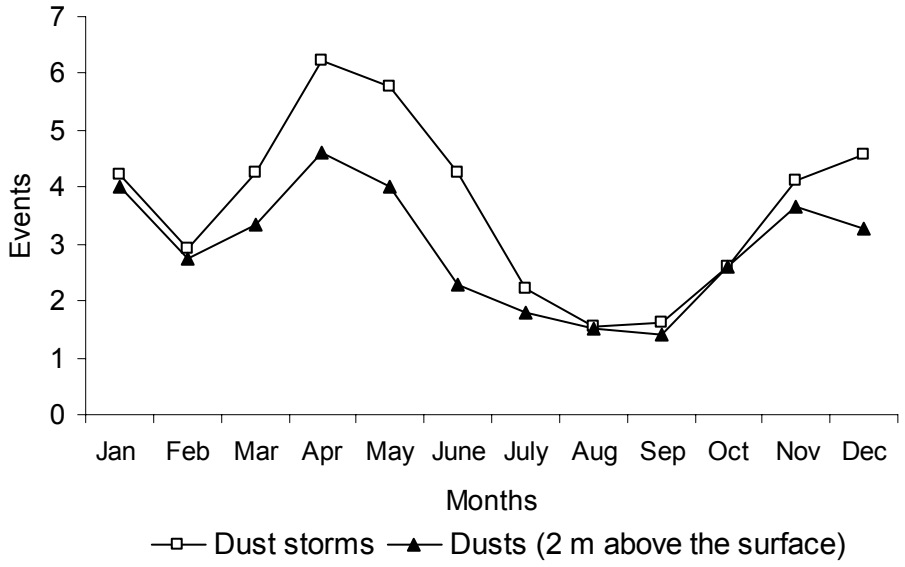

Figure 4.7 Annual variation of frequency of dust storms and dusts for 1970 - 2002, Bulgan soum, Mongolia (Hydrometeorology Institute, 2005)

Dusts hardly occurred after 1993, i.e., only 5 times in 1993 compared to 81 times in 1975 (Figure 4.8). In the years after 1993, dusts virtually disappeared. The

occurrence of dust storms after 1993 was almost 30-40 DSF more than dusts, with a peak of 62 dust storms (DSF) in 2002. Average DSF for 32 year period was 43. Maximum DSF was 98 times in 1984, and minimum 2 in 1971, with a general trend of decreasing dusts and increasing dust storms.

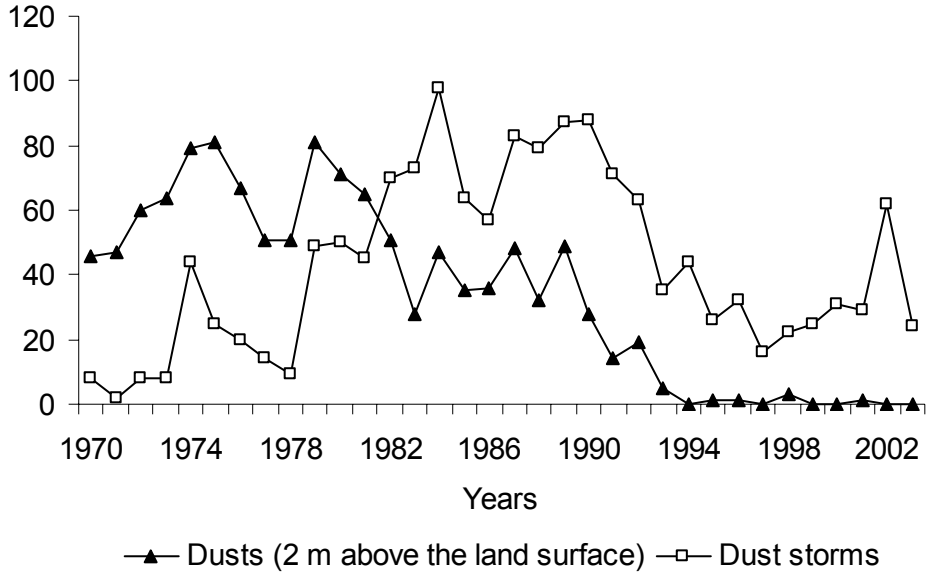

Figure 4.8 Changes in dust and dust storm frequency for 1970-2002. Bulgan soum, Mongolia (Hydrometeorology Institute, 2005)

Comparing the 1970-1986 and 1987-2002 periods, average MAP increased slightly from 120 mm to 130 mm, however with a reduction in the variability (Figure 4.9). Maximum MAP was 261 mm for the first 16 years, whereas it was 197 mm was for the following 16 years. Minimum MAP has slightly increased, from 57 mm in 1970-1986 to 61 mm for 1987-2002. In contrast, the average frequency of dust storms significantly increased from 39 to 56, with some change in variability. Maximum DSF was 88 in the period 1987-2002, compared to 70 DSF in the period 1970-1986.

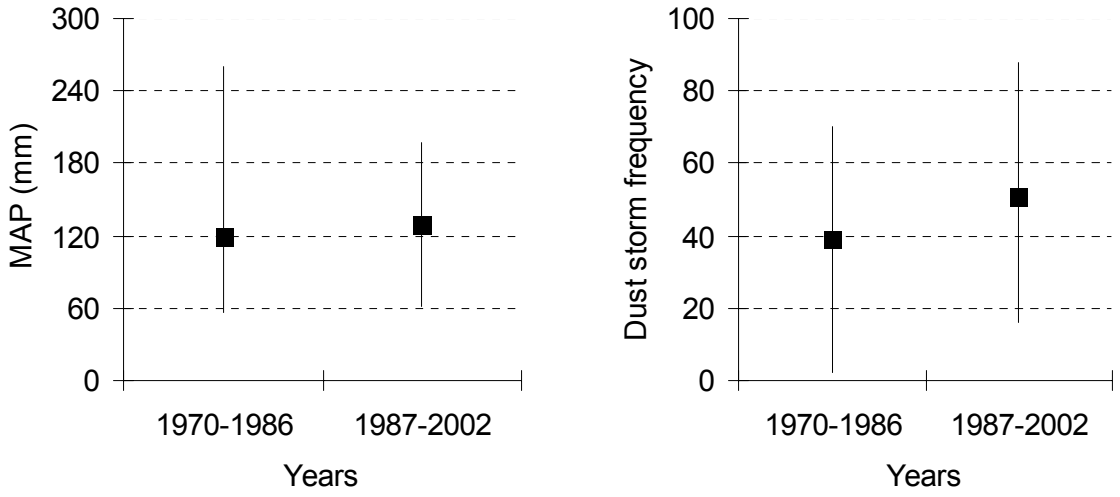

Figure 4.9 Mean annual precipitation (MAP) and dust storms frequency per year 1970-1986 and 1987-2002. Bulgan soum, Mongolia (Hydrometeorology Institute, 2005)

The linear regression analyses were conducted between plant biomass as a dependent variable and the climatic factors as independent variables. The regression analysis between aboveground biomass and growing-season rainfall between June and August is:

$$Plant\ biomass = 63.7 + 0.95 * rainfall,$$

r^2=0.39, p-value = 0.001 (Figure 4.10.a)

Thus, a 10-mm rainfall increase in the growing season is associated with a 9.5 kg ha^{-1} increase in aboveground plant biomass. The higher frequency of growing season rain fall below the 86-mm mean was higher than that of high rainfall. During the 32-year period (1970-2002), a below mean growing-season rainfall years occurred twenty times (Figure 4.10.a).

The aboveground biomass was also related to mean annual precipitation (MAP):

$$Plant\ biomass = 48.1 + 0.82 * MAP$$

r^2 = 0.38, p-value = 0.01

The results show that a 10-mm increase in MAP corresponds to an additional 8.2 kg ha^{-1} aboveground plant biomass per year. In fact, the correlation analysis reveals that MAP and growing-season rain were highly correlated, as about 80% of the rain falls during the growing season from May to August.

The next regression formula was developed as a base for calculation of the relationship between plant biomass and dust storm frequency per year:

$$Plant\ biomass = 177.6 - 0.99 * dust\ storms$$

r^2=0.24, p-value=0.005 (Figure 4.10.b)

Aboveground plant biomass decreased significantly with increasing number of dust storms. A tenfold higher frequency of dust storms per year are associated with a 9.9 kg ha^{-1} decrease in aboveground plant biomass.

To determine cause and effect relationship of increasing dust storms and decreasing plant biomass, a linear regression was computed between dust storm as a dependent and plant biomass as an independent variable.

$$Dust\ storm = 76.2 - 0.24 * plant\ biomass$$

r^2= 0.24, p-value = 0.005

Dust storm frequency decreases with increasing plant biomass; 10 kg ha^{-1} more plant biomass is associated with a 2.4 decrease in storm frequency.

The relationships of drought indices, namely SPI and Pedi, to plant biomass were significant. Decreasing plant biomass was observed during the drought years. Droughts appear with negative SPI values, but with positive Pedi values, so that plant biomass is negatively correlated with Pedi and positively with SPI:

$$Plant\ biomass = 154.3 - 27.3 * Pedi$$

r^2 = 0.40, p-value = 0.005 (Figure 4.10.c)

$$Plant\ biomass = 144.5 + 31.09 * SPI$$

r^2 = 0.39, p-value = 0.007 (Figure 4.10.d)

The underlying implication of the above results is that plant biomass is controlled by drought occurrences, and similar regression slopes (27.3 and 31.09) were obtained for both drought indices.

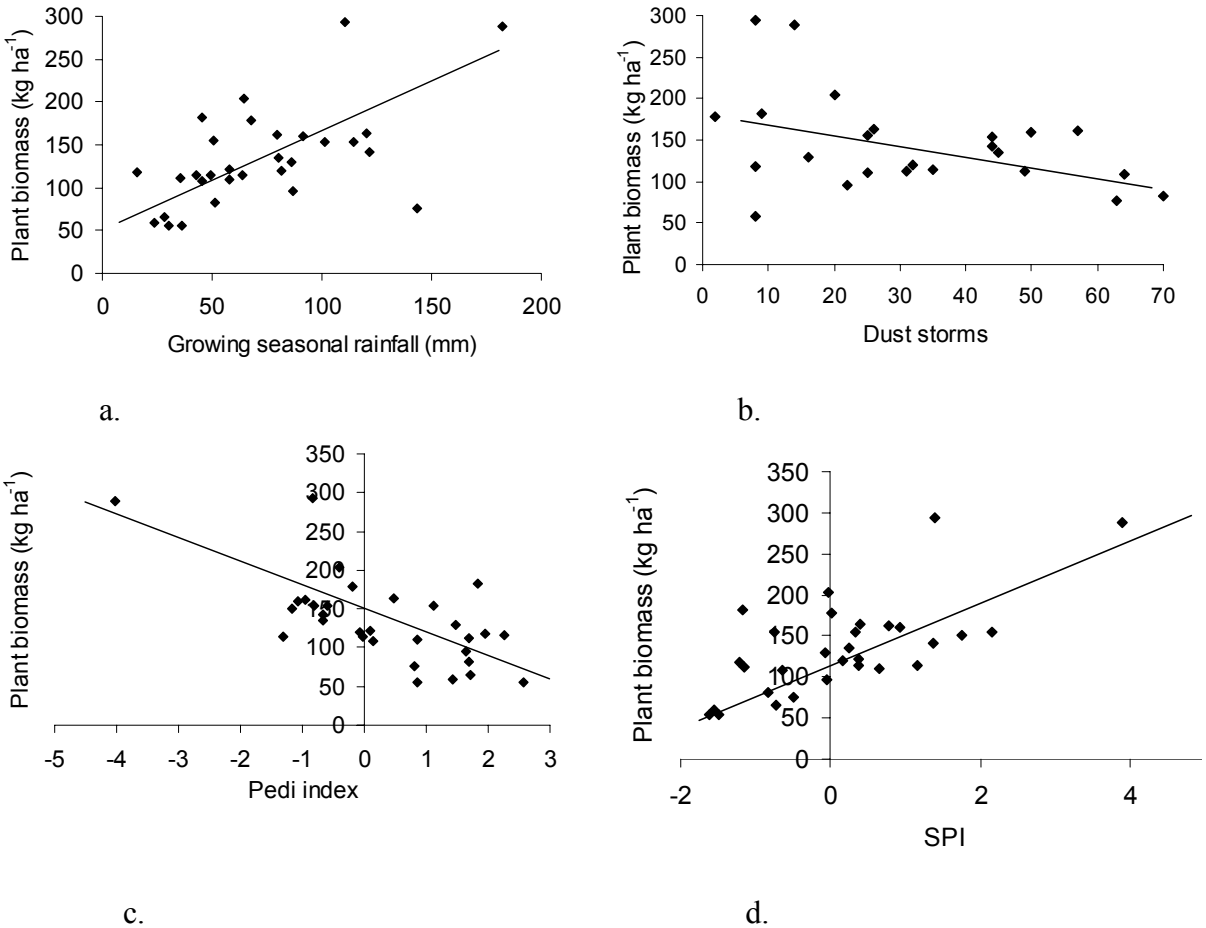

Figure 4.10 Relationship between aboveground plant biomass (kg ha^{-1}) and: a) growing season rainfall (June-August); b) annual dust storm frequency c) Pedi index; d) Standard precipitation index (SPI). Bulgan soum, Mongolia (Hydrometeorology Institute, 2005)

To evaluate the effects of combined growing season rainfall, MAP, MAT, drought indices and dust storms on aboveground biomass, a stepwise multiple regression analysis of aboveground biomass with respect to those factors was performed. It was computed by adding factors to the regression model in stages (Table 4.3) aimed at ascertaining which climatic factor or variable plays a more important role in controlling plant biomass.

Table 4.3 Stepwise multiple regression. Plant biomass as a dependent variable, climatic factors as independent variables. Bulgan soum, Mongolia

Equation	r^2	p-value
*63.6 + 1 * rainfall*	0.45	<.0001
98.5 + 0.97 rainfall – 6.06* MAT*	0.45	.0002
143+ 0.91 rainfall – 6.4* MAT – 0.86 * dust storms*	0.63	< 0.001
*83 -5.66 * Pedi + 0.85 *rainfall – 0.84* dust storms + 0.75 * dust*	0.76	<.0001
110 - 4.2 Pedi + 29.8 * SPI + 0.29 * rainfall -0.87* dust storms + 0.91* dust*	0.81	< .0001
9.18 – 0.86 dust storms + 0.92* dust + 0.41* rainfall - 3.4* Pedi*	0.95	<.0001

SPI and PEDI - drought indices, Rainfall - growing season rain from April to September, MAT – mean annual temperature

It was found that each climatic variable plays an important role, and particularly dust storms which increased the r^2 value by 0.18 (third regression from the top). When a single climatic variable is added, r^2 always goes up, as does the p-value. The final multiple regression reveals that, aboveground plant biomass was inversely related to dust storms, droughts and MAT and at the same time positively related to dusts (dust haze, 2 m above the land surface), and growing season rainfall (significant at p-value= 0.001). This finding also supports the premise that with less rainfall and high dust storm frequency, aboveground biomass is less than in years with high rainfall.

4.3.2 Time series forecasting

Time series forecasting analysis was done with SAS. Forecast modeling was executed by denoting growing season-rainfall, MAP, MAT, dust storms, dusts, as well as plant biomass as a time-dependent variable. Those variables were statistically significant in the previous linear and multiple regression models in relation to plant biomass. Linear and exponential smoothing (Table 4.4) yielded an increasing trend for dust storms and MAT, a decreasing trend for plant biomass, but no trend for rainfall, MAP and dusts. Dust storms show smoothed trends with 0.4 DSF, whereas trends were linear with MAT 0.05 ^{o}C and with plant biomass – 2 kg ha^{-1}. In line with desertification concerns, an overall decreasing trend in biomass with an increase in dust storms and MAT was predicted. In terms of global warming, the increase in of MAT 0.05^{o}C will result in high temperatures in the future.

Table 4.4 Time series forecasting of climatic factors up to 2020 based on 1970-2000 time series data, Bulgan soum, Mongolia

Climate factor	Trend type[a]	Trend value[b]	r^2	p- value
Plant biomass	Linear trend	-2.02	0.12	0.05
Dust storms	Damped trend exponential smoothing	0.4	0.58	0.001
MAT	Linear trend	0.05	0.35	0.003
Dusts	No trend			
Rainfall	No trend		0.002	
MAP	No trend		0.002	
Pedi	No trend			
SPI	No trend			
Snow	No trend			

[a]– type of trend. Linear trend denotes linear increase or decrease, is more accurate than any other trend, [b] – value indicates annual trend

Linear trends were found for MAT and plant biomass, namely decreasing plant biomass, and increasing MAT (Figure 4.11.a.b.). Long-term dust storm frequency data show some oscillation, thereby resulting in a damped trend of exponential smoothing. It suggests that the dust storm frequency per year may increase slightly in the future (Figure 4.11.c).

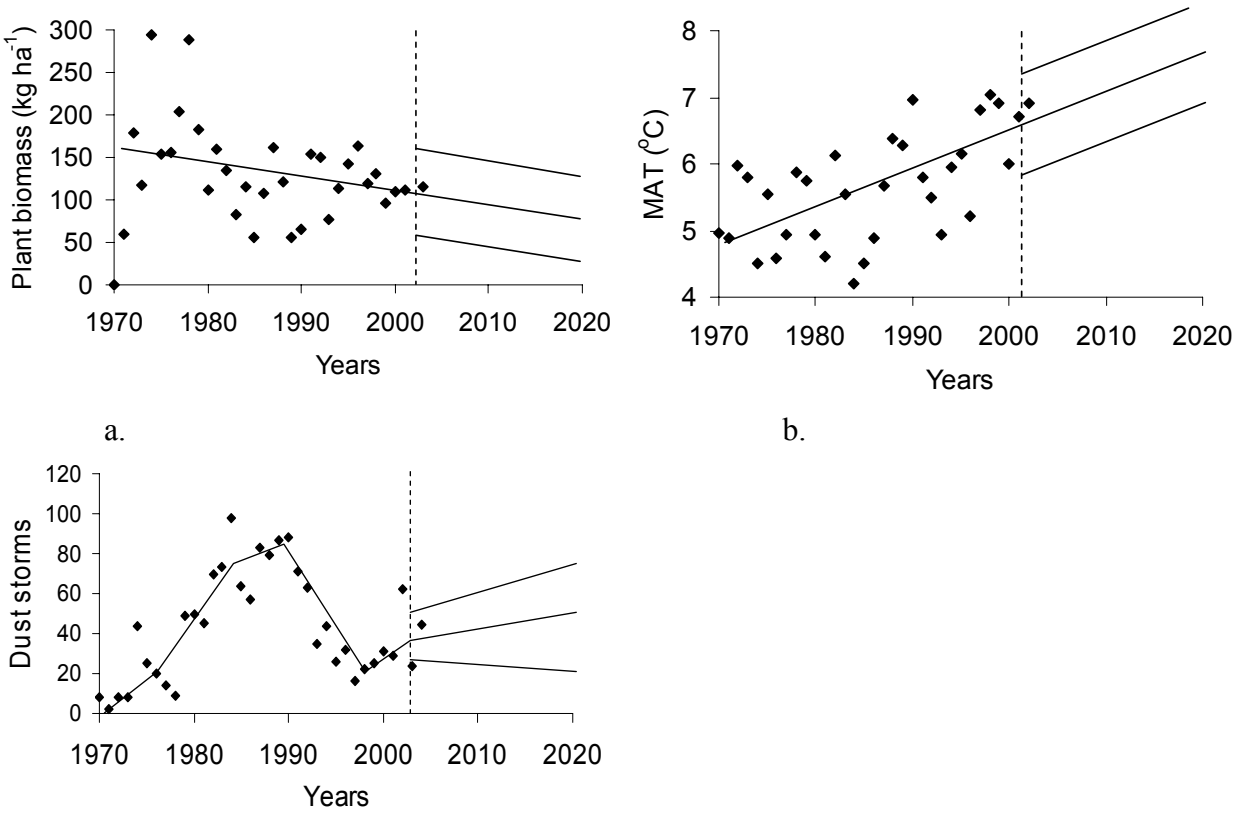

Figure 4.11 Time series forecasting from 1970 to 2020: a) Aboveground plant biomass (kg ha^{-1}); b) mean annual temperature – MAT (°C); c) dust storm frequency per year (DSF). Bulgan soum, Mongolia

Since no trend was found for most of the factors (dusts, rainfall, MAP, Pedi, SPI), a multiple regression was computed again on the variables that showed trends:

*Plant biomass = 240 – 11.3*MAT – 0.99* dust storms,* r^2= 0.27, p-value = 0.01

The values of dust storm forecasting of 0.4 DSF increase, 2.02 kg ha^{-1} decrease of plant biomass per each and 0.05 ^{0}C of MAT were used (Table 4.5). The prediction up to 2020 revealed that under the increasing dust storms and MAT conditions, plant biomass will decline up to 21% or 28 kg ha^{-1} (Table 4.5). An increase in dust storm frequency of 17% more is predicted till 2020. Mean annual dust storm frequency for 1970-2002 was 43, MAT was 5.5 ^{0}C, and aboveground plant biomass 130 kg ha^{-1}. Here the plant biomass data denote the long-term data obtained from the

monitoring site by the Mongolian-Russian expedition, therefore resulted in almost twice as much as amount than the present situation.

Table 4.5 Predicted dust storms, mean annual temperature-MAT (^{o}C) and plant biomass (kg ha$^{-1)}$ till 2020 derived from time series forecasting and multiple regression. Bulgan soum, Mongolia

Year	Dust storms (DSF)	MAT (^{o}C)	Plant biomass (kg ha$^{-1)}$
2006	44.6	5.7	122.7
2007	45	5.75	120.6
2008	45.4	5.8	118.6
2009	45.8	5.85	116.6
2010	46.2	5.9	114.6
2011	46.6	5.95	112.6
2012	47	6	110.6
2013	47.4	6.05	108.5
2014	47.8	6.1	106.5
2015	48.2	6.15	104.5
2016	48.6	6.20	102.5
2017	49	6.25	100.5
2018	49.4	6.30	98.5
2019	49.8	6.35	96.4
2020	50.2	6.4	94.4
Change by value	7.2	0.9	-28.2
Change by %	17	16	21

Probability of time series forecasting for dust storms using Eq 4.4 is:

$$Dust\ storms = \frac{50.2 - 43}{28} = 0.9$$

Where mean = 43, SD=28, y =50.2 (Table 4.4, till 2020*)*. The table of normal curve areas entry corresponding to z = 0.9 is 31%. It means the probability of dust storm increase lying in the DSF from 43 to 50.5 is 31%. MAT was calculated as:

$$MAT = \frac{6.4 - 5.5}{0.8} = 1.1$$

Where mean = 5.5, SD=0.8, y =6.05 (Table 4.4, till 2020). The table of normal curve areas entry corresponding to z = 1.1 is 37%. It means the probability of MAT increase lying in the temperature from 5.5 ^{o}C to 6.4 ^{o}C is 37%.

Probability of plant biomass decrease (Eq.4.4) is z = 0.71 or 26%.

4.4 Discussion

Rainfall is highly variable between years in the Bulgan soum. The climate is best described as non-equilibrium dynamic, with a CV of mean annual precipitation of 39% (Figure 4.2). MAP is low (117 mm) with high variability supporting the notion of Conrad (1941) that the lower the rainfall, the higher the variability of rainfall. Those manifestations confirm the temporally erratic character of rainfall. The MAP for 1987-2002 increased by 10 mm compared to the period 1970-1986 (Figure 4.3). The maximum growing season rainfall used to occur only in July for 1970-1986, however the maxima shifted to both July and August (an increase of 7 mm) in 1987-2002. Meanwhile snowfall during the winter months showed a slight increase for 1987-2002. The MAT was 1.8^{o}C higher in the 1990s than the long-term average, and showed warming of approximately 0.7°C over the last 30 years.

Drought frequency is one of the indicators of desertification. A comparison between SPI and Pedi index showed a high frequency of droughts (Figure 4.6). SPI indicated severe droughts six times over the studied 32 years. The Pedi index indicated drought 11 times. Both drought indices were related significantly to aboveground biomass production. The findings demonstrate frequent severe droughts but no long-term shifts in the magnitude of precipitation. Droughts occur once every two or three years (with 50% probability). This is twice as high as the drought frequency in African South Turkana, which once every five years (Coppock, 1993). Droughts in combination with cold harsh winters trigger livestock mortality that may catastrophically affect local populations in Southern Mongolia (Begzsuren, 2004; Squires, 2001).

Aboveground biomass was correlated with growing season rain, MAP, dusts, dust storms, MAT, SPI and Pedi indices over the period 1970–2002 (Figure 4.10). The slope of the regression analysis for dust storms, rainfall and MAP was similar. Plant growth is positively related to the growing season rainfall. Dust storms and drought occurrences are negatively related to plant biomass. The stepwise multiple regression analysis shows (Table 4.3) that the most controlling factor of plant growth is dust storms, but other climatic factors also control plant growth.

In terms of dust occurrences, dusts disappeared after 1993, but dust storms significantly increased 1987-2002 (Figure 4.8). Maximum dust storm frequency (60 in

1984 to 98 in 2002) was even higher than in the Sahel. The trend analysis shows increasing dust storm frequency with decreasing biomass (Table 4.5 and Figure 4.11). The time series forecasting till 2020 resulted in a 21% decrease in plant biomass (with 26% probability) accompanied by an annual increase of 0.4 dust storm frequencies per year (with 31% probability) and a 0.05 ^{0}C increase in mean annual temperature (with 37% probability). Therefore, the causes of desertification in Southern Mongolia, as elsewhere around the globe, are mainly caused by climatic factors, namely increasing dust storms and MAT. As far as global warming is concerned, increasing MAT will by accompanied by increased evapotranspitation, reducing soil moisture (Nicholson et al., 1998) and vegetation cover (Tucker et al. 1991) and further reducing rainfall amounts (Kelly and Hulme, 1993). This enhances the potential for dust mobilization and cause a decline of plant biomass, which will impact livestock pastoralism and the herding households dependent on nature. No increasing rainfall trend, however, was obtained. Even during short growing season (it corresponds to the short rainy season that spans June to September) the occurrence of sand storms indicates sparse vegetation cover, and loose and dry top soils.

5 VEGETATION AND SOIL DEGRADATION

5.1 Introduction

Aboveground plant biomass and soil texture are key factors in land degradation and soil compaction (Thiam, 2002). Soil compaction typically induces root thinning, increased bulk density of soil, runoff potentials, and decreases air-filled porosity, plant growth, hydraulic conductivity and soil infiltration rate (Engels, 2001; Froehlich and McNabb, 1984; Goldsmith et al., 2001). In turn, the soil is exposed to increased potential for erosion and changes in landscape hydrology, runoff and erosion loss of soil, eventually leading to degradation (Harr et al., 1979).

Soil compaction is related to the relative proportion and specific gravity of solid organic and inorganic particles, to the porosity of the soil and soil texture and overgrazing (Daddow and Warrington, 1983). Loams, clay loams and silt loam soils are generally more resistant to aggregate breakdown, and thus are more resistant to wind erosion. Clay-textured soils have less pore space than sandy-textured soils, while fine-textured soils may hold more water than coarse-textured soils, but compaction is more destructive to the water holding capacity of fine-textured soil. This restricts root growth and seedling establishment, and is responsible for shallow root growth. Heavy soils are less susceptible to gully and sheet erosion (Goldsmith et al., 2001).

Overgrazing leads to soil compaction, lower vegetation cover and biomass, loss of plant species and removal of roots (Oba et al., 2001). Coarse-textured soil bulk densities are less sensitive to grazing intensity, in contrast to fine-textured soils (with a significant clay fraction), which are more susceptible (Van Haveren, 1983). However, the ability of livestock to alter soil bulk densities is not the sole adverse effect of high stocking density. The removal of vegetation is the main cause of soil degradation, as vegetation protects soil from wind erosion by reducing the wind speed at the soil surface (Engels, 2001). In addition, the point at which bulk density hinders plant performance depends on soil types and plant species (Van Haveren, 1983).

A major objective of this study was to analyze the relationship between aboveground biomass, soil types, and soil bulk density as a result of degradation. The hypotheses are:

5.1. B*ulk density of soil has changed due to land degradation*.

5.2. P*rimary production is higher on coarse-texture soils than on fine texture soils (*Noy-Meir, 1973).

Sandy soils are more vulnerable to desertification (shifting sand dunes, and sand dune reactivation) independent of climate. Shifting sand dunes are spreading into the grasslands in the study area. This study will test inverse soil texture hypothesis (Hypothesis 5.2), as the region is highly subjected to low and variable rainfall, overgrazing and increasing desertification threat.

5.2 Methods

5.2.1 Plant samples

Based on the vegetation index change detection map, plant and soil samples were collected from the study area (40 km x 40 km). Plant and soil samples were taken from spots with no intact, slightly, moderately, and highly degraded and having similar elevations but different soil types. Before conducting the field work, 10 sample spots of each degradation category were selected representing different soil types using digital elevation model (DEM) and NDVI Landsat images. The location of sampled plots were matched by GPS with the selected spots and transferred to GIS (Figure 5.1).

After the field work, the sample information was entered into GIS, and overlaid with the MSAVI index and change maps (Section 3.3.1). All sample sites were classified based on the MSAVI change detection maps for 1973, 1990, 1991, 2002, and 2005, on which further analyses were conducted.

In the field, aboveground plant biomass was determined by clipping 1 m^2 (1 m x 1 m) plots located in a stratified random manner within 40 m x 120 m plots (Newbould, 1967). On each plot, plant cover was estimated, and 3 quadrates were clipped to ground level. At the time of clipping in the field, live species, aboveground dead material, and litter material were separated. Litter was collected by hand from the harvested plots. After being dried to a constant mass at 45^{o}C, aboveground plant biomass (g m^{-2}), and standing dead parts (g m^{-2}) were estimated. For each sampling plot, the geographic coordinates using GPS and climate data for the nearest weather station were obtained.

Plant cover was measured by laying out a 1 m x 1 m quadrant with 10-cm sub-squares on a low herbaceous cover of every 10 m area in the 40 m x 120 m plot. The cross points of the string grid were used to determine whether or not the vertical projection of the point intercepted plant species, litter, bare ground, or rock (Cummings and Smith, 2001). Plant species were recorded as annuals, perennials and shrubs.

5.2.2 Soil samples

Soil samples were taken at depths of 0-10 cm, 10-20 cm and 20-30 cm. In each plant sampling plot, six samples were taken randomly. A total of 246 soil samples (6 samples from 41 sample sites) were each placed in a bag, and then brought to the Geo-ecology Institute in Mongolia. They were sub-sampled, and their textures determined by the Hydrometer method and particle size analysis. Soil parameters were subsequently regressed against vegetation (cover and soil-sand percentage) using SAS, where the p-value was significant at .05. Soil samples were classified as coarse, medium, fine-textured using the hydrometer method (Hart lab, 2001) for textural analysis and USDA textural triangle.

The Soil Bulk Density Data Set contains the bulk density of the soil based on dry weight at depth 0-10 cm. Samples were collected at 41 different locations within the 40 km x 40 km study area during the growing season of 2005. These were averages for replicate measurements of 25 samples; 2 samples taken at each of the 41 locations within the study area, and brought to the Geo-ecology Institute, Mongolia for analysis.

A cylindrical metal sampler was pressed or driven into the soil to the desired depth and removed to preserve a known soil volume. Samples were taken from 0-10 cm depth. The total sample (approximately 100-150 grams) was dried in an oven at 105 ^{o}C for 24 hours. The dried samples were then weighed and the bulk density was calculated.

Porosity is an indirect measure of soil pore space (IUPUI, 2001). The mineral grains in many soils are mainly quartz and feldspar, so 2.65 is an adequate average mineral specific gravity for the sand fraction (particle density) (IUPUI, 2001). Under field conditions, pore spaces are occupied at all times by air and water. Porosity, when expressed as a percent, is the same as percent pore space (IUPUI, 2001). In fact, there is a formula:

$$Porosity(\%) = \left(1 - \frac{BulkDensity}{ParticleDensity}\right) * 100 \quad (5.1)$$

Table 5.1 General relationship among texture, bulk density and porosity of soils. Source: generalized from USDA-NRCS soil quality test kit guide (1999)

Textural Class	Bulk Density (Mg m^{-3})	Porosity (%)
Sand	1.55	42
Sandy loam	1.40	48
Fine sandy loam	1.30	51
Loam	1.20	55
Silt loam	1.15	56
Clay loam	1.10	59
Clay	1.05	60
Aggregated clay	1.00	62

Soil particles have irregular shapes, and thus the spaces or pores between them vary irregularly in size, shape and direction. Sandy soils have large continuous pores, while clays have small pores that transmit water slowly. Clays, however, contain more pore space than sandy soils, because of the pores inside of the soil peds. To growing plants, pore sizes are of more importance than total pore space.

5.3 Results

5.3.1 Identification of sample sites

Sample sites were pre-selected based on the LANDSAT image maps of August 1991 and 2002 after change detection. The map illustrated four degradation classes namely intact, slightly, moderately and severely degraded. A total of 41 sample plots were chosen. During the field work, some sample plots were altered slightly due to difficult access. The locations of the sample plots were noted down and later corrected in the GIS database. In total, 41 sample plots were visited during the field work in 2005 (Figure 5.1).

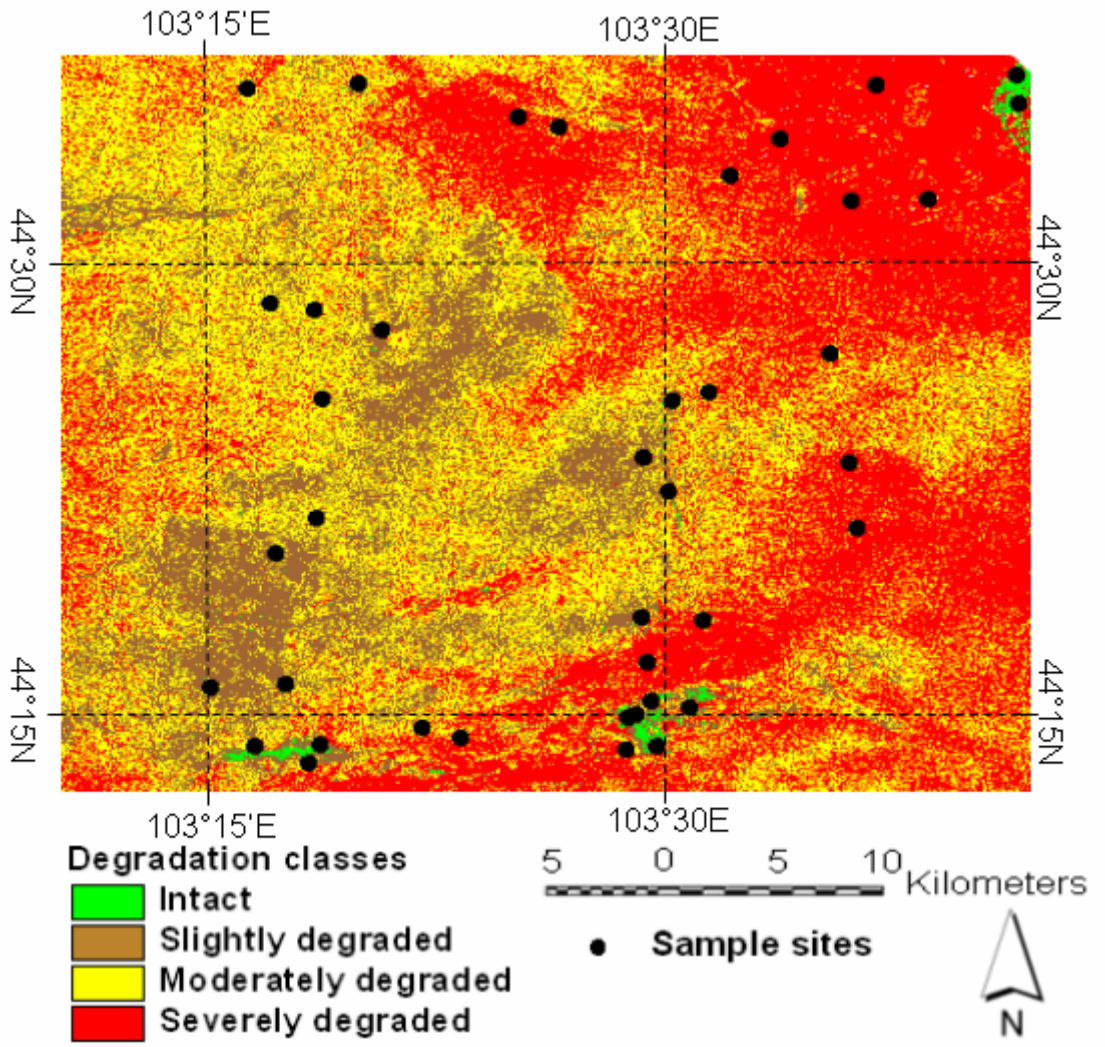

Figure 5.1 Sample sites and degradation classes within 40 km x 40 km area. Bulgan soum, Mongolia, 2005 (Figure 2.1)

5.3.2 Aboveground plant biomass and cover, soil bulk density and porosity

Aboveground biomass ranged from 14.6 g m^{-2} to 49.5 g m^{-2}, while aboveground plant cover ranged between 4% and 29% (Table 5.2). Slight variations occurred in plant cover and biomass among soil types of the coarse-textured soils. On average, mean biomass for the moderately coarse soils was 34.4 g m^{-2} (29 g m^{-2} standard deviation), and 33.1 g m^{-2} (18.9 g m^{-2} standard deviation) for moderately fine-textured soils. Aboveground biomass for moderately coarse-sandy loam soils was significantly higher than that of moderately fine- silt clay-loam soil. Aboveground biomass for medium loam soil was 28.1 g m^{-2} while cover was 3%. However, it was very close to the aboveground biomass of 20.5 g m^{-2} for loamy sand sandy soils. Plant cover, however, was almost identical, namely 11.7 % for coarse and 12.6 % for moderately coarse-textures soils and 13% for

fine-textured soils. Species number for differing soil groups was high for moderately coarse-textured soil, with a maximum of 20 species. In average, 8.5 species occurred on medium-textures, while 3 species occurred on moderately fine-textured soils and 8 species on coarse-textured soil.

Table 5.2 Aboveground plant biomass, cover, and species number in relation to soil texture from 41 sample spots within 40 km x 40 km area, Bulgan soum, Mongolia, 2005

Soil texture	Soil texture class	Biomass, g m^{-2}	Species number	Cover, %	Dominant species
Coarse	Loamy sand, sand	20.5 ± 12	7.7 ± 6.3	11.7 ± 13	Tree, shrubs
Moderately-coarse	Sandy loam	34.4 ± 29	7.8 ± 12.4	12.6 ± 14	Shrubs, perennials
Medium	Loam	28.1 ± 15	8.5 ± 1.5	6 ± 2.5	Shrubs
Moderately-fine	Silt clay loam	33.1 ± 18.9	3 ± 1	13 ± 15	Shrubs, perennials

The regression analysis between soil sand percentage to aboveground plant biomass, species number, and plant cover were not significant. Thereby, the results do not support the inverse soil texture Hypothesis 5.2, which indicates that other factors in this region are affecting plant biomass.

Regression analysis (Figure 5.2) of aboveground biomass (a), plant cover (b) and number of species (c) against bulk density again show no statistically significant relationship. There was no relationship with plant biomass and plant cover. All insignificant relations might be due to the small sample spots. Therefore Hypothesis 5.1 (bulk density of soil has changed due to land degradation) was rejected.

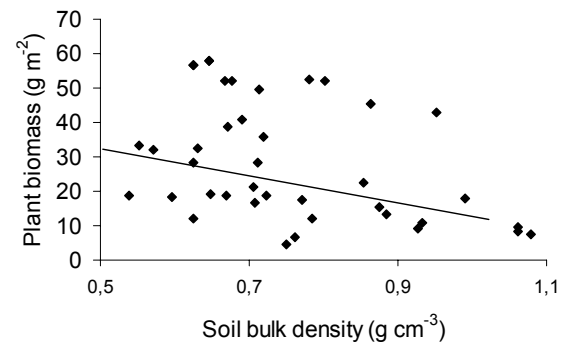

a.

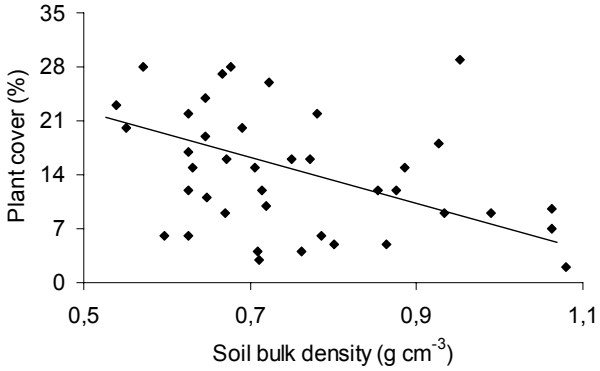

b.

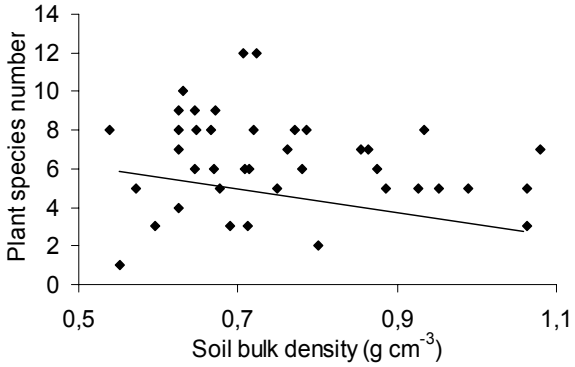

c.

Figure 5.2 a) Relationship between aboveground plant biomass (g m^{-2}) and soil bulk density (g cm^{-3}); b) relationship between aboveground plant cover (%) and soil bulk density (g cm^{-3}); c) relationship between number of plant species and soil bulk density (g cm^{-3}), Bulgan soum, Mongolia. 2005.

However, bulk density of soil fluctuated between 0.6 and 1.2 compared to 0.5-1.05 for non-degraded soils. Maximum bulk density of loamy sand–coarse-textured soils was 0.6 g cm^{-3}, which was lower than the normal bulk density rate (1.60 g cm^{-3}).

Sand percentage of soil in relation to soil bulk density was examined to determine possible relationships. A linear regression revealed a bulk density increase along increasing sand percentage. This rejects Hypothesis 5.1 that the bulk density of the soils in the Bulgan soum have not changed. The result of the regression is:

$$\textit{Bulk density} = 0.476 + 0.004 * \textit{sand \%}, \; r^2 = 0.24, \text{ p-value}=0.05$$

Soil porosity (used Eq. 5.1) fluctuated between 73 and 89%, with a mean of 79% for coarse, 76% for moderately coarse and 83% for moderately fine-textured soils.

High porosity means more pores for air and water and less compaction. The lowest porosity (73%) porosity was found in sandy loam followed by 64 % for loamy sand.

5.3.3 Plant species among the soil textural groups

The number of plant species ranged between 1 and 20. On the loamy-sand–coarse textured soils, one tree (*Haloxylon ammodendron)* and several shrubs *(Reaumuria soongorica, Salsola passerina, Anabasis brevifolia, Convolvulus fruticosa* and *ammanii, Nitraria sibirica)* had significantly high cover averaging 7%. Shrubs (*Artemisia gobica, Anabasis brevifolia, and Nitraria sibirica*) and perennials (*Achnatherum splendens*) dominated on moderately coarse-textured soils sandy loam averaging 9% (5%-11% cover), while medium-textured loam soils were dominated by shrubs (*Artemisia gobica* and *sphaeracoph, Nitraria sibirica,* and *Salsola passerina*). The fine-textured soil (Silt clay loam) was dominated by perennial bunch grass (*Stipa gobica*), and shrubs (*Oxytropisa acyphylla*), with a 2-5% cover. *Artemisia adamscii,* and *Carex duriuscula* (grazing tolerant sedge) contributed most to the vegetative cover close to households and water (Table 5.3).

Table 5.3 Plant species among soil textural groups, 40 km x 40 km area, Bulgan soum, Mongolia, 2005.

Soil texture	Soil type	Dominant plant species
Coarse	Loamy sand	Tree (*Haloxylon ammodendron),* shrubs *(Reaumuria soongorica, Salsola passerina, Anabasis brevifolia, Convolvulus fruticosa* and *Nitraria sibirica)*
Moderately coarse	Sandy loam	Shrubs (*Artemisia gobica, Anabasis brevifolia, and Nitraria sibirica*) and perennials (*Achnatherum splendens*)
Medium	Loam	Shrubs (*Artemisia gobica, Nitraria sibirica and Salsola passerina*).
Fine	Silt clay	Perennial bunch grass (*Stipa gobica*), and shrubs (*Oxytropisa acyphylla*), and grazing tolerant species *Carex duriuscula* and *Artemesia adamskii*

Overall, a high percentage of shrub cover was found on the majority of plots, and the number of plant species decreased with decreasing sand percentage; however, this was not statistically significant. A total of 48 species were distributed over the 41

sampling plots including 1 tree species, 21 shrub species, 22 perennial species and 3 annual species (Table 5.4).

Table 5.4 Plant species from 41 sampling plots, Bulgan soum, Mongolia, 2005

Tree	Shrubs	Perennials	Annuals
1. Haloxylon ammodendron	*2. Potaninia mongolica* *3. Reaumura soongorica* *4. Anabasis brevifolia* *5. Nitraria sibirica* *6. Convolvulus fruticosa* *7. Artemisia xerophytica* *8. Brachanthemum gobica* *9. Oxytropis aciphybla* *10. Ptilotrichum canescens* *11. Caragana norzinskii* *12. Cauligonium mongolica* *13. Zyogophyllum xantoxylon* *14. Z. rosovii* *15. Artemisia globosa* *16. A. adamscii* *17. Kalidium foliatum* *18. Artemisia gobica* *19. Astrathamnus centraliasiatica* *20. Ajania fruticulosa* *21. Eurata ceratoides* *22. Salsola passerina*	*23. Stipa gobica* *24. Cleistogenes soongorica* *25. Convolvulus ammanii* *26. Ferula bungeana* *27. Allium mongolicum* *28. A. polyrrhizum* *29. Scorzonera diruricata* *30. S. pseudodivaricata* *31. Carex stenophybloides* *32. C. duriuscula* *33. Astragalus monophyblus* *34. Iris bungei* *35. I. teninfalia* *36. Asparugus gobicus* *37. Dondestomon sinilis* *38. Lagochilis ilicifolius* *39. Psamchlaea villosa* *40. Phragmites communis* *41. Arnebia fembriata* *42. Peoganium nigellastrum* *43. Achnatherium solendens* *44. A. splendens* *45. Pheum nanum*	*46. Bassia dasyphybla* *47. Carispermum mongolicum* *48. Halogeton glomeratus*

5.3.4 Vegetation and soils in relation to degradation classes

The degradation classes map (Chapter 3) was overlaid with 41 sample plots, and the relationships to vegetation and soil features were examined. As the abundance of shrubs and annuals is not conducive to livestock consumption, it is an expression of

degradation. Therefore, the abundance of vegetation types partially indicates the stages of land degradation (Figure 5.3).

In terms of vegetation types, the tree species was found only in areas with good plant biomass or within the intact degradation classes. Shrubs were usually distributed commonly on intact, slight and moderately degraded classes. In contrast, severely degraded classes harbored twice as many perennials as shrubs. Overall, the findings indicate that shrubs are commonly found on all soil texture and degradation classes, while annual species indicate degradation processes.

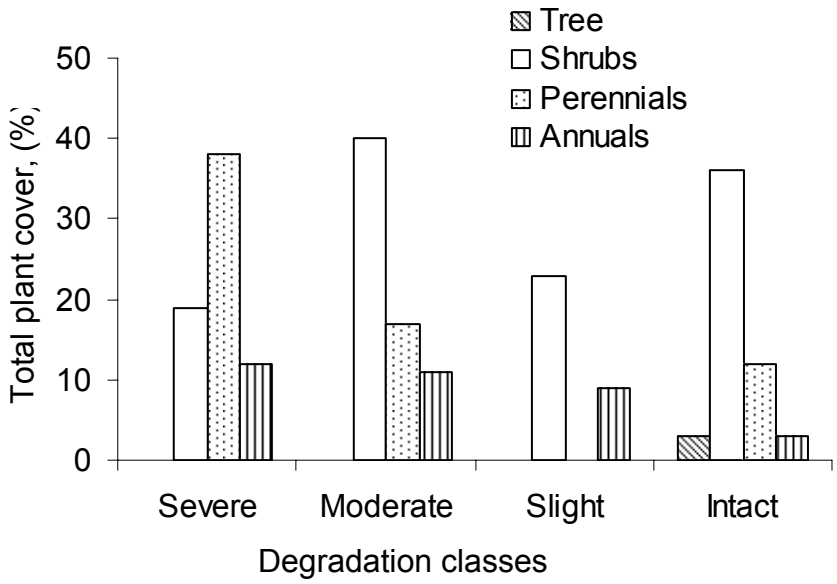

Figure 5.3 Total plant cover percentage of plant types for all the 41 sites in relation to degradation classes, Bulgan soum, Mongolia, 2005

5.4 Discussion

On average, mean aboveground plant biomass was 36 g m^{-2} at the Bulgan soum in June 2005. This falls within the sample plant biomass range of 30-200 g m^{-2} found by Noy-Meir (1973) for arid zones, and was much lower than the lower limit of 100 g m^{-2} yr^{-1} in semi-arid zones. The plant biomass was close to that of short grass steppe (97 g m^{-2}) in the Central Plains Experimental Range in Colorado, USA, where annual precipitation is 321 mm (Laurenroth and Sala, 1992). It was much lower than that in the *Leymus chinensis* steppe of neighbouring China (248.6 g $m^{-2)}$ with 313 mm precipitation (Xiao et al., 1996). The low plant biomass can be, however, an underestimate, as the field work was conducted in June, early in the growing season.

The inverse texture hypothesis (Noy-Meir 1973) "primary production is higher in coarse soil texture" was not supported by the field work data, which shows higher productivity in fine textured soils than in coarse textured-soils (Table 5.2).

Compaction can also result in a change in the proportion of pore sizes, which has an influence on four physical properties: bulk density, soil strength, pore size distribution and aeration (Daddow and Warrington, 1983). In the present study bulk density was mostly below the normal range, and ranged between 0.55 and 1.2. The findings do not support Hypothesis 5.1, as less aboveground biomass was observed along increasing bulk density.

Plant species types in relation to degradation classes showed a dominance of perennials over shrub species in severely degraded areas (Figure 5.3). For the other degradation classes, shrubs were found to be dominant. Even trees appeared on well vegetated intact landscapes. In general, in terms of species composition, shrubs were found on most of the sites, which is similar to the invasion of grasslands by shrubs in US grasslands when land degrades (Schlesinger et al., 1990). In present study, aboveground plant biomass decreased in the long term.

Aboveground plant biomass in fenced and non-fenced plots is commonly used for analyzing grazing effects and also changes in aboveground biomass in the long run and between years (Figure 5.4). This study on overgrazing states a 20% lower biomass in non-fenced than in fenced plots in the 1970s, however, this was almost 50% in 2002 (Gordeeva, 1978; Davaajamts, 1974; Sanjid, 2004). This also indicates that overgrazing leads to loss of vegetation, which in turn accelerates desertification.

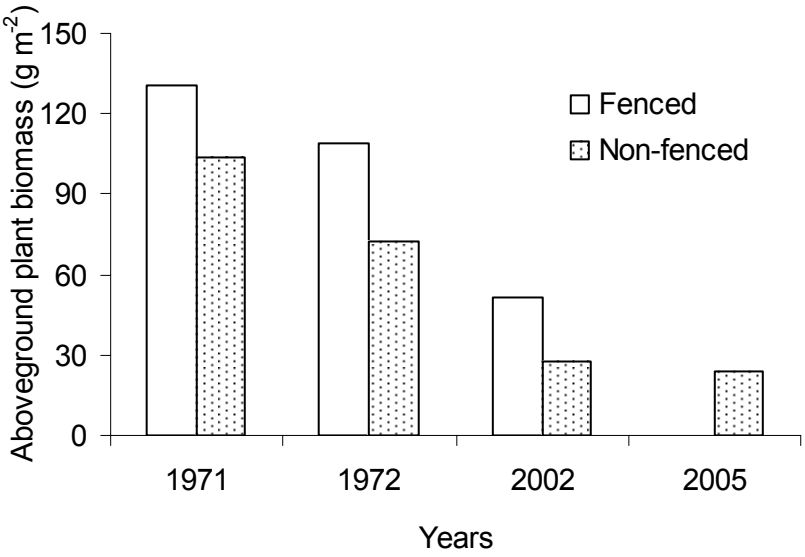

Figure 5.4 Aboveground plant biomass in plot with fence and without fence from 1 June to 21 July, for 1971, 1972 and 2002 and 2005, Bulgan soum, Mongolia (Gordeeva, 1978; Davaajamts, 1974; Sanjid, 2004)

In relation to the degradation classes obtained from LANDSAT image processing, overall species number decreased along the degradation gradient. Aboveground plant cover was less related to the degree of degradation.

6 HERDERS AND LAND DEGRADATION

6.1 Introduction

In general, desertification is conceived as the extension and intensification of desert conditions and involves a decline in resource quality and quantity (Johnson, 2004). Desertification, especially in developing countries, aggregates conditions of poverty, induces malnutrition and disease, and consumes the basis of the national economy. Desertification then leads to a decline in the socio-economy of the local population previously hindered by remoteness and lack of funds (FAO, 2006). Furthermore, desertification is the most threatening phenomenon that impacts the livelihoods of the poor (UNCCD, 2006a). A theoretical definition of degradation that eventually leads to desertification, however, suggests a tie between resource quality and the impact of resource degradation on rural households. Namely, this impact is on the small and poor herders' livelihoods and their standard of living. Furthermore, desertification is the result of the interaction between a harsh, unpredictable climate, the sensitive dry land environment, and the use of human labor in an effort to make a living (UNCCD, 2006a).

Mongolia has a long history of nomadic pastoralism. The country represents the largest remaining contiguous area of common pastureland in the world. Pasturelands make up approximately 82% of the land area and are currently home to 23.9 million head of livestock. Pastoral life and production still render the basis of existence for at least 30% of the population or 176,000 herding families accounting for 45% of employment (National report, 2002). In those rural areas, the economic sectors or wealth groups are expressed by the size of livestock holdings. Typically, wealthy herders have more available management options and higher economic returns through their livestock product marketing, and are limited in their vulnerability to any livestock loss (Agrawal, 1993). Access to resources is differentiated. Typically, richer families have more access to inputs that can compensate for shorter growing periods and intensive use of land (Sneath, 2004).

Pastoral systems are labor intensive, with high risks and low returns from an economic perspective. In addition, nomadic pastoralism requires a maximum amount of flexibility and movement of livestock (Coughenour, 1991), yet, some families with few members cannot afford frequent movement, causing sedentarization and land

degradation. Herding households normally bear more children than urban households, and a high child birth rate may increase not only a household's needs but, more importantly, may be perceived as a way to increase a household's ability to accumulate wealth by providing pastoral labor (Cain, 1981). In conditions of degradation, large family size may be considered a coping strategy for multiple livelihood options and many children are seen as one way for households to cope with poverty (Cain, 1981). Water access is also important. In most cases, the good grazing in remote areas remains under-utilized for want of investment to provide an adequate water supply, transportation infrastructure, and access to markets (Mearns, 2004).

With the economic transition to privatization in Mongolia in 1990 and in the absence of alternative livelihood opportunities, many people turned to livestock production to support their families. Livestock privatization, giving state owned livestock to former herders, brought a sharp increase in livestock numbers without regard of land carrying capacity (PALD, 1997). Species composition of livestock, which was proportional during the socialist period, has changed in response to world cashmere prices. Goats particularly have increased as a share of total livestock from 20% in 1990 to 40% in 2005. Some people postulate, however, that the recent severe spring dust storms may have been aggravated by the larger number of goats present across the Gobi region (UNDP, 2004).

This chapter explores the relationship between land degradation and land use by herders. The results provide some insight into the socioeconomic causes of and responses to desertification. Plant biomass degradation is used as an indicator of land degradation. In addition, land degradation was measured using remotely sensed LANDSAT images for 1991, 2002 and 2005, and the MSAVI differences showed the degradation classes (Chapter 3). Socioeconomic questionnaire surveys were integrated with the remotely sensed data to determine the association between degradation and the socioeconomic conditions of the herders. Integration of this socioeconomic information on herders with remote sensing and GIS may allow the mapping of the social aspects of land degradation. Two Hypotheses were tested:

6.1. *Desertification is accelerated in the grazing areas of large, rich households, and occurs more slowly in the grazing areas of small and poor families*.

6.2. *The gap between rich and poor herding households has been widening over the period 2000-2005*.

6.2 Methods

6.2.1 Questionnaire

To establish the perception of herders concerning degradation, a questionnaire survey (Appendix 5) was carried out in the study area (40 km x 40 km). A total of 42 independent herding households were interviewed. The questionnaire was structured and open-ended and took 60-90 minutes to complete. Thirty-one items were built into the initial screening survey to investigate how herders react to degradation, how they change their behavior, etc. The questionnaire was prepared in four modules: 1) household profile (demography, livestock number, and properties); 2) livestock reproduction (reproduction per year; 3) movements (frequency, cause of less movement); and 4) environmental degradation (pasture use duration, grazing land, indicator and response to degradation, fuel wood collection). Demographic information (age, number of people per family), number of livestock holdings of five main livestock types (horses, camel, cattle, sheep and goats) and geographic location of each household were included.

The herding households were divided into three wealth categories: 1) “poor” up to 200 SSU; 2) “medium” from 200 to 500 SSU; and 3) “rich” over 500 SSU. SSU refers to standard stock units for five livestock species: (camel = 7 SSU, horse = 6 SSU, cattle = 5 SSU, sheep = 1 SSU, and goat = 0.9 SSU). This wealth structure is often utilized by the Government of Mongolia, and the National Office of Statistics.

The interview was analyzed based on four different degrees of desertification resulting from the remote sensing images and the three wealth categories. The Chi-square test was calculated by SAS 8.1. to determine whether there is a relationship between degradation and:

- wealth groups (based on livestock numbers – SSU)
- age of household head
- family size
- movement frequency

Significance is indicated when the p-value is lower than 0.05 for all analysis.

The Gini coefficient (a measure of inequality in a population) was used to measure the income inequality in herder's population for different years. The coefficient comes from the Lorenz curve, a cumulative frequency curve, comparing the distribution of a specific variable with the uniform distribution that represents equality (Figure 6.4). The Lorenz curve of livestock number is a cumulative frequency curve showing the distribution of a proportion of herder's population. If the distribution of household livestock number is equal, the plot will be shown as a straight diagonal (45^0). The greater the deviations of the Lorenz curve from this line, the greater the inequality (Mathworld, 2003). The Gini coefficient ranges from 0 to 1. 0 representing perfect equality and 1 representing total inequality.

6.2.2 Remote sensing and GIS processing

Once the satellite image with the change detection had been processed, the questionnaire survey was carried out. Afterwards the latitude and longitude coordinates of the households from the questionnaire survey were entered into GIS, and the points were overlaid onto a Digital Elevation Model (DEM) to determine the elevation of each point. The DEM was converted into aspects with Arc-View. The corresponding values of DEM, aspect and degradation classes were obtained in ARC view by extracting the grid values of each point.

To test Hypothesis 6.1, livestock density maps for present (2005) and before (2000) in relation to wealth groups were created in GIS. The density maps were subtracted to underline the change in livestock density, particularly the density of goats. On these resultant livestock density change images, the pixels at positions (plant biomass) corresponding to the ground sampling plots were extracted. Linear regression analysis was computed between aboveground biomass and livestock density, when p-value considered significant at 0.05. The subtracted density map was overlaid with MSAVI map of 2005 (Chapter 3) to determine if livestock or goat density induces reduced vegetation index or severe degradation. To depicts the actual biomass decrease under grazing, the produced map from the multiple regression (dependent on grazing density change and MSAVI) was compared with the biomass map from MSAVI calculated from formula 7.1 (Chapter 3.3).

6.3 Results

6.3.1 Herding households

Degradation classes were obtained from 1990, 2002, and 2005 LANDSAT MSAVI image maps. The more negative change (red in Figure 6.2) represents the more decreased MSAVI or degraded areas. The total number of herding households was 42 in 2005 (Figure 6.2). Most of the families resided in the south of the study area, more in the steppe zone. Winter shelters were located near the mountains or the north of the area. Most of the time, however, only a few families were found there due to unavailability of water. The locations of the families in regard to degradation differed: most of the families (18) were found in heavily degraded, 11 families in moderately degraded areas, and the remaining 12 families in intact and slightly degraded areas. The interview results are given in Appendix 4.

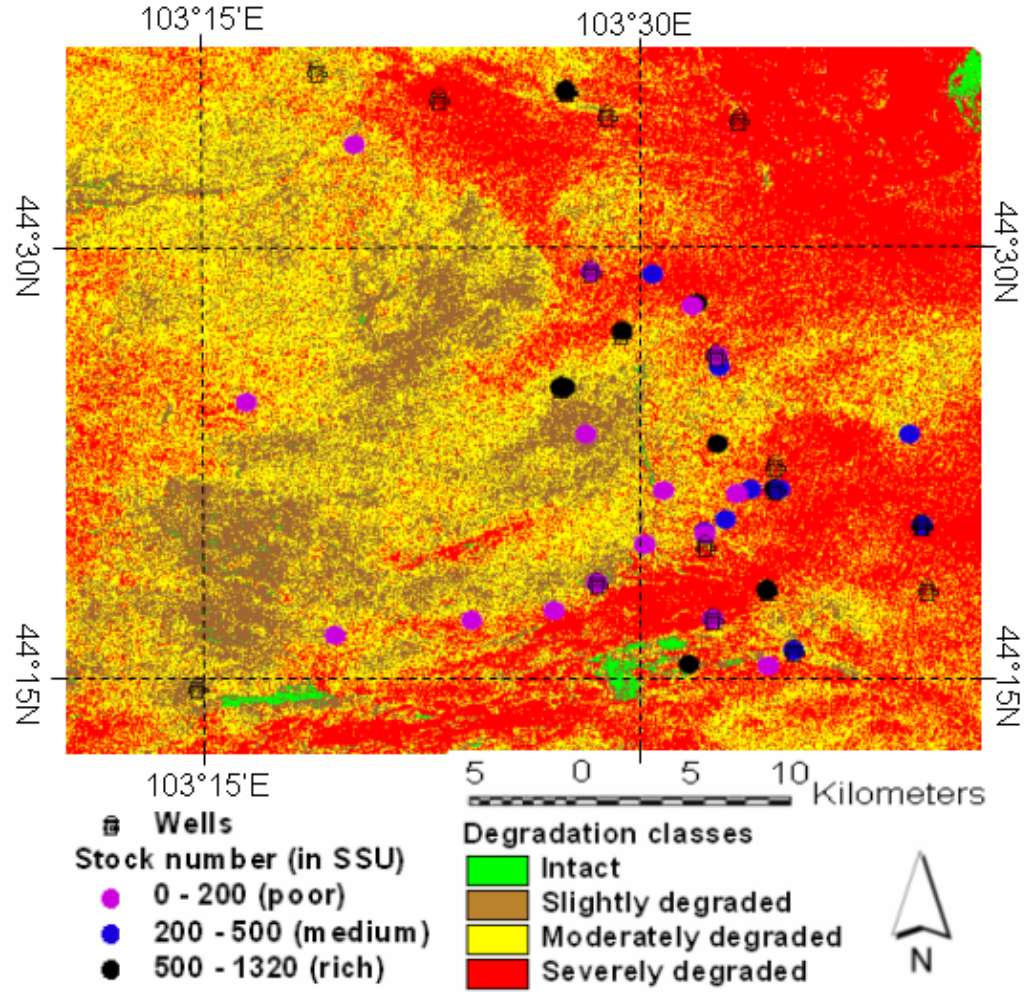

Figure 6.2 Location of households, livestock numbers, wells and degradation classes, Bulgan soum, Mongolia, 2005 (The location of the study area is shown in Figure 2.1)

6.3.2 Family size

Total family size was significantly correlated with degradation classes (Figure 6.3.b). Most families consisted of 2-3 children, father and mother. Grandparents, living in a different house but next to the son or daughter, were considered a separate family. The Chi-square test showed that families with 1-2 members tended to cause less degradation than those with 3-12 family members. This suggests that family labor availability is an important determinant of degradation.

Overall, the data suggest that there is a close association between family labor availability and degradation in the Gobi desert zones. In addition, the Chi-square test between wealth groups and family labor showed that the higher the number of family members, the more livestock. Therefore, family size is the main determinant of wealth, and triggers degradation due to the large stock numbers.

6.3.3 New-old herders and age

About 35% of herders were new, while and the remaining were traditional herders. In general, newcomers to herding were young, less skilled and experienced in livestock production, tended to move less frequently and remained closer to settlements, roads and other points of market access (UNDP, 2004).

Degradation appeared be lower in areas with younger herders (18-40 years old), whereas older herders (>40 years old) degradation was more severe (Figure 6.3.a). Age was also correlated with wealth differentiation. The older the age of the herders, the more livestock they had accumulated.

6.3.4 Livestock ownership and wealth classes

Livestock holdings are typically considered as status of wealth differentiation in rural area of Mongolia. Therefore, total livestock numbers for the Bulgan soum were analyzed to explore relative changes in the distribution of livestock holdings among households over the economic transition period. Here used the Gini coefficient, shown here in its graphical form, is a measure of inequality. If all households have exactly the same livestock holdings (i.e. the same share of total livestock), the Lorenz curve forms a straight line from the origin, representing perfect equality. The further away from this straight line is the actual Lozenz curve, the greater the degree of inequality. Hypothesis

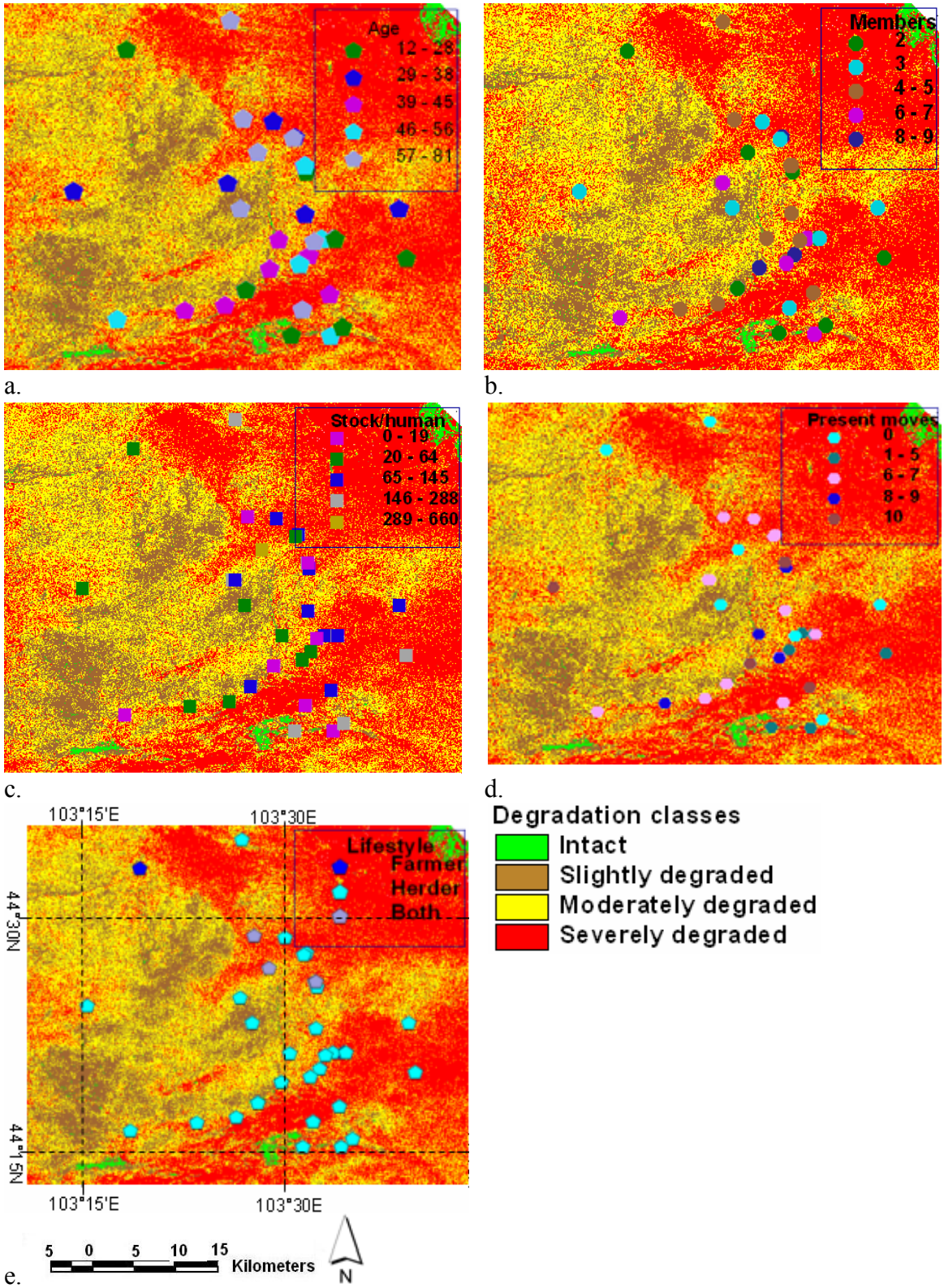

Figure 6.3 Figure 6.3 Socio-demographic information for household within the 40 km x 40 km study area. a) age of household head; b) family members per household; c). livestock (SSU) and human ratio; d) number of moves until 2005; e) lifestyle, either herder or farmer. Bulgan soum, Mongolia (The location of the families is shown in Figure 6.2)

6.2 assumed that the gap between rich and poor herding households had widened over the period 2000-2005 (Figure 6.4). Around 50% of herders in the Bulgan soum have 35% of the total livestock. The poor remained poor and the rich become richer in 2005 than they were five years before. The herding households of upper middle wealth status (upper bar in the distribution) had managed to increase their herds most rapidly in 2005.

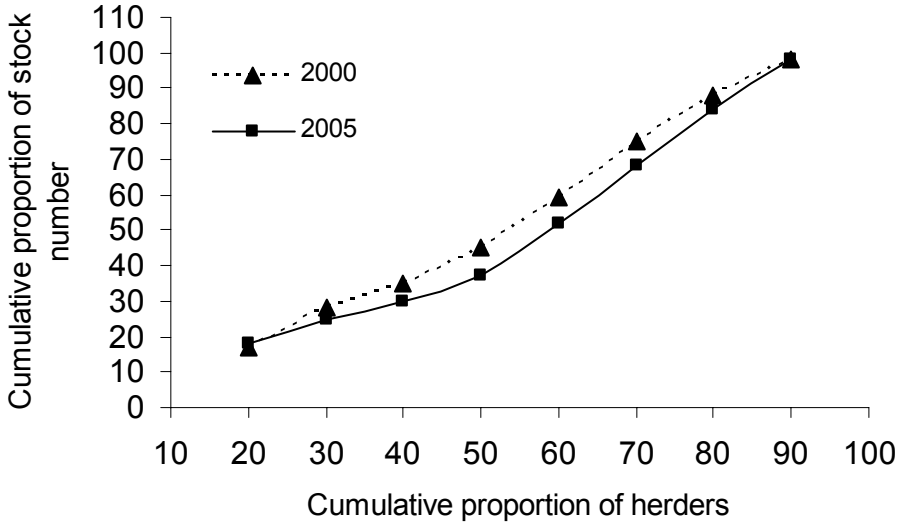

Figure 6.4 Inequality of wealth expressed by the number of livestock holdings at Bulgan soum, Mongolia, 2000 and 2005

Livestock and human ratio ranged between 1 and 660 SSU (Figure 6.3.c). In average of 73 SSU per person was found. Average livestock holdings for the 40 km x 40 km area were 5 camels, 6 cattle, 12 horses, 41 sheep and 142 goats in 2005. Nine families were rich (over 500 SSU), 22 were medium (200-500 SSU), and 11 families were poor. In other words, 37% families were poor, 43% medium, and 21% were rich. Wealth classes (poor, medium, rich) expressed by the number of stock were related degradation to classes (Chi-square test p-value=.05) (Table 6.2). Thereby, rich families with the largest number of stock were found to degrade lands in 2005, while medium and poor families were found on land with less degradation or to be causing less degradation. This can be explained by the decreasing number of moves (2 times less compared to 1990s), which has become the heaviest work in livestock production due to economic and social constraints. The movements of herding households are no longer based on the traditional nomadic pattern, but moves use of cars and expensive gasoline.

This creates problems even for rich households. However, camels and horses are still used by about 50% of the households.

The grazing radius of livestock varied for wealth groups. Rich families grazed animals within a range of 5 to 20 km, medium 7-8 km, and poor herding households 2-5 km. Grazing resources closest to the households or community group settlements were the first to be degraded and to become less productive. Independent of grazing radius and wealth groups, the areas closest to human settlements (1-3 km) were almost always heavily degraded. When creating a grazing radius in GIS, a 7-km radius per herding household was applied. This radius was selected because most of the families belonged to medium wealth classes, and livestock mostly grazed in most cases within a 3-7 km radius.

Livestock density in 2005 per km^2 was in general 6.5 goats, 15 SSU and 8.9 stock; the latter was 7.4 stock in 2000 (Figure 6.5). Stock density in SSU km^{-2} ranged between 1 and 37 in 2005, and the majority of the households had 10-35 SSU km^{-2}. Goat density per km^{-2} fluctuated between 2 and 16 (Figure 6.5.c), while stock numbers ranged between 1 and 30 in 2005 (Figure 6.5.a). Since the herders remembered the number of livestock for 2000, a change detection was carried out by subtracting a density map for the 2000 and 2005 in real stock numbers (Figure 6.5.a). Change detection analysis (Figure 6.5.d) shows that livestock density increased up to 14 stock per km^2. Only in a few areas, there was a decrease by 0.5 stock km^{-2}.

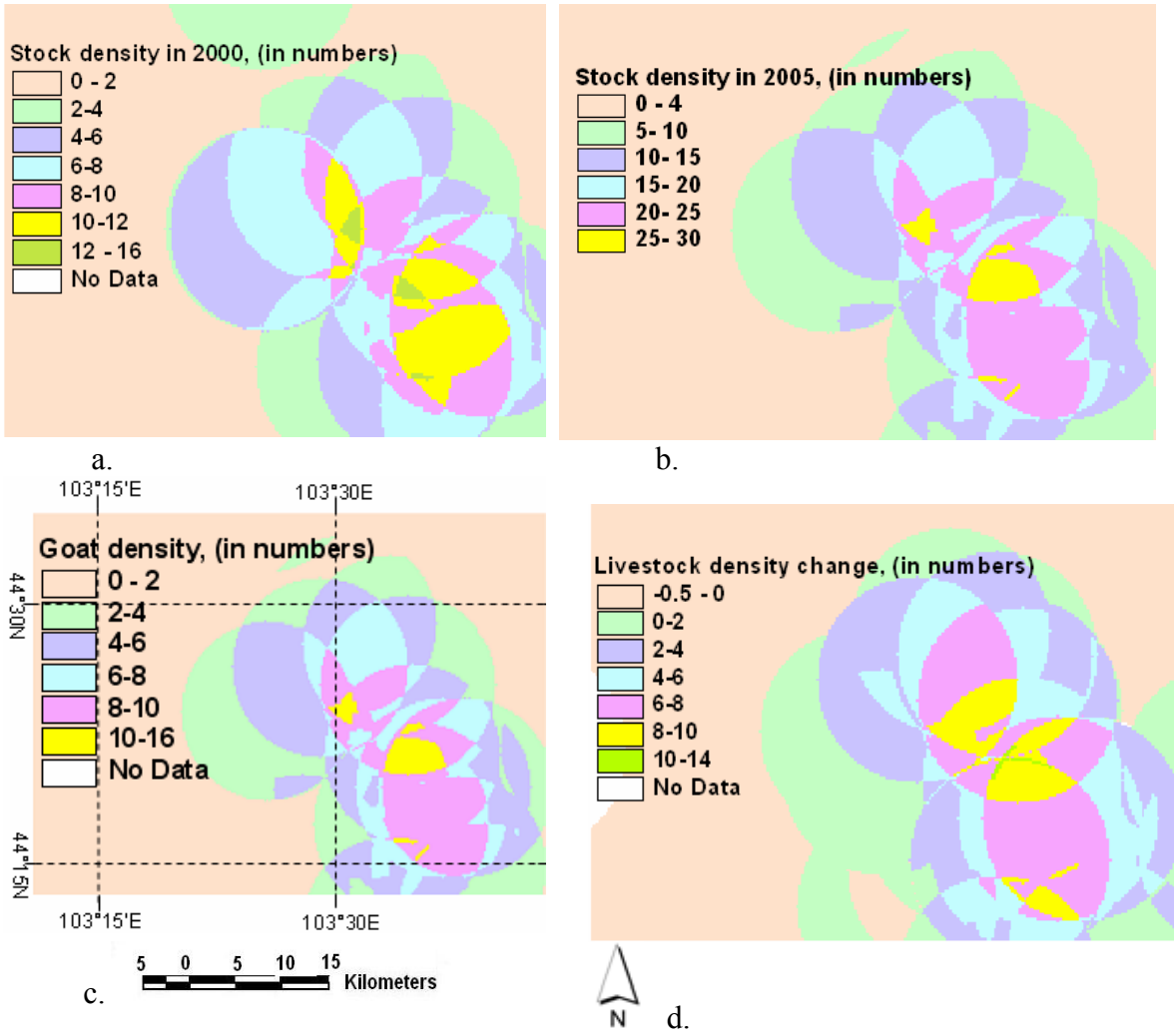

Figure 6.5 Livestock density in the 40 km x 40 km study area, based on questionnaire results in 2005: a) stock density in 2005; b) total stock density in 2000; c) goat density. d) stock density change maps (2000-2005). Bulgan soum, Mongolia (The location of families is shown in Figure 6.2)

The average livestock density changed from 11 SSU km^2 in 2000 to 15 in 2005 (Table 6.1). The maximum stock density increased from 26 SSU to 37 SSU km^2 within the 5-year period. The number of goats increased significantly since 2000, reaching at 9 goats km^{-2} in 2005. Total stock density and goat density change maps show an overall increase by 3 stock and 3 goats km^{-2} (average).

Table 6.1 Total livestock and goat density map, Bulgan soum, Mongolia. Livestock numbers are expressed in stock numbers

	Total stock density, stock km^{-2}			Goat density, goats km^{-2}		
	2000	2005	Change	2000	2005	Change
Mean	11	15	4	6	9	3
Max	26	37	11	8	16	8
SD	0.6	0.8	0.4	0.2	0.6	0.4

The result of areal percentage of livestock density change (Figure 6.5.d) is shown in Table 6.2. The largest percentage of area, 31% showed no livestock increase or no change. Minority of families reside in this area. The remaining 69% of area was subjected to increasing stock density changes, and the second largest 21% area supported 0-2 stock density changes, 17% for 2-4, and 13% for 4-6 stock density changes.

Table 6.2 Areal percentage of livestock density change for 2000-2005 (in real stock numbers), 40km x 40 km study area, Bulgan soum, Mongolia

Year	Areal percentage of livestock density change						
	-0.5-0	0-2	2-4	4-6	6-8	8-10	10-14
2000-2005	31	21	17	13	10	6	2

Afterwards, multiple and linear regression analysis was conducted on the corresponding plant biomass (MSAVI) of 2005, and livestock density change. The assumption was increasing livestock density (Table 6.1) leads to overexploitation of the land, leading to low plant production. Specifically, increasing stock density results in declines of vegetation biomass. The multiple regression analysis of plant biomass as a dependent variable with the MSAVI and livestock density was the following:

$$\textit{Plant biomass} = 98.6 - 1.5 * \textit{livestock density} - 156 * \textit{MSAVI}, \quad r^2 = 0.32, \text{ p value} = 0.05$$

To answer if plant biomass was reduced under overgrazing or increased, the comparison analysis between plant biomass under livestock pressure and actual plant biomass map obtained from Eq. 7.1 resulted in approximately 12% decrease in most of the cases, i.e., when grazing is applied, plant biomass decreases by 12%.

The locations of each family and the respective stock density were overlaid with MSAVI change detection map (Table 6.3). Average stock units, stock units by livestock type, and livestock to human ratios increased with increasing wealth groups.

Degradation classes were associated with wealth groups, the greater the livestock numbers, and the greater the degradation of the land. Elevation and aspects were not significantly correlated to degradation classes. The wealth groups of herders were based on the government poverty classification.

Table 6.3 Degradation classes related to ecological and social factors, Bulgan soum, Mongolia. Livestock numbers are expressed in SSU

Degradation classes	Wealth groups	Range of stock units	Mean stock unit	Mean age	Family size	Stock human ratio	Elevation (m.a.s.l.)	Aspect
Intact	poor	0-200	51	34	3.2	48.5	1700	south
Slight	poor	200-500	60	38	4.5	99.6	1800	south
Moderate	medium	200-500	210	42	5	112.4	2000	north
Severe	rich	>500	500	47	6.1	140	1900	north

6.3.5 Forecasting for livestock numbers

Time series forecasting analyses were carried out for the types of livestock to identify trends (Table 6.4) based on the total livestock number in the Bulgan soum, 1990-2000 obtained from Hydrometeorology Institute, Mongolia (Appendix 3). Livestock numbers and individual species are expected to increase, except camels. A particular steep trend can be seen for the goats (0.9), which is about nine times higher than for any other type of livestock species. Each year, 7000 additional livestock is expected, which poses a serious threat to the land carrying capacity for the coming years.

Table 6.4 Time series analysis for livestock types per year. Trend denotes SSU in thousands. Bugan soum, Mongolia

	Trend types[a]	Trend value[b]	r^2	p- value
Camels	Damped trend exponential smoothing	-0.04	0.29	0.05
Horses	Log linear trend	0.11	0.81	0.007
Cattle	Linear trend	0.14	0.57	0.03
Sheep	Log linear exponential smoothing	0.06	0.80	0.01
Goats	Damped trend exponential smoothing	0.9	0.84	0.04
Total stock (in SSU)	Linear trend	7.07	0.35	0.01

[a]– *type of trend. Linear trend denotes linear increasing or decreasing trend; more accurate than any other trend,* [b] *– value that can increase or decrease per year*

Linear trends were found for total stock numbers, cattle, and horses, a linear exponential smoothing trend for sheep, and a damped trend exponential smoothing for goats (Figure 6.6). The rare linear trend might be attributed to the scarcity of the data for only eight years; therefore a general trend was assumed for all stock types.

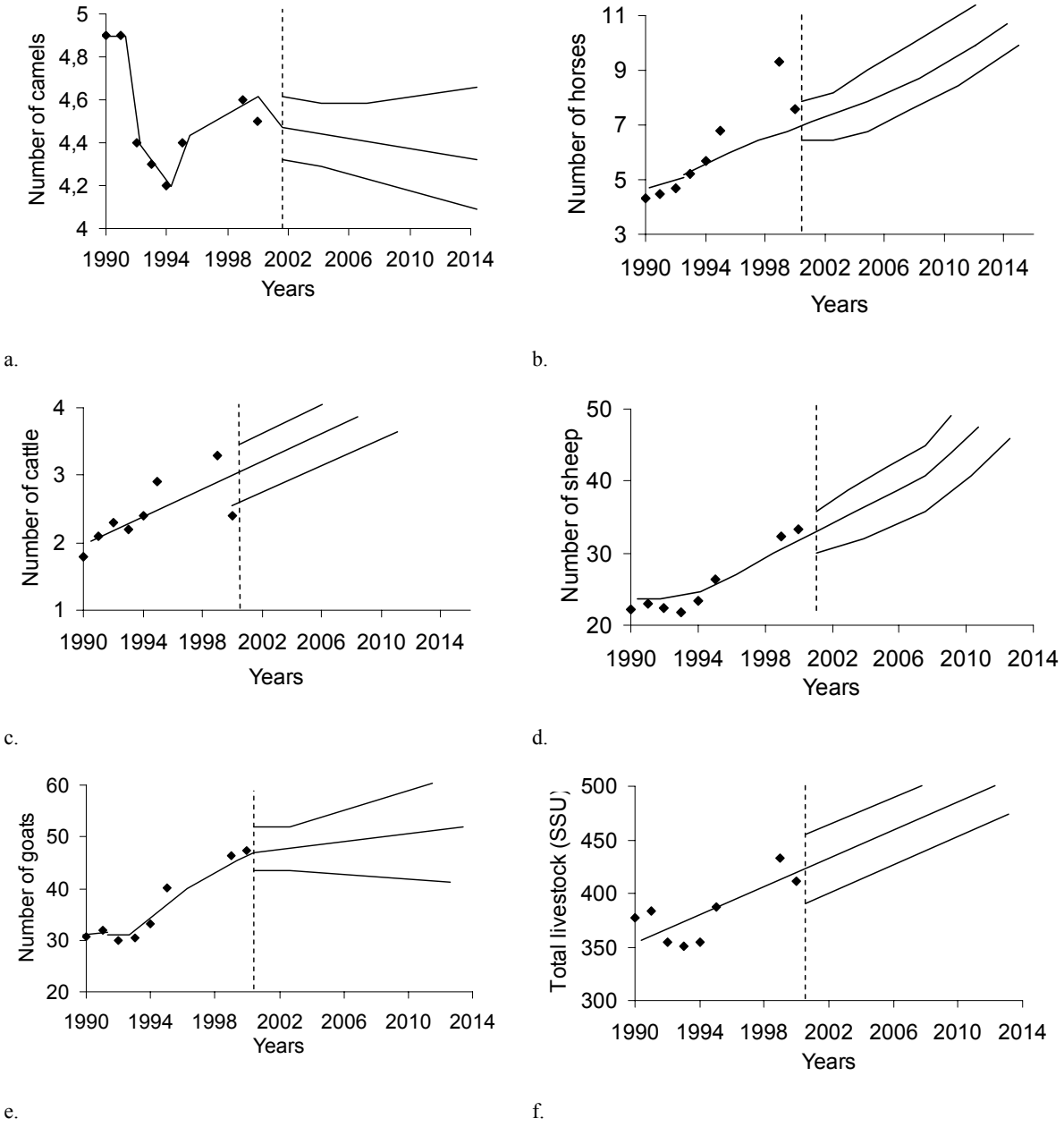

Figure 6.6 Time series forecasting. a) number of camels; b) number of horses; c) number of cattle; d) number of sheep; e) number of goats; f). total stock number in SSU at the Bulgan soum, Mongolia (Hydrometeorology Institute, Mongolia)

6.3.6 Wells

Water supply at the Bulgan soum is normally provided by groundwater wells. As mentioned earlier, all the aboveground water sources (rivers and lakes) have completely dried out. Many of the 14 wells in the study area were no longer operating. The wells were built during the socialist regime, the majority operated with motors requiring gasoline. When socialism collapsed, these expensive mechanic wells was no longer affordable, thus only hand operated wells remained.

Almost all wells were hand operating, except a few wells by animals. The only open water source, close to Arst Bogd mountain, was said to be used primarily by horses due to its sulphur content. Livestock dependency on a limited number of wells as sources of water was causing concentration of livestock on nearby pastures. One well supplies 11.4 km^2 or 540 SSU, which causes overgrazing around the wells.

6.4 Discussion

Most families resided in the mid elevated areas (1600-2000 m), where there are better water supplies, in the Ongi river basin, supporting higher plant biomass. The Bulgan soum is oriented east-west. Therefore, most of the aspects face north and south. The west aspect is characterized by high wind speeds as high as 25 m s^{-1}, and is not ideal for the location of winter shelters. In contrast, the north and south facing aspects are protected from the wind. However, Chi-square tests revealed no relation between aspect and location of households. As expected, over 50% of the households reside on the north and south facing aspects, covering 65% of the study area.

Age of the households had a significant relation to degradation classes and wealth groups. For the 18-40 year group, herders tended to be poorer (67.2%), while in the 40-55 and over 55 age groups, the number of richer families increased. A family tended to reach its economic peak (become rich) when the household head was between 42 and 56 years old. It might be attributed that privatization in 1992 transferred larger numbers of livestock to the older herders than to the younger herders, which was due to their working years for collectivization, thus creating wealth for old families. Another explanation might be that older herders might be more experienced than younger herders and were better in accruing wealth. Age also effect to the differences between new and existing herders, therefore, affect the herding household's level of wealth, and

skill and experience. In fact, those factors have strong influence on the mobility of herders and their animals as well as their choice or grazing area (UNEP, 2004).

The correlation between degradation classes and number of family members were positive. Among the 1-2 member families, only 2.3% were wealthy, whereas 25% of the families with 3-12 members were wealthy. Poor households generally have fewer animals, greater labor constraints, and are less able to respond to market opportunities than wealthier households (Agrawal, 1993). In addition, the number of family members is very important for pastoralists because of labor demands. Critical labor periods occur in spring and throughout the summer due to herding, watering, movement, and preparing and harvesting livestock products.

Hypothesis 6.1 was confirmed stating that the richer and larger herding families accelerate land degradation. Interacting factors namely large family size, older age of herders, and thus higher number of livestock and decreased number of seasonal moves are all leading to overgrazing and desertification. This increasingly applies to the majority of rich families. The most important reasons for the decline in mobility include transport and labor constraints, desire to have access to social services and market opportunities. Another reason is that herders have to guard winter pastures from seasonal trespassing by other herders (UNDP, 2004).

Hypothesis 6.2 was confirmed by Gini coefficients, the livestock owning equality in 2000 as the diagonal line was almost straight. However, 5 years later in 2005, income inequality had increased. The medium class households seemed to be able to increase their stock, more significantly than poorer households. The range of herd sizes is widening and with it is the gap between the incomes of the richest and poorest groups in the herding sector.

In the study area, the ratio of herd sizes between the highest and lowest wealth classes ranged from 4:1. Livestock density per km^{-2} ranged between 1-35 SSU per km^{-2} in 2005 with high a livestock pressure on the land. Livestock human ratio 73 SSU per person in the Bulgan soum is much higher than 2.25:1 in India, and 55 SSU per person - over half times higher than the Ngorongoro Conservation Area in Africa (Ellis and Galvin, 1994). Time trend forecasting analysis (Table 6.4) also suggests further increases in livestock numbers, 7000 SSU per year, particularly goats. Goats are by far the most detrimental animal with regard to land degradation as they consume the plants

with their roots. The high livestock growing rate is continuously expected due to the increased interest of increasing livestock of herders, economic inflation of the country, and livestock as the only source for herder's livelihood (Fernadez Gimenez and Allen-Diaz, 1999). If this trend persists it might bring significant degradation to the land, its productivity, and peoples' livelihood. Yet, some episodic livestock mortality due to droughts and severe winter snow will perhaps lessen the livestock increase (Begzsuren et al., 2004; Ellis and Galvin, 1994).

In the study area, around 90% of the population relies on nomadic pastoralism and thus depends on income generated by animal husbandry. People that live in this area have age-old strategies of nomadic herding. In the decades after the collapse of socialism, however, their strategies have become less practical due to changing economic and political circumstances and a trend toward more settled communities and less movement. The lack of economic power of Mongolia, one of the poor nations in the world, contributes in the vulnerability of the pastoral systems (Ojima, 2001). There is no legislation in Mongolia that limits the number of livestock that a herder can have on this land. Therefore, in many cases, unregulated access to land resources may lead to individuals maximizing their own gains by overexploiting the land at the expense of the community as a whole. Thus, urgent measures such as the introduction of best quality animals, rotational grazing, and maintenance of traditional knowledge are imperative. Land and grazing conservation practices need to be carefully defined and demonstrated, and the families need to be encouraged to adopt these practices.

7 DESERTIFICATION ASSESSMENT

7.1 Introduction

To monitor, control and reverse land degradation effectively, the severity of degradation and spatial distribution of degraded land have to be assessed through realistic indicators and indices derived from remote sensing (Liu et al., 2004). Many indicators have been proposed and successfully implemented using GIS and remote sensing methods. Desertification in West Asia has been estimated by examining the decrease in forage productivity and vegetation cover (i.e., using NDVI), by calculating a temperature index in China, and by comparing the results of multi-temporal remotely sensed images with NDVI coefficients of variation (CoV) in Saudi Arabia (Kharin et al., 1999; Jing, 2002). The temporal changes of vegetative cover, sand dunes and sand sheets were investigated in India and globally using both MSS and IRS data (Mishra et al., 1994; Tripathy, 1996). A new index called the Moving Standard Deviation Index (MSDI) has been proposed to study degradation by moving a standard deviation filter across the red band of satellite images to measure landscape heterogeneity (Tanser and Palmer, 1999).

Remote sensing in combination with linear mixture modeling, based on the computation of vegetation, soil, and parent material indicators, has been successfully implemented in mapping land degradation in semiarid environments, the Mediterranean regions of Europe, and the eastern Andes of Bolivia (Hill et al., 1995a; Metternicht, 1996). The combinations of satellite derived vegetation (NDVI) and soil indices (bare soil, brightness, redness, and topsoil grain size indices) linked to vegetation and soil properties have been used by several researchers (Ray et al., 2005; Rikimary and Miytake, 1997; Xiao et al., 2006). Ringrose et al. (1992) and Serrano (2004) used linear regression models based on land cover, human and livestock population, and rainfall statistics to identify the causes of range degradation and generate green vegetation cover from satellite VI measurements. Likewise, Purevdorj et al. (1998) estimated vegetation cover in Mongolia using second-order polynomial regression from AVHRR derived NDVI. Bayasgalan and Dash (2002) made desertification and carrying capacity of land assessments based on AVHRR derived NDVI, and the Pedi index, meanwhile Erdenetuya (2000) found an overall decrease in vegetation cover for the last two decades using long-term NDVI AVHRR data.

Land degradation of Bulgan soum has been particularly severe for the last two decades, for two reasons. First, low precipitation, marching sands, decreasing plant productivity and increasing dust and sand storms are exacerbating desertification. Second, overgrazing by ever increasing stock in this fragile ecosystem is widespread.

The main objective of this chapter is to devise a methodology for realistically assessing desertification and its trend by taking into account climatic factors. Linear and multiple regression models were developed to extrapolate information obtained from satellite images, field work, and long-term climatic data over the study site. The specific objectives of this study were:

1. To assess and depict the current status of land degradation using the vegetation index (MSAVI) and soil spectral index (GSI);
2. To highlight trends in land degradation hazard by taking into account long-term climatic attributes.

Four indicators have been determined as critical to the assessment of desertification severity in the study area, namely vegetation biomass, coarsening of topsoil, extent of drifting sand, and water body shrinkage. The indicators are the most direct indicators of land degradation and derivable from satellite imagery. They were combined to indicate degradation severity degrees: intact, slight, moderate and severe (Table 7.1). Here, drifting sand and water body shrinkage were classified as severe degradation class.

Table 7.1 Indicators and corresponding change values in the assessment of land degradation severity degrees

Indicator	Severity level		
	Slight	Moderate	Severe
Vegetation biomass change (%)	<15	15–35	35-100
Soil coarsening (%)	<15	15–35	35-100
Extent of drifting sand (%)			100
Water body shrinkage (%)			100

7.2 Methods

Four types of data were used, long term climatic and vegetation biomass data, field work in 2005 and indices derived from remote sensed images. From many vegetation indices, MSAVI was selected after verifying that it was in closest agreement with plant biomass data collected at 41 sites during field work in summer 2005. The GSI was selected as it corresponded well to the sand percentage of soil from those same sites (Chapter 3).

7.2.1 Sand movement change

Sand looks very bright on Landsat bands 2 and 3. Therefore, the values for those bands were added and divided by two, and a constant threshold value was used for images from the four years to depict sand.

Mechanisms of sand erosion, sand transportation and sedimentation were analyzed by Geerken and Hansman (2000). They used multitemporal Landsat TM images to give hints on the origin, extent, and intensity of degradation through sand accumulation, which enabled them to derive trends in sand movements. Sandy areas were displayed in yellow colors, and gypsum in cyan based on the band combination of 7,4,1 coded RGB (Geerken and Hansman, 2000). Based on this, comparisons between band combination 2 and 3 and band combinations of 7, 4, and 1 were made to distinguish sand encroachment.

7.2.2 Water body change

Longer wavelength visible and near infrared radiation is absorbed more by water than shorter visible wavelengths. Thus, water typically looks blue or blue-green due to stronger reflectance at these shorter wavelengths, and darker if viewed at red or near infrared wavelengths (CCRS, 2006). In addition, the water bodies from 1942 topographic maps were digitized to distinguish long-term water body change.

7.2.3 Integration of indicators

The following significant indicators selected from the previous chapters are combined to access desertification severity:

Natural factors: MSAVI - vegetation biomass, GSI – topsoil coarsening

Plant biomass was calculated from MSAVI images for differing years based on the linear regression result (Chapter 3) (Eq. 7.1).

$$Plant\ biomass = 90.3 + 213.7 * MSAVI \quad (7.1)$$

The result contained 4 possible combinations according to Eq. 7.2, and divided into classes from slight degradation to very severe degradation (Table 7.1). Each indicator was assigned an upper and lower threshold, corresponding to a severity rank (Figure 7.1).

To eliminate the minus values in MSAVI and make MSAVI values correspond to GSI values, the value of 1 was added to MSAVI. Afterwards, combinations of MSAVI and GSI were created for each year by simply combining those images in Erdas Imagine. Change detection by subtracting the combined images of MSAVI and GSI for each year was conducted. The resulting image was classified into degrees of degradation severity classes according to Table 7.1.

It was assumed that there was no interaction between indicators, and the products of each indicator layer were summed without the addition of weightings and divided by the number of combination factors as following (Eq.7.2):

$$Desertification\ assessment = \frac{plant\ biomass + topsoil\ coarsening + sand\% + water\ body\ change\%}{4} \quad (7.2)$$

Long-term time series forecasting analysis was calculated using SAS. Only dust storms, mean annual temperature, and aboveground plant biomass showed the trend (Chapter 4.3.2), therefore, they were used to predict the desertification trend up to 2020. Here, plant biomass was calculated with a multiple regression dependent on mean annual temperature and dust storms based on the time series forecasting model.

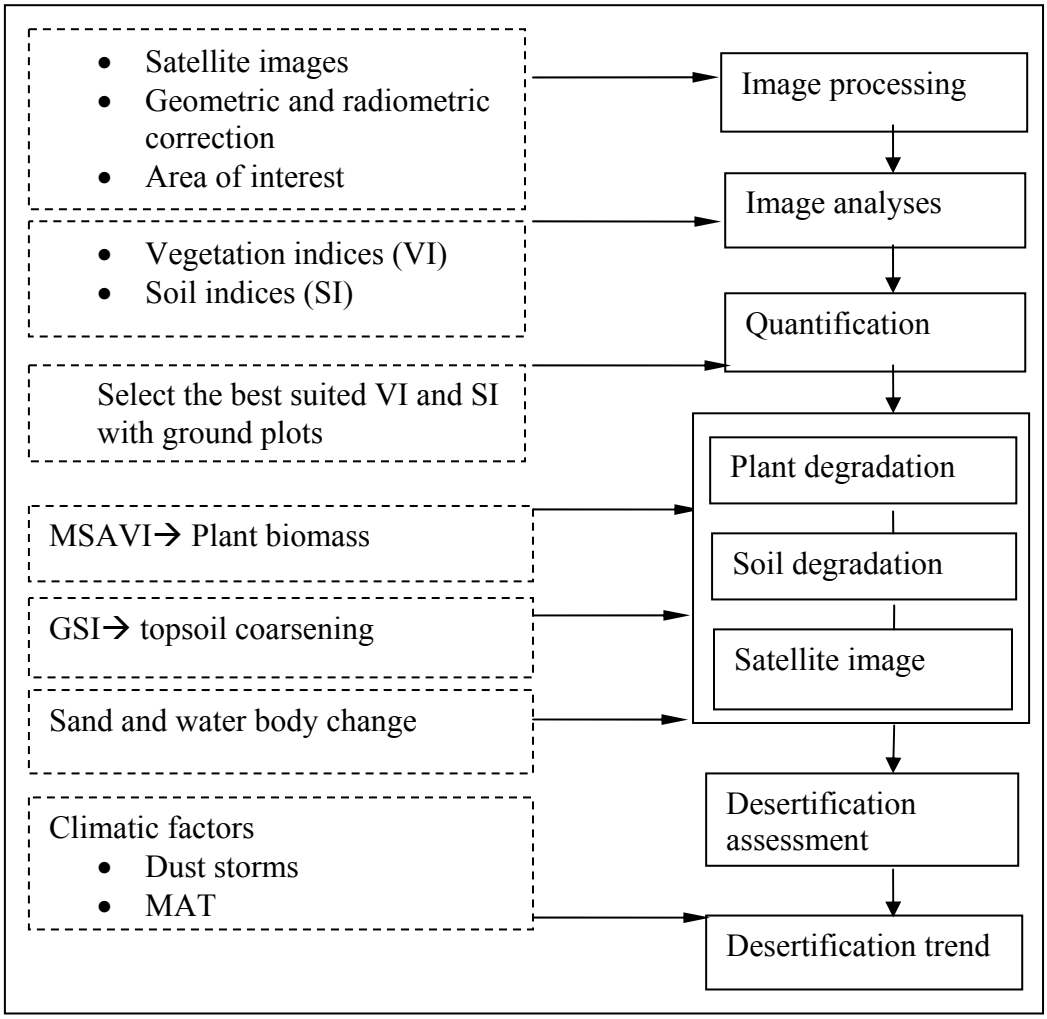

Figure 7.1 Satellite image pre-processing, desertification assessment and trend analysis methods used in this study

7.3 Results

7.3.1 Vegetation degradation

To map plant biomass, the linear regression equation Eq 7.1 was used across the Landsat MSAVI images from all years. The resultant vegetation biomass values for five different years are given in Table 7.2. As seen from the table, the maximum and mean values of vegetation biomass decreased through time. Comparing 1990 and 1991, the biomass of 1991 was slightly higher in terms of mean and maximum plant biomass. It is attributed to the fact that the 1990 image was acquired in September, corresponding to the end of growing season, whereas the 1991 image was acquired in July, the peak of growing season. The plant biomass estimates decreased along the time periods, and

average biomass estimates were almost half in 2005, what they were 15 years earlier. Standard deviation rapidly increased through the time period, from 13 kg ha^{-1} in 1990 to 38 kg ha^{-1} in 2005.

Table 7.2 Vegetation biomass (kg ha^{-1}) derived from MSAVI, Bulgan soum, Mongolia

	1973	1990	1991	2002	2005
Mean	112	92	100	60	58
Max	222	207	208	180	178
St. Dev	42	13	17	34	38

The results in Table 7.2 are summarized in Table 7.3. The highest vegetation biomass appears to represent non-degraded natural vegetation. Vegetation biomass for 1973-2005 has a wide range of values ranging from 1–222 kg ha^{-1}. The years 1973 and 1990 contain more vegetated areas compared to the later years. The years 2002 and 2005 include small portions of high-biomass vegetation, around 10% displays high vegetation. The rest of the areas are low vegetation, where the plant biomass ranges from 1-60 kg ha^{-1}. The 15-30 kg ha^{-1} plant biomass was virtually nonexistent in the images of 1973 and 1991. It looks as if the vegetation biomass was the highest in the south of the Bulgan soum in early years, but decreased in later years due to climatic and human factors. The largest areas for differing years were the following: 51% for 15-30 kg ha-1 in 2005, 48% for 15-30 kg ha^{-1} in 2002, 43% for 95-22 kg ha^{-1} in 1991, 36% for 60-75 ha^{-1} in 1990, and 43% for 75-90 kg ha^{-1} in 1973. Almost 90% of the areas supported 45 - 222 kg ha plant biomass for 1973-1990, while 90% supported 1-45kg ha plant biomass for 2000-2005.

As mentioned earlier, the highest plant biomass in 1990 and 1991 was attributed to those years had the highest rainfall in a 32 year period (1970-2002). In addition, the monthly rainfall pattern for those years show that both dates of 1990 and 1991 images were acquired after the highest rainfall (80 mm). In addition, early growing season of June 1991 resulted in higher plant biomass than the latest growing seasonal month of September 1990.

Table 7.3 Areal percentage of biomass classes, Bulgan soum, Mongolia

Plant biomass classes, kg ha^{-1}	Years				
	6/1973	9/1990	6/1991	7/2002	6/2005
0-15	0	0	0	15	12
15-30	0	0	0	48	51
30-45	0	10	0	22	22
45-60	15	26	5	9	5
60-75	21	36	9	9	4
75-90	43	10	22	7	6
90-95	3	7	21		
95-222	18	11	43		

7.3.2 Combination of vegetation and soil indices

The combination of vegetation index (MSAVI) and soil index (GSI) derived from satellite image indicates land degradation. Figure 7.2 depicts the results of the combination of those indices for each year. Figures 7.2.a and 7.2.b show non-degraded areas in green in most of the areas. Only a small portion is in light yellow and classed as slight degradation, constituting 45% in 1990 and 21% of the Bulgan soum in 1991. The slightly degraded area, in yellow in Figure 7.2.b. is a sand-covered area. Degradation intensified in 2002 and 2005, with almost the entire area showing moderate and severe degradation, illustrated in brown and dark brown. Intact areas are hardly found in those years.

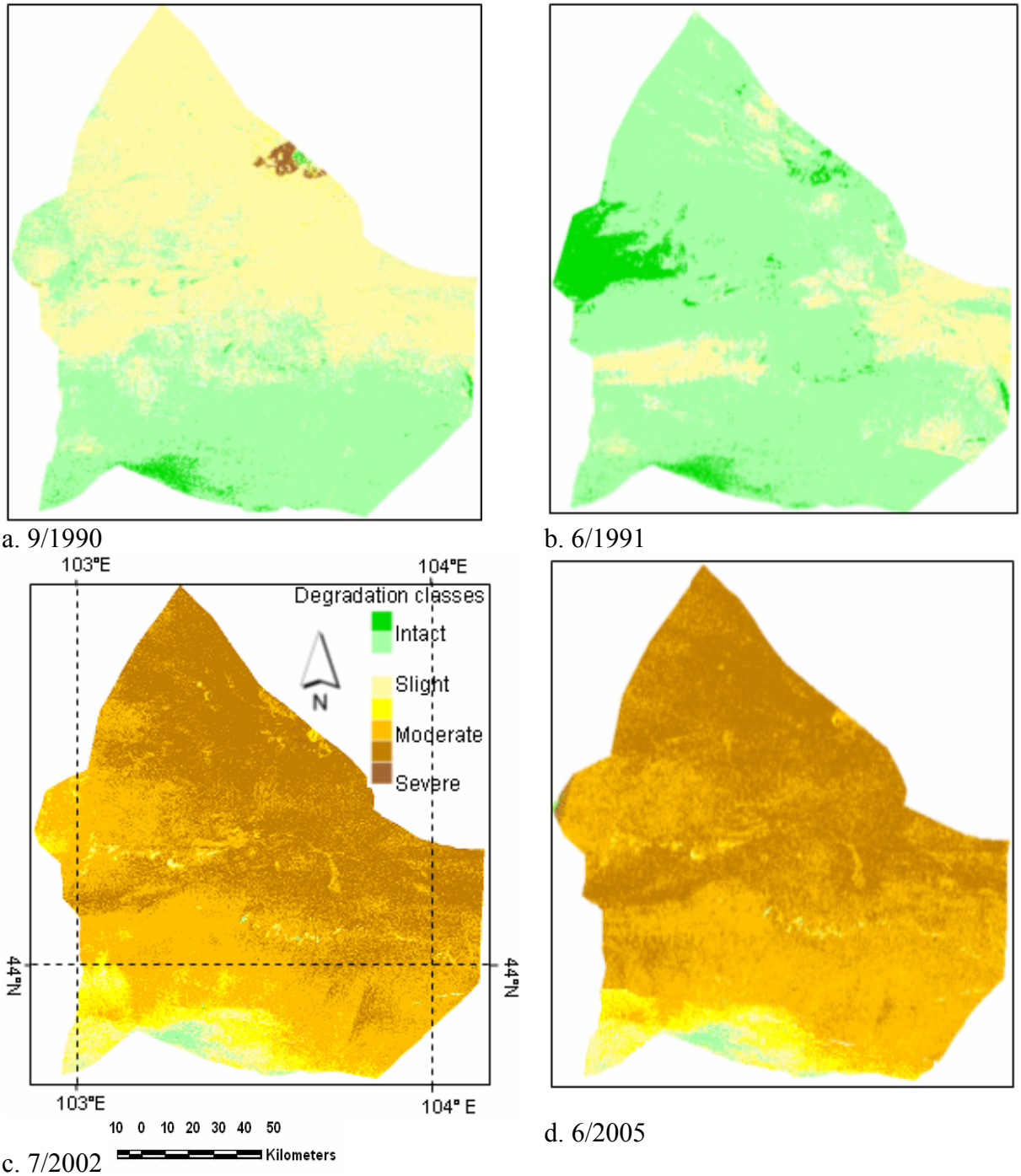

Figure 7.2 The combination of MSAVI and GSI for the year of: a) 9/1990; b) 6/1991; c) 7/2002; and d) 6/2005. It indicates the degree of land degradation. Bulgan soum, Mongolia

The images of combinations of MSAVI and GSI (Figure 7.2) were further employed in change detection by subtracting images on a pixel-by-pixel basis (Table 7.4). The degraded areas encompass the largest area for the period 1990 - 2002, while the intact areas constitute a relatively large proportion of the Bulgan soum in the 1991 -

2005. As mentioned earlier, this feature was attributed to the high rainfall of 1991. The result shows that 12% of the area remained in the vegetated area (intact) between the 1990 and 2002 dates, and a 31% remained intact between 1991 and 2005. The degrees of degradation classes were similar for the two difference images (1990-2002 and 1991-2005).

Table 7.4 Changes of degradation classes based on the MSAVI and GSI combination for 1990 - 2005, Landsat TM and ETM+ images. Bulgan soum, Mongolia

Desertification classes	1990-2002 Area (%)	1990-2002 Hectare	1991-2005 Area (%)	1991-2005 Hectare
Intact	12	85000	31	231000
Slightly degraded	20	145000	14	101000
Moderately degraded	39	281000	31	223000
Severely degraded	29	209000	24	165000

7.3.4 Sand encroachment

The Bulgan soum has the strongest winds in Mongolia, therefore it is highly subject to accelerating sand movements. The encroachment of blowing sand into adjacent shrub lands has dramatic impacts on the landscape, and is considered one of the indicators of desertification (Schelesinger, 1998).

Black color indicates the progressive appearance of sand mobilized from west to east (Figure 7.3). A topographic map from 1980 and Landsat MSS and TM images of the Bulgan soum from 1973, 1980, 1991, 2002, and 2005 were processed to display sands.

Shifting sand areas increased in the valley between Gurvansaikhan and Ikh saikhan mountain ranges, and other low topography areas. Sand-covered area accounts for 35% of the total area in 2005. The prevailing soil types are aridisols and entisols, young, not well developed soil with high sand content. Those soils are considered highly subject to land degradation.

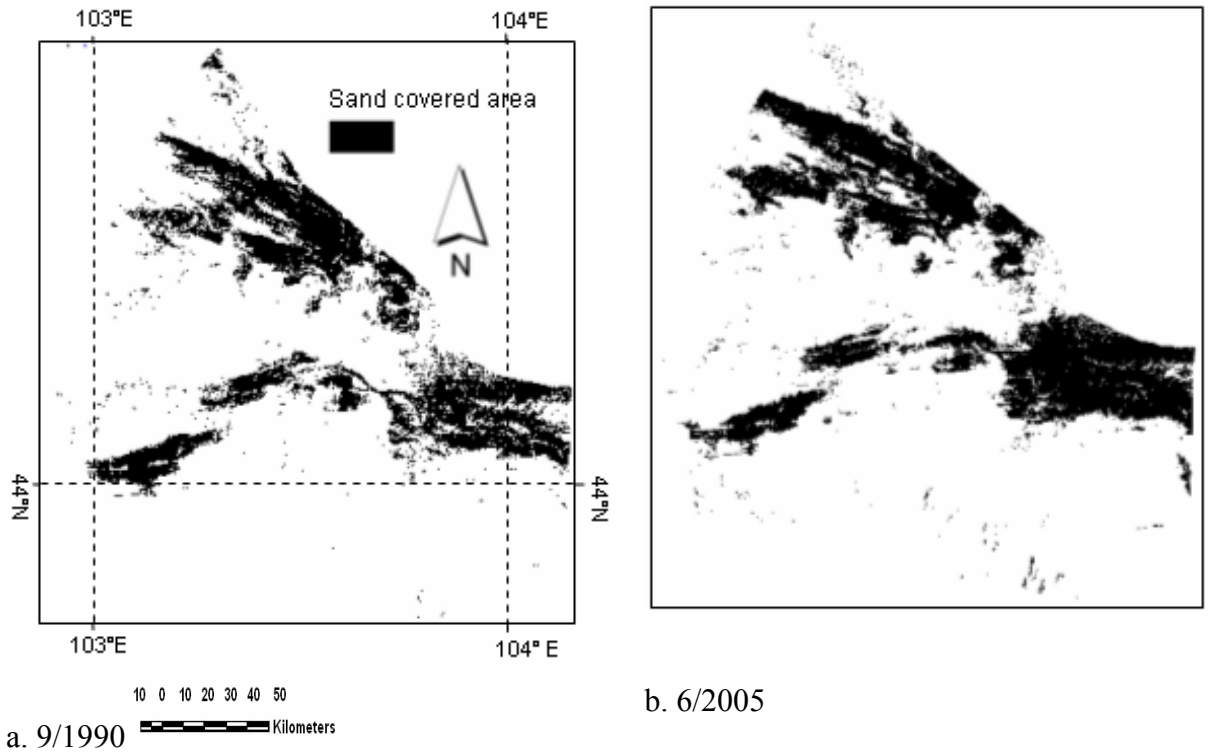

a. 9/1990 b. 6/2005

Figure 7.3 Areal changes of sand-covered area, Landsat image for the year of: a) 9/1990: b) 6/2005. Black area denotes the moving sand. Bulgan soum, Mongolia

Compared to 1973, the sandy area increased by 137000 ha (19%) in 2005 (Table 7.5). In 2005, the sand covered 35%, which equals 0.6% sand encroachment per year. However, in some years, namely 2005 and 1991, the sand covered area decreased by 2-3% for one to three years. The year 1991 was the highest rainfall year resulting in high plant productivity, and thus the sand cover decreased compared to the previous year. It can be interpreted that sands do not always march forward at a certain pace, but that in some years the sands do not move depending on rainfall. In general, the Bulgan soum has been moderately affected by drifting sands, some which are mobile sand dunes, with a height ranging from 3 to 5 m, and occasionally as high as 10 to 20 m. This demonstrates ongoing degradation.

Table 7.5 Change matrix of sand and water bodies in Bulgan soum, Mongolia

	Total sand area (ha)	Sand area (%)	Increase of sand area (ha)	Water (ha)	Water, area (%)
1973	115000	16		12750	1.7
1980	158000	22	43000	4500	0.6
1990	209000	29	51000	0	0
1991	187000	26	-22000	0	0
2002	266000	37	79000	0	0
2005	252000	35	-14000	0	0

7.3.5 Quantity and quality of water resources

Aboveground freshwater resources are essential components of pastoral systems. The Bulgan soum has limited water resources; surface water comprises only one lake, Ulaan, and other small seasonal rivers and the Ongi river. A total of 1.7 % of the area was water body according to topographic maps in 1973 (Table 7.5). However, the water bodies on these maps had decreased or disappeared in the satellite images of 1991. In the satellite image from 2002 the soil types solonchak and tykire were all that remain of Ulaan lake, but these too had disappeared in the 2005 image. The Ongi River was completely dried by 1993 due to gold mining.

7.3.6 Assessment of overall degradation and its trend

The four maps independently produced from the plant biomass, topsoil coarsening, sand coverage and water body change were combined to form an overall map so that degradation could be assessed more efficiently. This was achieved through linearly adding the four variables with a weight of 4 assigned to each (Eq 7.2).

Figure 7.4 contains continuously varying pixel values that had to be categorized into four groups in order to effectively visualize the spatial distribution of degradation severity. The overall severity map shows four levels of degradation severity: severe, moderate, slight, and intact. Roughly 94% of the study area has been affected by degradation to various levels of severity.

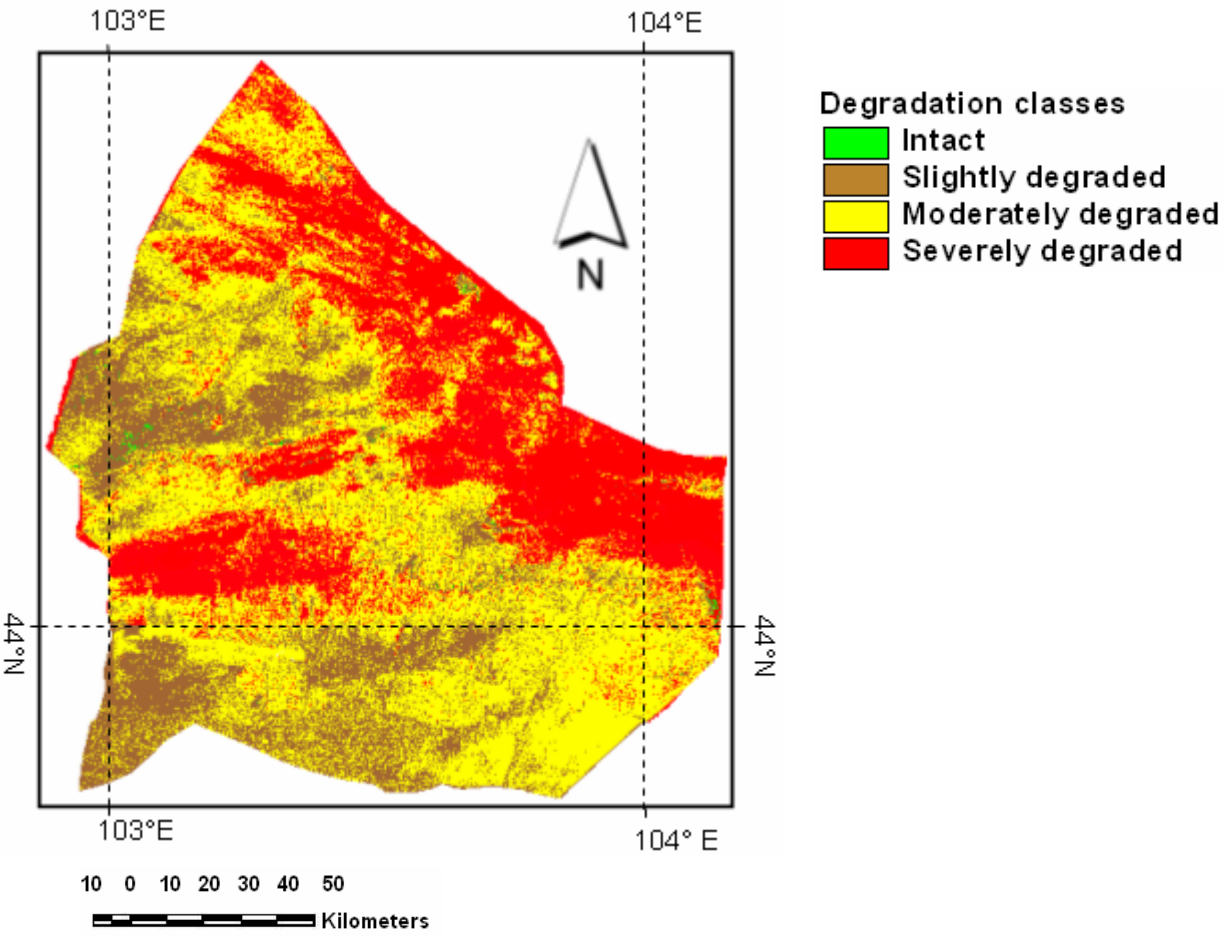

Figure 7.4 Overall degradation assessment map for Bulgan soum, Mongolia. Map shows distribution pattern of degradation classes in 2005

Table 7.6 (a summary of Figure 7.4) displays the results of the degradation severity changes between 1990 and 2005. A small part of the Bulgan soum is illustrated in green. Those areas are considered as intact (no change or slight change compared to the previous years). Degradation is relatively light, and the sites still resemble the original undisturbed state. Severely degraded areas make up the second largest class at 38% or 272 500 ha. Moderately degraded areas comprise the largest class of the four at 44% or 320 000 ha^{-1}. Slightly degraded areas (12% or 85 000 ha) make up the third most common severity class. The areas that have not yet been affected by degradation make up exactly 6% or 42 500 ha of the study area.

Table 7.6 Degradation classes based on all the indicators from 1990 to 2005. Bulgan soum, Mongolia

Degradation classes	1990-2005 (%)	hectares
Intact	6	42500
Slightly degraded	12	85000
Moderately degraded	44	320000
Severely degraded	38	272500

If land is degrading, it is essential to determine how much of the area is degraded after a certain period of time under changing environmental conditions. To reach this objective, the trend analysis presented in Section 4.3.2 was used. The plant biomass degradation was calculated based on the increasing dust storms and mean annual temperature trend up to 2020. Figure 7.5 depicts the future trend of land degradation for the Bulgan soum up to 2020. Plant biomass is forecasted to decrease by 20%. The result is tragic, as 90% of the landscape will hold 1-40 kg^{-1} ha aboveground plant biomass (in red and yellow), which is well within the severe degradation classification, while good vegetated pasture land is hardly found.

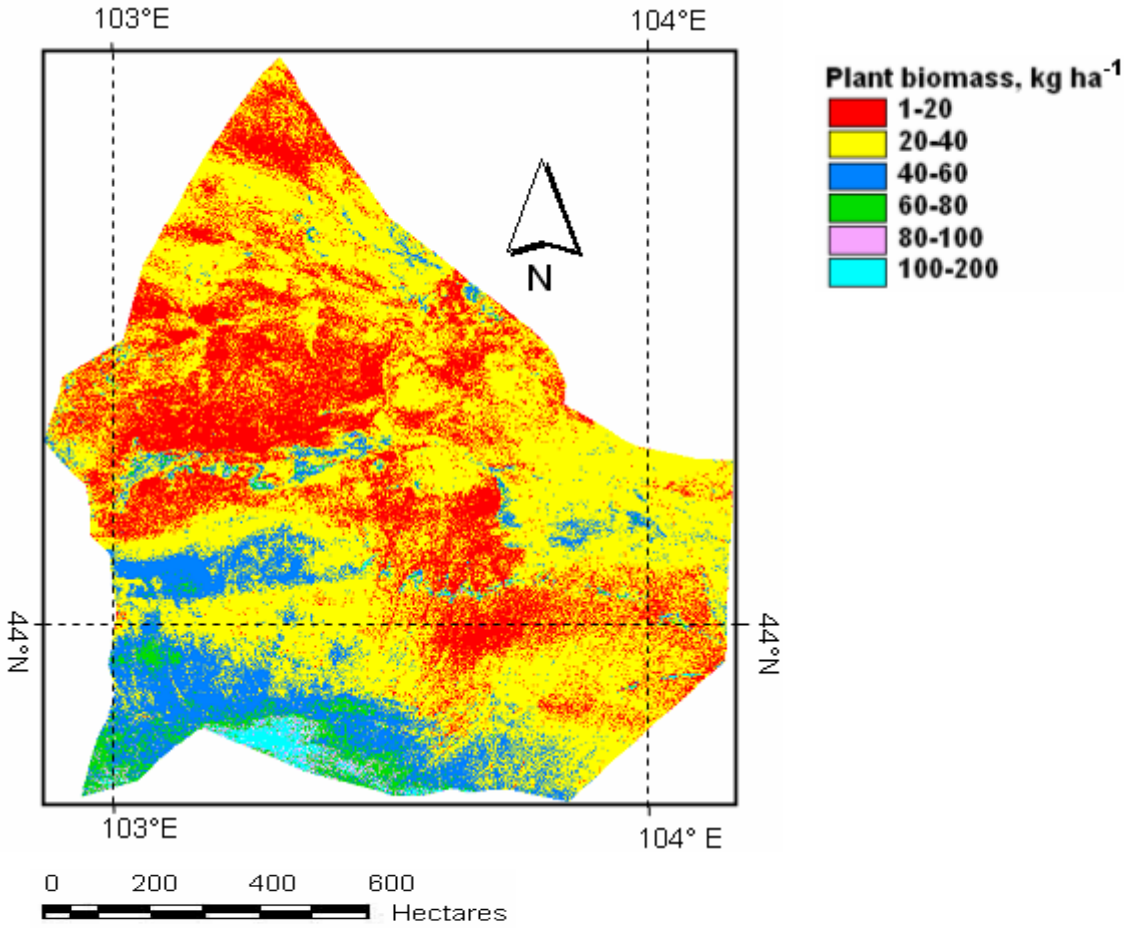

Figure 7.5 Degradation trend up to 2020. Based on plant biomass (kg ha^{-1}) deterioration under increasing dust storms and mean annual temperature. Bulgan soum, Mongolia

Time series forecasting analyses were carried out for the types of livestock to identify trends (Table 6.4). Livestock numbers and the individual species are expected to increase, except for camels. A particularly steep trend (i.e., 0.9) is seen for goats, which is about nine times more than for any other type of livestock. Seven thousand additional total stock are expected every year, which poses a serious threat to the land carrying capacity for the coming years.

Since the area is extensively utilized for grazing animals, an aim was to predict the number of animals to be supported in the future based on plant biomass production (Table 7.7). Carrying capacity was calculated using methods specific to Mongolia (Tserendash, 1990):

$$CC = \frac{YS}{TG} \qquad (7.3)$$

Where *Y* is yield, (kg ha), S is pasture area, (ha), G is grass amount grazing by 1 SSU, kg $day^{-1,}$ T is number of grazing days.

The number of livestock predict to be present by 2020 was 140 000 SSU, an increase of 7000 per year for 20 years (Table 7.8). In 2000, the area contained 411 000 SSU. That value plus 140 000 SSU yields 551 000 SSU by 2020. Aboveground plant biomass is going to decrease by 20%. A present, 720 000 ha of land produces an average of 46 kg forage per ha, yielding 33 120 t forage. Here, the growing season is considered to be 5 months, from May to September, thereby the average forage (46 kg ha) was multiplied by 5. Annual grass consumption per sheep was computed by the Mongolian method (Table 7.8), yielding 684 kg of forage consumption per SSU per year. The capacity of Bulgan soum to support livestock is therefore 205 363 SSU. If we assume that livestock are going to reach 551 000 SSU by 2020 and the carrying capacity of Bulgan soum will support 205 363 SSU, then stocking is going to exceed capacity by 345 637 SSU, or a factor of 2.5 more than the carrying capacity of land. Even today, the carrying capacity of the study area has been exceeded by a factor of 2 based on the same methods of calculation and average biomass per ha as 46 kg plant biomass. Many regions of the Gobi Desert of Mongolia have had an increase in unpalatable vegetation because of overgrazing, so there is little doubt that the area can not support the ever increasing stock in the future.

Table 7.7 Carrying capacity of land to support number of animals (SSU) in the Bulgan soum till 2020 based on plant biomass. The calculation of future trend includes increasing dust storms and MAT. Bulgan soum, Mongolia

Years	SSU	Biomass (kg $ha^{-1)}$	ANPP[a] (kg $ha^{-1)}$	Total biomass (tonn)	Carrying capacity (SSU)	Exceeded (SSU)	Exceeding rate
2000	411000	56	280	201600	294736	116264	0.5 times
2005	446000	46	230	165600	242105	203895	0.9 times
2020	551000	39	195	140400	205263	345637	1.5 times

[a-] *Annual Net primary production. Biomass values multiplied by 5 (growing season months).*

Table 7.8 Annual grass consumption per SSU (Tserendash, 1990)

	Grass amount (kg day$^{-1)}$	Grazing days	Annual biomass consumption (kg)
Summer	2.5	90	225
Fall	2.5	90	225
Winter	1.3	90	117
Spring	1.3	90	117
Total			684

Another way of calculating capacity is using the western method (PFRA, 2003), where 1 sheep = 120 pounds body mass, or 0.20 animal unit equivalent (AUE). The amount of forage required by one animal unit (AU) for one month is called an Animal Unit Month (AUM), and 1 AUM (sheep) is 71 kg. One sheep requires 852 kg fodder per year. Stocking rate is the number of animals on a pasture during a month or growing season. For instance, 100 animals grazing in an area for 12 months is 1200 AUM. Then total plant biomass is 720 000 ha x 46 kg ha fodder x 5 growing season months = 165 600 t total forage. Research in 2000 showed that one cattle with 100 kg body weight needs 2.5 kg of dry forage and that the annual requirement of dry forage for one cattle is 912.5 kg. Then, when 100 kg body weight equals 2 SSU (912:2=456 kg), the carrying capacity calculation will be 129 600 000 kg / 456 kg = 363 157 AUM.

In 2005, AUM for the Bulgan soum was: 411 000 SSU per 12 months or 411 000 * 12 months = 493 2000 AUM. Furthermore, 720000 ha / 493 2000 = 0.15 AUM ha. In the study area (40 km x 40 km), average livestock density was 11 SSU per km^2, or 6 stock per km^2.

7.4 Discussion

Since the study area has been used for animal husbandry for thousands of years, the indicator of plant production, MSAVI, should be a primary indicator because it is relevant to animal husbandry. The GSI, an indicator of topsoil coarsening, was applied in combination with MSAVI, since it is not as easily changed by rainfall as is MSAVI. Afterwards, temporal changes of the combined images of MSAVI and GSI were conducted for each year. Desertification severity indicators included aboveground biomass, topsoil coarsening, water body shrinkage, and sand movement. Those indicators were directly derivable from remotely sensed data.

The accuracy of the degradation map (Figure 7.4) was verified during a field visit in June - August 2005. In total, 41 sample spots were selected. Field-observed severity of degradation at 37 of these points was consistent with its counterpart shown in the map, leading to an accuracy of 91 %. Admittedly, this high accuracy level is related to the fact that degradation was mapped at only four categories of severity. The accuracy would certainly be lower had the severity been visualized with more categories. Nevertheless, a high accuracy level of 91% was achieved. It shows that overall, 75% of the area under study has been affected by degradation of various levels of severity.

Overlay of desertification severity layers (slight, moderate, severe) revealed that the spatial extent of desertified land in the area expanded during the 32-year study period (1973-2005). It particularly worsened during the last two decades with degraded areas accounting for 94% of the total area in 2005, and a far worse trend was found when extrapolated to 2020 (Table 7.6). Slightly degraded area encompassed 12%, moderate classes 44% and severely degraded 38% of the Bulgan soum. The comparison of the long-term plant productivity decline by Erdenetuya (2000) supports the finding that the Bulgan soum is being subjected to desertification.

Up to severe degradation classification, when plant productivity falls to 50% to 66%, land degradation is assumed reversible because restoration of land is still feasible. After this stage, land degradation is presumably irreversible (Katyal and Vlek, 2000). However, the actual degree of reversibility and resilience is not well described in this research. The classification was based upon the actual values of plant biomass (MSAVI) and soil coarsening (GSI) over the satellite imageries of 1970s, 1990s and 2000s. Indeed, plant production in non-equilibrium environments is largely controlled by the amount and duration of rainfalls. To overcome the relationship of plant production with rainfall, the use of topsoil grain size index (GSI) proposed by Xiao et al. (2006) made this research appropriate. Yet, the absence of a SWIR band or band 5 for the earliest image, Landsat MSS, did not permit generating this index for the 1973. Nevertheless, the increasing topsoil coarsening in the 2000s compared to the 1990s supports the premise of undergoing desertification.

The concept of ‘encroaching desert’, ‘moving desert’ or ‘advancing desert’ illustrating desert encroachment over productive areas have been largely rejected

(Dregne and Tucker, 1988; Mainguet, 1994; Warren and Agnew, 1988). Particularly the marching desert in the form of a readily measurable front of mobile sand dunes has been increasingly criticized (Binns, 1990; Pearce, 1992; Thomas 1997). The finding in the present study bolsters this criticism by validating decreasing moving sand encroachments between the years 1990-1991 and 2002-2005 (Table 7.5). Moving sands at the Bulgan soum is more like a 'sporadic rush than an advancing tide' (Goudie, 1996). It was highly dependent on plant production in association with rainfall. It is particularly true for 1-3 year intervals, yet, the area of moving sand has increased by 19% since 1973, with 0.6% encroachment per year.

Carrying capacity calculations according to western and Mongolian methods show that the Bulgan soum is currently supporting twice as many livestock as its carrying capacity. If this increasing trend of livestock density continues, the Bulgan soum will need to support even a factor of 2.5 more stock units than its actual carrying capacity by 2020. Carrying capacity of livestock in 200 mm of annual rainfall region based on ANPP was 6 SSU km^2 in tropical Africa (Hocking and Mattick, 2000). In the Bulgan soum, average stock density of 11 SSU was twice as much as suggested carrying capacity rate by Hocking and Mattick. Exceeding carrying capacity beyond natural limits remains a major cause of the deteriorating status of rangelands, leading to desertification (Katyal and Vlek, 2000). Land degradation will worsen in the future, but the number of livestock has and will seldom be adjusted to this changing scenario.

Mounting grazing pressure, which is the direct cause of overgrazing (Hilbig 1995) and shrinkage of water bodies have been identified as the driving forces of desertification. There is no clear trend in the spatial distribution of the desertified land within the study area. In general, all the indicators support that desertification is underway in the Bulgan soum (Table 7.9)

Table 7.9 Indicators of desertification showing that desertification is underway. Bulgan soum, Mongolia

Observation and results	1973 →→→→→→→ 2005
Vegetation biomass (MSAVI)	decrease
Number of water bodies	decrease
Sand drift	increase
Topsoil coarsening (GSI)	increase
Mean annual temperature	increase
Dust storms	increase
Livestock numbers and goats	increase

8 SUMMARY AND CONCLUSIONS

From the multiple calculated vegetation indices, the NDVI, SAVI, MSAVI were correlated with ground plant biomass compared to other vegetation indices. In general, none of the vegetation indices were correlated to the ground plant cover. MSAVI appeared to correlate with the ground plant biomass quantity. The GSI showed the highest correlation with the soil sand percentage, and was thus selected as an indicator of soil degradation.

The integrated desertification assessment by combining both plant and soil satellite-derived indices shows a 33% difference in the desertified area between three dates (1990, 1991 and 2005). Overall, 90% of the area is subjected to land degradation (1990–2005), of which the severely degraded area increased by 23%, whereas the moderately degraded area decreased by 9%, and the slightly degraded area increased by 9% compared to 1990-2002. Land degradation appeared mostly on pastures, grassland areas and water bodies. The annual rate of desertification was 2% for 1990 - 2005.

In terms of climatic factors, frequent severe droughts, and long-term shifts in the magnitude of precipitation characterized the Bulgan soum. Growing season MAP decreased by 2.4 mm for 1987-2000 compared to 1970-1980, and the maximum rainfall occurred one month later in August. MAT increased by 0.7 °C over the last 30 years, especially increasing trend were found and 1.8 °C higher than the long term average after 1990s. The maximum dust storm frequency increased from 60 times (1984) to 98 times (2002), while dust occurrence above 2 m from the ground surface disappeared along the time period. This postulates that sands fly at greater height than before due to increasing degradation. Plant biomass was controlled by growing season rain, MAP, MAT, drought indices (SPI, Pedi) and dust storms over the period 1970–2002. Statistical trend analysis found increasing dust storm frequency and MAT, but decreasing plant biomass. The forecasting till 2020 shows a 21% decrease in plant biomass for livestock, with an annual 0.4 increase in dust storms frequency and 0.05 °C increase in MAT. Increasing dust storms and temperatures will result in less water available to the ground and consequently reduced plant production. An increase in precipitation and rainfall was not proven, which might be due to lack of long-term data.

Related to soil factors, mean aboveground plant biomass was 36 g m^{-2} at the Bulgan soum in 2005. Higher productivity in fine textured soils was found than in coarse textured soils. Bulk density and porosity were mostly below the normal range, except for 12 sample sites, which were close to average bulk density rate

In terms of socio-demographic and human induced factors, age showed a significant relationship to degradation classes and wealth groups based on livestock holding. For the 18-40 year group, herders tended to be poorer, while in the 40-55 and over 55 age groups, the number of richer families increased. The relationship between degradation classes and the number of family members was positive, i.e., 6-12 family members tended to create degradation. The range of herd sizes is widening and with it the gap between the incomes of the richest and poorest groups in the herding sector. The ratio of herd sizes between the highest and lowest wealth classes ranged from 4:1. In general, large family sizes, older age, former herding households and decreased amount of moves lead to overgrazing. Those factors interact with each other, eventually leading to wealthy households. Livestock density per km ranged from 1-35 SSU per km^2 in 2005.

Time trend forecasting analysis shows increasing trend of livestock numbers namely 7000 SSU per year, particularly goats. A rangeland may, however, be degraded for cattle and sheep, goats. Land degradation in Mongolian has been caused by the increasing number of goats due to the growing cashmere market. It seems that rich families are causing land degradation, and poor families are increasing. However, livestock production system in non-equilibrium environments always faces episodic mortality; therefore, it can not be strictly projected that livestock will increase by 7000 SSU per year. In any case, an increasing trend of livestock is projected, while the number of nomadic moves by herders may remain the same. Typically, less moves resulting in intensive year-around grazing by animals left hardly any room for regeneration. Traditional knowledge on livestock management systems that respect nature has almost been forgotten by the young and middle-age herders, and livestock grazing is carried out with little consideration for vegetation and land restoration. If this trend continues, herders will eventually be pushed out of their age-old grazing territories due to declining rangeland quality and declining carrying capacity. Therefore,

improvement of the quality of livestock and regulation of the stocking rate equivalent to grazing capacity must be given high priority.

Based on general desertification assessment obtained from the combination of satellite images desertified land in 2005 is 94% of Bulgan soum. The severely degraded area covered 38%, moderately degraded 44%, and slightly degraded 12%. The area covered by sand increased by 137000 hectares or 19% from 1973 to 2005, covering 35%. Aboveground water resources in 1942 accounted for 1.7%, but were all completely dried due to human factors.

Desertification indicators are dynamic at time scales longer than a year. Thus, to ascertain progressive desertification and land degradation, a longer record needs to be examined, at least satellite images of ten different years with the same rainfall record. Furthermore, long-term remote sensing, climate and livestock data are needed for integrated ecosystem assessment to monitor, detect and analyze the degradation or desertification processes in the Mongolia Desert. Particularly, the response of primary production to precipitation, and rain use efficiency (RUE) should be used as an indicator of desertification.

To combat desertification, favorable tax and fee policies should be carried out to encourage herdsmen to participate in combating desertification. Economic incentives must be also provided to rural populations through planting vegetables, crops, trees that would generate additional values such as those that contain or generate medicinal and herbal essence, and fodder and other commercially valuable non-timber products. Attention must be paid to the preservation of existing desert vegetation and to the development of desert tourism. Engaging agriculture by harvesting run-off water from mountains should be ideal in Mongolian situation.

9 REFERENCES

Adyasuren T. and Dash D. 2001. Reasons of land degradation and its current situation in Mongolia In: Abstracts of open symposium on Change and Sustainability of Pastoral Land Use Systems in Temperate and Central Asia. Ulaanbaatar, Mongolia, pp. 25-28.

Aharoni B. and Ward D. 1997. A new perspective tool for identifying areas of desertification: a case study from Namibia. Desert. Cont. Bul. 31:12-18.

Agrawal A. 1993. Mobility and cooperation among nomadic shepherds: the case of the Raikas. Human Ecology. 21(3): 261-279.

Bannari A., Morin D., Bonn F., and Huete A.R. 1995. A review of vegetation indices. Rem. Sen. Rev. 13:95–120.

Batjargal Z. 2001. Lessons learnt from consecutive *dzud* disaster of 1999-2000 in Mongolia in Asia. In: Abstracts of open symposium on Change and Sustainability of Pastoral Land Use Systems in Temperate and Central Asia. Ulaanbaatar, Mongolia, pp. 35-38.

Baret F., Guyot G., and Major D.J. 1989. TSAVI: a vegetation index, which minimizes soil brightness effects on LAI and APAR estimation. In: Proceedings of the 12th Canadian Symposium on Remote Sensing, IGARRSS'90. Vancouver, BC, Canada, 10–14 July, volume 3.

Bayasgalan M. and Dash M. 2002. Drought and desertification assessment. In: Strengthening capacity for mitigating drought impact and desertification control proceedings. Ulanbator, Mongolia, pp. 29-35.

Bedunah D.J. and Schmidt S.M. 2000. Rangeland of Gobi Gurvan Saikhan National Park, Mongolia. Rangelands. 22(4):18-24.

Begzsuren S., Ellis J.E, Ojima D.S, Coughenour M.B. and Chuluun T. 2004. Livestock responses to droughts and severe winter weather in the Gobi Three Beauty National Park, Mongolia. J. Arid. Environ. 59:785-796.

Behnke R.H. and Scoones J. 1993. Rethinking range ecology implications for rangeland management in Africa. In: R.H. Behnke, I. Scoones, and Kerven. (eds), Range Ecology at Disequilibrium. Overseas development Institute, London, UK, pp.1-30.

Bettis A. 1983. Gully erosion. http://www.igsb.uiowa.edu/browse/gullyero/gullyero.htm

Binns T. 1990. Is desertification a myth? Geography. 75: 106–113.

Bolle H.J. 1994. Remote Sensing in desertification studies. In Desertification in a European context - Physical and socio-economic aspects. Report EUR. 15415.

Burton I. 2001. Vulnerability and adaptation to climate change in the drylands. http://www.undp.org/drylands/docs/cpapers/Vulnerability%20and%20Adaptation%20to%20Climate%20Change%20in%20the%20Drylands.doc

Cain M. 1981. Risk and Insurance: Perspectives on Fertility and Agrarian Change in India and Bangladesh. Popul. Dev. Rev. 7(3):435-475.

CCRS. 2006. Canada centre for remote sensing. Radiation – target interactions http://www.ccrs.nrcan.gc.ca/resource/tutor/fundam/chapter1/05_e.php

Chognii 0. 1990. Features of Restoration of Heavily Grazed Land for the Forest-steppe and Steppe Zones of Mongolia, Mongolian Academy of Science, Ulaanbaatar. Mongolia.

Chrapko D. 2001. An introduction to wind erosion control. Agriculture food and rural development. http://www1.agric.gov.ab.ca/$department/deptdocs.nsf/all/agdex3524

Clevers J.G.P.W. 1989. The application of weighted infrared red vegetation index for estimating leaf area index by correcting for soil moisture. Rem. Sen. Env. 29:25-37.

Conacher A.J. and Sala M. 1998. Land degradation in Mediterranean environments of the world: nature extent, causes and solutions. Wiley and Sons, pp 491.

Conrad V. 1941. The variability of precipitation. Mon. Wea. Rev. 69:5–11.

Coppock D.L. 1993. Vegetation and Pastoral Dynamics in the Southern Ethiopian Rangelands: Implications for Theory and management. In: Behnke R.H., Scoones I. and Kerven C. (Ed.) Range Ecology at Disequilibrium, London: Oversees Development Institute, pp. 42-62.

Coughenour M.B. 1991. Biomass and nitrogen responses to grazing of upland steppe on Yellowstone's northern winter range. J. App. Ecology. 28:71-82.

Cummings J. and Smith D. 2001. The line intercept method. A tool for introductory plant ecology. http://www.zoo.utoronto.ca/able/volumes/vol-22/13-cummings.pdf

Daddow R.L. and Warrington G.E. 1983. Growth limiting soil bulk densities as influenced by soil texture. WDG report, SADA forest service.

Dashnyam L. 1986. Vegetation in Southern Mongolia. Structure and dynamics of steppe and deserts in Mongolia (in Mongolian).Ulaanbaatar, Mongolia.

Davaajamts Ts. 1974. Research on plant roots biomass in the desert steppe of Mongolia. In: Structure and dynamics of steppe and deserts in Mongolia (in Mongolian). Ulaanbaatar, Mongolia.

Deering D.W. and Haas R.H. 1980. Correlations of rangelands brush canopy covery with Landsat MSS data. J. Range. Manag. 12:25-61.

Dregne H.E. and Chou Nan-Ting. 1993. Global desertification dimensions. In Degradation and Restoration of Arid Lands (eds: Dregne H.E.). International Center for arid and semiarid studies, Texas tech University, Lubbock, Texas, USA. Pp 249-282.

Dregne H.E. and Tucker C.J. 1988. Desertification encroachment. Deserti. Control. bullet. 19:6-18.

Ellis J.E. and Chuluun T. 1993. Cross-country survey of climate, ecology and land use among Mongolian pastoralists. Conference on Grassland Ecosystems of the Mongolian Steppe, 4-7 November 1993. Wingspread Center, Racine, WI, pp. 117-121.

Ellis J. and Galvin K.A. 1994. Climate patterns and land use practices in the dry zones of Africa. Bioscience. 44(5):340-348.

Ellis J.E. and Swift D.M. 1988. Stability of African pastoral ecosystems: Alternate paradigms and implications for development. J. Range Manag. 41:450-459.

Ellis J., Prince K., Yi F., Christensen L. and Yu M. 2002. Dimensions of desertification in the drylands of northern China. In: Stafford Smith (Ed) Global Desertification: Do humans cause deserts? Dahlem University Press.

Engels C.L. 2001. The effect of grazing on soil bulk density. http://www.ag.ndsu.nodak.edu/streeter/99report/soil_bulk.htm .

Erdenetuya A. 2000. Pastureland monitoring using NOAA/AVHRR data. In: Proceedings of International conference Central Asian ecosystems. Ulaanbaatar, Mongolia, pp.115-120.

Escadafal R. and Bacha S. 1996. Strategy for the dynamic study of desertication. proceedings of the ISSS International Symposium Ouagadougou, Burkino Faso, 6–10 February 1995 (Paris: Orstom editions), pp 19–34.

Escadefal R. and Huete A.R. 1991. Improvement in remote sensing of low vegetation cover in arid regions by correcting vegetation indices for soil noise. C.R. Acad. Sc. Paris. 312(2): 1385-1391.

Escadafal R, Girard M.C. and Courault D. 1989. Munsell soil color and soil reflectance in the visible spectral bands of Landsat MSS and TM data. Remote Sens. Environ. 27:37-46.

FAO. 2006. Gender and dryland management: Drylands, opportunities, and challenges. lada.virtualcentre.org/eims/.

Fassnacht K.S., Gower S.T., Mackenzie M.D., Nordheim E.V. and Lillesand T.M. 1997. Estimating leaf area index of north central Wisconsin forest using the Landsat Thematic Mapper. Rem. Sen. Env. 61:229-245.

Fernandez-Gimenez M.E. and Barbara Allen-Diaz. 1999. Testing a non-equilibrium model of rangeland vegetation dynamics in Mongolia. J. App. Ecology 36:871-885.

Fox G.A., Sabbagh G.J. and Searcy S.W. 2003. Radiometric normalization of multi-temporal images using the soil line transformation technique. Trans. ASAE 46:851–859.

Froehlich H.A. and McNabb D.H. 1984. Minimizing soil compaction in Pacific Northwest forests. p. 159–192. In: Stone E.L. (Ed.) Proc. Forest Soils and Treatment Impacts Conf., 1983. Univ. of Tennessee, Knoxville, TN.

Fu H., Wang Y., Wu C. and Ta L. 2002. Effect of grazing on soil physical and chemical properties of Alxa desert grassland. J. Desert Res. 22:339-343.

Gad A. and Daels L. 1986. Assessment of desertification in the lower Nile Valley (Egypt) by an interpretation of Landsat MSS color composites and aerial photographs. Remote Sensing for Resources Development and Environmental Management, In: Damen M. C. J. (Ed). Proceedings of the 7th ISPRS Commission VII Symposium, vol. 2, Rotterdam, Balkema, pp. 599–605.

Geerken R. and Hansmann B. 2000. Combating desertification in the near east identification of rehabilitation measures and impact monitoring. In: Hongbo J. (Ed.), Workshop of the Asian regional thematic programme network on desertification monitoring and assessment. UNCCD, Tokyo, pp.56-69.

Goldsmith W., Silva M. and Fischenich C. 2001. Determining optimal degree of soil compaction for balancing mechanical stability and plant growth capacity. U.S. Army Engineer research and development center. http://www.wes.army.mil /el/emrrp.

Gordeeva T.K. 1978. Vegetation variety, cover and biomass in the Mongolian desert steppe. In: Geography and dynamics of flora and fauna in Mongolia. (in Russian).

Grunblatt J., Ottichilo W.K. and Sinange R.K. 1992. GIS approach to desertification assessment and mapping. J. Arid. Env. 23:81-102.

Goudie A.S. 1983. Dust storms in space and time. Prog. Physic. Geog. 7:502-530.

Goudie A.S. and Middleton N.J. 1992. The changing frequency of dust storms through Time. Climat. Change. 20:197-225.

Goudie A. S. 1996. The geomorphology of the seasonal tropics, in: Adams W. M., Goudie A. S. and Orme A. R. (Ed.) The Physical Geography of Africa, Oxford University Press, pp. 148-160.

Gunin D.P., Elizabeth A.V., Nadezda I.D., Pavel E.T. and Clanton C.B. 2000. Vegetation Dynamic of Mongolia, Geobotany 26, Kluwer Academic Publishers, the Netherlands.

Hanan N.P., Prevost Y., Diouf A. and Diallo O. 1991. Assessment of desertification around deep wells in the Sahel using satellite imagery. J. App. Eco. 28:173–186.

Hardin G. 1968. The tragedy of commons. Science. 162:1243-1248.

Harr R.D., Fredriksen R.L. and Rothacher J. 1979. Changes in stream flow following timber harvest in south western Oregon. USDA For. Serv. Res. Paper PNW-249. Pacific Northwest For. and Range Exp. Stn., Portland, OR.

Hart Lab, 2001. Soil texture protocol. Hydrometer method. http://www.for.nau.edu/mosaddphp/Hartlab/LabProcedures/SoilTextureProtocol.pdf

Hayes M.J., Svobody M.D., Wilhite D.A. and Vanyarkho O.V. 1999. Monitoring the 1996 drought using the standardized precipitation index, Bull.Am. Meteorol. Soc. 80:429-438.

Hennemann R. 2001.a. Elective on land degradation, assessment, monitoring and modelling soil science division, ITC, Enschede, The Netherlands.

Hennemann R. 2001.b. Some notes about soil and land degradation in the Naivasha rangeland zone, pp 3, Soil science division, ITC, Enshede, The Netherlands.

Hilbig W. 1995. The vegetation of Mongolia. SPB Academic Publishing, Amsterdam.

Hill J., Megier J. and Mehl W. 1995.a. Land degradation, soil erosion and desertification monitoring in Mediterranean ecosystems. Rem. Sen. Rev. 12(1-2):107-130.

Hill J., Sommer S., Mehl W. and Megier 1995.b. Use of earth observation satellite data for land degradation mapping and monitoring in Mediterranean ecosystems: towards a satellite observatory. Env. Monitor. Assessment. 37(1-3):143-158.

Hocking D. and Mattick A. 2000. Dynamic carrying capacity analysis as tool for conceptualizing and palling range management improvements, with a case study from India. http://www.odi.org.uk/pdn/papers/34c.pdf.

Huete A.R. 1988. A soil adjusted vegetation index (SAVI). Rem. Sen.Env. 25: 295-309.

Huete A., Liu H.Q., Batchily K. and Van Leeuwen W. 1997. A comparison of vegetation indices over a global set of TM images for EOS-MODIS. Rem. Sen. Env. 59:440–451.

Huete A., Post D.F., and Jackson R.D. 1984. Soil spectral effects on 4-space vegetation discrimination. Rem. Sen. Env. 15:155–165.

Hydrometeorology Institute. 2005. Maps and information on Mongolia. Ulaanbaatar, Mongolia.

Idso C.D. and Idso K.E. It's happed before. It can happen again. Science. 2(6):15. http://www.co2science.org/scripts/CO2ScienceB2C/articles/V2/N6/EDIT.jp

Ingo H., Schwartz H., Pieters V.H.C. and Moster C. 1996. Land degradation in African pastoral systems and the destocking controversy. Ecolog. Model. 86:227-233.

IPCC. 2001. Intergovernmental panel on climate change. http://www.ipcc.ch.

IUPUI. 2001. Bulk density determination. http://www.geology.iupui.edu /research/SoilsLab/procedures/bulk/Index.htm.

Javzandulam Ts, Tateishi R. and Tsolmon R. 2002. Multitemporal analysis of vegetation indices for characterizing vegetation dynamics in Mongolian grassland.150-155pp. In: First international workshop on land cover study in Mongolia using remote sensing and GIS, Research and hydrometeorology Institute, Ulanbator, Mongolia, pp.75-80.

Jano A., Jefferies R.L. and Rockwell R.F. 1998. The detection of vegetational change by multitemporal analysis of Landsat data: the effects of goose foraging. J. Ecology. 86:93-99.

Jing L. 2002. Desertification monitoring and estimation in China from AVHRR data http://www.gisdevelopment.net/aars/acrs/1999/ps4/ps4241.asp.

Johnson D.L. 2004. Nomadism and desertification in Africa and the Middle east. Geo.J. 31(1):51-66.

Justice C.O., Townshend J.R.G., Holben B.N. and Tucker C.J. 1985. Analysis of the phenology of global vegetation using meteorological satellite data. Int. J. Rem. Sen. 6:1271–1318.

Karnieli A., Kaufman Y.J., Remer L. and Wald A. 2001. AFRI- aerosol free vegetation index. Rem. Sen. Env. 77:10-21.

Katyal J.C. and Vlek P.G.L. 2000. Desertification – concept, causes and amelioration. ZEF- Discussion papers on development policy, Bonn, Germany. Number 33.

Kaufman Y.J. and Tanre D. 1992. Atmospherically resistant vegetation index (ARVI) for EOS-MODIS. IEEE Transaction. Geoscience. Rem. Sens. 30:261-270.

Kharin N., Tateishi R. and Harahsheh H. 1999. Degradation of the drylands of Asia. Center for environmental remote sensing, Chiba university, Japan.

Kelly M. and Hulme M. 1993. Desertification and Climate change. Tempo 9. http://www.cru.uea.ac.uk/tiempo/floor0/archive/issue09/t9art1.htm.

Laurenroth W.K. and Sala O.E. 1992. Long term production of north American short grass steppe. Ecologic. Applicat. 2(4): 397-403.

Lillesand T.M. and Kiefer R.W. 1994. Remote Sensing and Image Interpretation. John Wiley, New York.

Linacre E. and Geerts B. 2002. The climate of the Kalahan desert. http://www-das.uwyo.edu/geerts/notes/chap10/kalahari.html.

LeHouerou H.N. 1992. An overview of vegetation and land degradation in world arid lands. In: Dregne H.E. (Ed.) Degradation and Restoration of Arid Lands. International center for arid and semiarid land studies, Texas Tech Univeristy, Lubbock, Texas, USA. pp 127-164.

Liu Y., Zha Y., Gao J. and Ni S. 2004. Assessment of grassland degradation near Lake Qinghai, West China, using TM and in situ reflectance spectra data. Int. J. Rem. Sen. 25(20): 4177-4189.

Luk S.H. 1983. Recent trends of desertification in the Maowusu Desert, China. Environment. Conserv. 10:213–224.

Mainguet M. 1994. Desertification natural background and human mismanagement. Springler_Verlag, Berlin, Germany.

Major D.J., Baret F. and Guyot G. 1990. A ratio vegetation index adjusted for soil brightness. Int. J. Rem. Sen. 11:727–740.

Mathworld Wolfram. 2003. Gini coefficient. http://mathworld.wolfram. com/GiniCoefficient.html.

McKee T.B., Doesken N.J. and Kleist J. 1993. The relationship of drought frequency and duration to time scales. Preprints, 8th Conference on applied climatology, 17-22 January, Ahaheim, California, pp. 179-184. http://www.wrcc.dri.edu/spi/ explanation.html.

Mearns R. 2004. Decentralization, rural livelihoods and pasture land management in Post-Socialist Mongolia. Eu. J. Dev. Res. 16(1): 133-152.

Metternicht G.I. 1996. Detecting and monitoring land degradation features and processes in Cochabamba Valleys,Bolivia: a synergistic approach. ITC, Enschede, The Netherlands, pp. 390.

Mishra J.K., Joshi M.D. and Devi R. 1994. Study of desertification process in Aravalli Environment using remote sensing techniques. Int. J. Rem. Sen.15:87–94.

Mouat D., Lancaster J., Wade T., Wickham J., Fox C. and et al.1997. Desertification evaluated using an integrated environmental assessment model. Environ. Monit. Assess. 48: 139–156.

Mumby P.J., Green E.P., Edwards A.J. and Clark C.D. 1997. Coral reef habitat mapping: how much detail can remote sensing provide? Marine Biology 130(2): 133-134.

National desertification report. 2002. National Report on Combating Desertification and Promoting the Synergistic Implementation of Inter Linked Multilateral Environmental Conventions. http://www.unccd.int/regional/asia/meetings/ meetings.php.

National report. 2000. Statistical center of Mongolia, Ulaanbaatar. Mongolia. pp.105 (in Mongolian)

National report. 2002. Statistical center of Mongolia, Ulaanbaatar. Mongolia pp.107 (in Mongolian)

NDMC National Drought Monitoring Center. 2006. What is drought: Understanding and defining the drought. http://www.drought.unl.edu/whatis/concept.htm.

NETC. 2005. Sheet erosion. http://www.netc.net.au/enviro/fguide/sheeterosion.html

Newbould P.J. 1967. Methods for estimating the primary production of forests. IBP handbook Number 2. Blackwell Scientific Publ. Oxford. England.

Nicholson S.E., Tucker C.J. and Ba M.B. 1998. Desertification, drought, and surface vegetation, an example from the west African Sahel. Bullet. Americ. Meteorolog. Society. 79:815–829.

Noy-Meir I. 1973. Desert ecosystems: environment and producers. Annual. Rev. Ecology. Systematic. 4:25-51

Ojima D. 2001. Critical drivers of global environmental and land use changes in temperate East Asia. In: Abstracts of open symposium on Change and Sustainability of Pastoral Land Use Systems in Temperate and Central Asia, pp 32. Ulaanbaatar, pp 75.

Qi J., Chehbouni A., Huete A., Kerr Y.H. and Sorooshian S. 1994. A modified soil adjusted vegetation index. Rem. Sen. Environ. 48:119–126.

Qu J.J., Xianjun H., Kafatos M and Wang L. 2006. Asian dust storms monitoring combining terra and aqua MODIS SRB measurements. IEEE Geoscience Rem. Sen. Letters 3(4):484-486.

PALD. 1997. Study of extensive livestock production systems TA. Opportunities and Constraints Reports. Ulaanbaatar. Mongolia.

Pearce F. 1992. Mirage of shifting sands. New Scientist. 12: 38–42.

Pech R.P., Davis A.W., Lamacraft R.R. and Graetz R.D. 1986. Calibration of Landsat data for sparsely vegetated semi-arid rangelands. Int. J. Rem. Sen. 7: 1729–1750.

Pickup G. and Chewings V.H. 1988. Forecasting patterns of erosion in arid lands from LandsatMSS data. Int. J. Rem. Sen. 9: 69-84.

PFRA. 2003. Animal unit months, stocking rate and carrying capacity. http://www.agr.gc.ca/pfra/land/fft1.htm.

Prince S.D., Brown De Colstoun E. and Kravitz L.L. 1998. Evidence from rain-use efficiencies does not indicate extensive Sahelian desertification. Global Change Biology 4: 359-374.

Prince S.D., Haskett J., Steininger M. and Strand H. 2001. Net primary production of U.S. midwest croplands from agricultural harvest yield data. Ecological. App. 11: 1194-1205.

Proctor J.D. 1999. The limits to growth debate and future crisis in Africa: a case study from Swaiziland. Land. Degrad. Rehabilit. 2:135-155.

Purevdorj Ts., Tateishi R., Ishiyama T. and Honda Y. 1998. Relationships between vegetation cover and vegetation indices. Int. J. Rem. Sen. 19 (18): 3519-3535.

Raina P., Joshi D. and Kolarkar A.S. 1993. Mapping of soil degradation by using RS on alluvial plain, Rajasthan, India. Arid. Soil. Res. Rehabilit. 7(2):145-161.

Ray S.S., Singth J.P., Garhi D. and Sushma P. 2005. Use of high resolution remote sensing data for generate site-specific soil management plan. Int. Archives. Photometry, RS. Spat. Infor. System.

Rikimary A. and Miyatake S. Development of forest density mapping and monitoring model using indices of vegetation, bare soil and shadow. http://www.gisdevelopment.net/aars/acrs/1997/ts5/ts5006pf.htm.

Ringrose S., Matheson W., Tempest F. and Boyle T. 1992. The development and causes of range degradation features in southeast Botswana using multi-temporal Landsat MSS imagery. Photogram. Engineer. Rem. Sen. 56:1253–1262.

Rubio J.L. and Bochet E. 1998. Desertification indicators as diagnosis criteria for desertification risk assessment in Europe. J. Arid Environ 39:113–120.

Sabins F.F. 1987. Remote sensing: principles and interpretation. W.H. Freeman, New York.

Sanjid J., Dugarjav Ch., Hongor Ts. and Arnon K. 2004. Lifestyle changing characteristics of plants due to drought. Research reviews from the Institute of Botany, 14 Mongolia. pp: 58-61.

Schlesinger W.H., Reynolds J.F., Cunningham G.L., Huenneke L.F. and Jaerel WM, Virginia R.A. and et al. 1990. Biological feedbacks in global desertification. Science. 247:1043-1048.

Sehgal J.L. and Abrol I.P. 1994. Soil degradation in India: Status and Impact. Oxford and IBH Publishing Co. Pvt.LTd., New Delhi, India.

Seligman N.G. and Leulen N.V. 1989. Herbage production of a Mediterranean grassland in relation to soil depth, rainfall and nitrogen: a simulation study. Eco. Model. 47:303-311.

Serrano S.M.V., Lasanta T. and Romo A. 2004. Analysis of Spatial and Temporal Evolution of Vegetation Cover in the Spanish Central Pyrenees: Role. Human. Manag. Environ. Manag. 34(6):802-218.

Sharma K.D. 1998. The hydrological indicators of desertification. J. Arid. Env. 39:121-131. Singh A. 1989. Digital change detection techniques using remotely sensed data. Int. J. Rem. Sen. 10(6): 989-1003.

Singh A. 1989. Digital change detection techniques using remotely sensed data. Int. J. Rem. Sen. 10:989-1003.

Sneath D. 1998. State policy and pasture degradation in Inner Asia. Science. 28:1147-1148.

Sneath D. 2004. Land use, the environment and development in Post-socialist Mongolia. Oxford Development Studies. 31(4):441-459.

Squires V.R. 2001. Dust and sand storms: an early warning of impending disaster. In: Global alarm: dust and sandstorms from the world's drylands.pp.15-28. Asian regional coordination unit and secretariat of UNCCD press, UN.

Sommer S., Hill J. and Megier J. 1998. The potential of remote sensing for monitoring rural land use changes and their effects on soil conditions. Agricul. Ecosystems. Environ. 67(2-3):197-209.

Stewart B.A, Lal R. and El-Swaify S.A. 1992. Sustaining the resource base of an expanding world agriculture. In: Lal R and Pierce F.J. (Ed.) Soil management and sustainability. Soil and water conservation society, Ankey, Iowa, USA, pp.125-145.

Sujatha G., Dwivedi R.S., Sreenivas K.S. and Venkaratathan L. 2000. Mapping and monitoring of degraded lands in part of Jaunpur district of Uttar Pradesh using temporal spaceborne multispectral data. Int. J. Rem. Sen. 21(3):519-531.

Tanser and Palmer A. 1999. The application of remotely sensed diversity index to monitor degradation patterns in semi arid, heterogeneous, South African landscape. J. Arid. Env. 43:477-484.

Tchayi M.G.M., Bertrand J.,Legrand M., and Baudet J. 1994. Temporal and spatial variations of the atmospheric dust loading throughout West Africa over the last thirty years. Ann. Geophys. 12:265-273.

Thiam A.K. 2002. The causes and spatial pattern of land degradation risk in southern Mauritania using multitemporal AVHRR-NDVI imagery and field data. Land. Degrad. Develop. 14(1):133 – 142.

Thomas D.S.G. 1997. Science and the desertification debate. J. Arid. Env. 37, 599–608.

Tripathy G.K., Ghosh T.K. and Shah S.D. 1996. Monitoring of desertification process In Karnataka state of India using multi-temporal remote sensing and ancillary information using GIS. Int. J. Rem. Sen.17:2243–2257.

Tserendash D. 1990. Carrying capacity calculation. In: Livestock pastoralism development. Ulaanbaatar. Mongolia. (in Mongolian).

Tsunekawa A. 2000. Methodologies of desertification monitoring and assessment. pp.44-55. In: Proceeding of workshop of the Asian regional thematic programme network on desertification monitoring and assessment . UNU, Tokyo, Japan press. pp.251.

Tucker C.J., Fung I.Y., Keeling C.D. and Gammon R.H. 1986. Relationship between atmospheric CO2 variations and a satellite-derived vegetation index. Nature 319:195– 199.

Tucker C.J., Dregne H.E. and Newcomb W.W. 1991. Expansion and contraction of the Sahara Desert from 1980 to 1990. Science 253:299-301.

Tucker C.J., Townshend J.R.G. and Goff T.E. 1985. African land-cover classification using satellite data. Science 227:369-375.

USDA-NRCS soil quality test kit. 2000. http://soils.usda.gov/sqi/files/KitGuide Complete.pdf

UNCCD. 2004. Fact sheets on UNCCD. http://www.unccd.int/publicinfo/factsheets/menu.php

UNCCD. 2006a. Down to earth, News and Views on desertification. Issue 26. UNCCD. Bonn. Germany in the desert recreation sector. UNEP DTE , and world tourism organization. France

UNCCD. 2006b. In those countries experiencing serious drought and desertification, Particularly in Africa. UNCCD secretariat.

UNDP. 2004. United Nations development program in Mongolia. www.undp.mn/modules.php.

UNEP. 1998. Report of expert meeting on meteorology for desertification assessment and mapping. Ulaanbaatar, Mongolia.

UNEP. 2002. United Nations Environment Programme. Mongolia: State of the environment. Pathumthani, Thailand: regional resource center for Asia and Pacific. 2002. pp. 3-7.

Warren A. and Agnew C. 1987. An assessment of desertification and land degradation in arid and semi-arid areas. Drylands paper 2. International Institute for Environment and Development, London, UK.

Williams M.A.J. 2001. Desertification: General debates explored through local studies. Progress. Env. Science. 2(3): 229-251.

Westoby M, Walker B. and Noy-Meir I. 1989. Opportunistic management for rangeland at equilibrium . J. Range. Manag. 42:266-274.

Weins J.A. 1984. On understanding a non-equilibrium world: Myth and reality in community patterns and processes. In: Strong D.R., Simberloff, D., Ebele, L.C. and Thistle A.B. (Ed). Ecological Communities: Conceptual Issues and the Evidence. Princeton, N.J. Princeton University Press.

WMO. 2006. World meterological organization. World day to combat desertification, Climate and land degradation. WMO-No. 989. Geneva. Switzeland**,** pp. 32.

Xiao X., Jiang S., Wang Y., Ojima D.S. and Bonham C.D. 1996. Temporal variation in aboveground biomass of *Leymus Chinense* steppe from species to community levels in the Xilin Basin, Inner Mongolia, China. Vegetatio. 123:1-12.

Xiao J., Shen Y., Tateishi R. and Bayer W. 2006. Development of grain size index for monitoring desertification in arid land using remote sensing. Int. J. Rem. Sen. 27(12):2411-2422.

10 APPENDICES

Appendix 1 Vegetation and soil index values of Landsat ETM+ oft images corresponding to sample plots, Bulgan soum, Mongolia, 2005.

Site	NDVI	TNDVI	ARVI	SARVI	SAVI	MSAVI	BI	RI	R	NIR	BSI	GSI
1	-0.107	0.622	0.096	0.144	-0.17	-0.247	189	2	130	103	0.194	0.193
2	-0.129	0.606	0.026	0.027	-0.2	-0.304	175	1	113	91	0.163	0.121
3	-0.127	0.611	0.021	0.022	-0.19	-0.288	173	1	118	89	0.157	0.102
4	-0.129	0.609	0.055	0.033	-0.19	-0.294	196	2	137	101	0.178	0.152
5	-0.133	0.592	0.027	0.035	-0.2	-0.306	182	1.37	132	103	0.127	0.147
6	-0.15	0.592	-0.01	-0	-0.23	-0.335	179	1	122	90	0.119	0.101
7	-0.134	0.61	0.045	0.068	-0.19	-0.308	177	1.92	118	93	0.165	0.140
8	-0.136	0.603	0.042	0.063	-0.2	-0.312	171	1.81	115	88	0.165	0.136
9	-0.115	-0.617	0.062	0.093	-0.17	-0.257	176	2	118	96	0.150	0.147
10	-0.135	0.604	0.04	0.06	-0.2	-0.211	170	1.35	117	88	0.177	0.146
11	-0.123	0.613	0.037	0.05	-0.19	-0.281	191	1	131	101	0.146	0.109
12	-0.128	0.61	0.068	0.105	-0.19	-0.288	175	2	138	107	0.177	0.152
13	-0.137	0.606	0.046	0.069	-0.2	-0.318	209	2	143	109	0.147	0.138
14	-0.132	0.606	0.035	0.053	-0.2	-0.303	173	1.02	117	90	0.163	0.129
15	-0.14	0.61	0.034	0.051	-0.21	-0.315	168	1.49	114	87	0.158	0.124
16	-0.128	0.606	0.031	0.085	-0.2	-0.292	157	1.97	118	93	0.160	0.150
17	-0.123	6.14	0.029	0.06	-0.18	-0.278	182	1	122	96	0.154	0.118
18	-0.119	0.617	0.066	0.105	-0.18	-0.27	198	2	137	111	0.180	0.179
19	-0.14	0.597	0.026	0.033	-0.21	-0.325	187	1.12	114	92	0.173	0.123
20	-0.131	0.61	0.042	0.057	-0.2	-0.299	186	1.15	130	98	0.155	0.128

Appendix 1 continued

Site	NDVI	TNDVI	ARVI	SARVI	SAVI	MSAVI	BI	RI	R	NIR	BSI	GSI
21	-0.137	0.602	-0.01	-0.03	-0.21	-0.316	173	1	116	87	0.146	0.087
22	-0.132	0.609	0.054	0.087	-0.18	-0.302	167	2	120	97	0.194	0.183
23	-0.136	0.603	0.042	0.063	-0.2	-0.312	171	1.81	115	88	0.163	0.125
24	-0.115	-0.617	0.062	0.093	-0.17	-0.257	176	2	118	96	0.157	0.112
25	-0.135	0.604	0.04	0.06	-0.2	-0.311	170	1.35	117	88	0.178	0.154
26	-0.123	0.613	0.037	0.05	-0.19	-0.281	191	1	131	101	0.127	0.149
27	-0.14	0.61	0.034	0.051	-0.21	-0.315	168	1.49	114	87	0.119	0.112
28	-0.128	0.606	0.031	0.085	-0.2	-0.292	157	1.97	118	93	0.165	0.141
29	-0.123	6.14	0.029	0.06	-0.18	-0.291	182	1	122	96	0.165	0.135
30	-0.119	0.617	0.066	0.105	-0.18	-0.271	198	2	137	111	0.150	0.149
31	-0.14	0.597	0.026	0.033	-0.21	-0.304	187	1.12	114	92	0.177	0.135
32	-0.134	0.61	0.045	0.068	-0.19	-0.302	177	1.92	118	93	0.146	0.119
33	-0.136	0.603	0.042	0.063	-0.2	-0.301	171	1.81	115	88	0.177	0.142
34	-0.115	-0.617	0.062	0.093	-0.17	-0.216	176	2	118	96	0.147	0.128
35	-0.135	0.604	0.04	0.06	-0.2	-0.301	170	1.35	117	88	0.163	0.130
36	-0.128	0.61	0.068	0.105	-0.19	-0.298	175	2	138	107	0.158	0.123
37	-0.137	0.606	0.046	0.069	-0.2	-0.307	209	2	143	109	0.160	0.152
38	-0.132	0.606	0.035	0.053	-0.2	-0.301	173	1.02	117	90	0.154	0.119
39	-0.14	0.61	0.034	0.051	-0.21	-0.306	168	1.49	114	87	0.180	0.176
40	-0.128	0.606	0.031	0.085	-0.2	-0.284	157	1.97	118	93	0.173	0.125
41	-0.123	6.14	0.029	0.06	-0.18	-0.268	182	1	122	96	0.155	0.119

Appendix 2 Long term climatic data, Bulgan soum. (Hydrometeorology Institute, Mongolia)

Year	MAT, ^{o}C	MAP	Dust storms	Dusts	Rainfall	Plant biomass, kg ha	Pedi	SPI
1970	5,0	60	8	46	24	59	1,4	-1,6
1971	4,9	118	2	47	68	179	-0,2	0,0
1972	6,0	72	8	60	16	118	2,0	-1,2
1973	5,8	155	8	64	110	294	-0,8	1,4
1974	4,5	130	44	79	101	154	-0,8	0,3
1975	5,5	88	25	81	51	155	1,1	-0,8
1976	4,6	122	20	67	65	204	-0,4	0,0
1977	4,9	262	14	51	183	288	-4,0	3,9
1978	5,9	74	9	51	45	182	1,8	-1,2
1979	5,7	74	49	81	35	112	1,7	-1,2
1980	4,9	152	50	71	92	160	-1,1	0,9
1981	4,6	127	45	65	80	135	-0,7	0,2
1982	6,1	87	70	51	51	82	1,7	-0,8
1983	5,5	132	73	28	64	115	0,0	0,4
1984	4,2	57	98	47	36	55	0,9	-1,6
1985	4,5	93	64	35	46	108	0,1	-0,6
1986	4,9	146	57	36	80	162	-0,9	0,8
1987	5,7	131	83	48	58	121	0,1	0,4
1988	6,4	62	79	32	30	55	2,6	-1,5
1989	6,3	91	87	49	29	65	1,7	-0,7
1990	7,0	197	88	28	115	154	-0,6	2,2
1991	5,8	183	71	14	143	150	-1,2	1,8
1992	5,5	99	63	19	43	76	0,8	-0,5
1993	4,9	161	35	5	122	114	-1,3	1,2
1994	6,0	169	44	0	120	142	-0,7	1,4
1995	6,1	132	26	1	82	164	0,5	0,4
1996	5,2	124	32	1	87	120	-0,1	0,2
1997	6,8	115	16	0	87	130	1,5	-0,1
1998	7,0	116	22	3	58	96	1,7	0,0
1999	6,9	142	25	0	49	110	0,9	0,7
2000	6,0	133	31	0	78	112	0,3	0,4
2001	6,7	88,4	29	1	61	113	5,0	-0,8
2002	6.2	133	62	0	69	115,3	5,8	-0,8

Appendix 3 Total livestock number, Bulgan soum. (Hydrometeorology Institute, Mongolia)

Year	Camel	Horse	Cattle	Sheep	Goat	SSU
1990	4,9	4,3	1,8	22,1	30,6	377,3
1991	4,9	4,5	2,1	23	32	383
1992	4,4	4,7	2,3	22,4	29,9	353,9
1993	4,3	5,2	2,2	21,7	30,4	350,8
1994	4,2	5,7	2,4	23,3	33,2	354,6
1995	4,4	6,8	2,9	26,3	40,1	387,5
1999	4,6	9,3	3,3	32,3	46,4	433,4
2000	4,5	7,6	2,4	33,4	47,3	411,2

Appendix 4 Socio-demographic results from questionnaire survey. Bulgan soum, Mongolia, 2005.

	Head of households	Herding years	Stock (2005)	Stock (2000)	Age	Family member	SSU	Stock: Human
1	man	1960	500	500	48	5	1140	228
2	man		400	300	38	5	260	43
3	man	20 years	500	200	42	6	830	92
4	man		100	200	37	9	150	17
5	man		10	100	49	8	23	3
6	women	60 years	10	50	25	4	15	4
7	man	1983	100	200	70	2	110	55
8	women	30 years	400	50	45	9	220	24
9	man	20	200	100	68	4	120	30
10	man	whole life	100	200	40	8	203	25
11	women	whole life	40	130	36	3	50	17
12	women	whole life	0	130	77	2	1140	570
13	man	whole life	400	200	74	2	212	106
14	man	whole life	500	300	55	6	306	51
15	man	whole life	150	50	32	4	160	40
16	man	whole life	200	300	28	2	62	31
17	man	whole life	40	10	55	6	10	2
18	man	20 yr	60	60	76	4	50	13
19	man	whole life	100	100	42	4	70	18
20	man	1970	200	150	45	5	50	10
21	women	whole life	150	100	50	6	138	23

Appendix 4 continued

	Head of households	Herding years	Stock (2005)	Stock (2000)	Age	Family member	SSU	Stock: Human
22	women	whole life	200	300	19	2	90	45
23	man	whole life	50	100	25	3	150	50
24	man	whole life	100	120	65	3	156	52
25	man	whole life	500	500	28	2	600	300
26	man	whole life	100	200	81	5	182	36
27	man	whole life	400	300	32	3	370	123
28	man	whole life	20	100	45	5	46	9
29	man	wholyre life	10	20	55	6	21	4
30	women	whole life	120	60	56	7	50	7
31	women	1950	700	300	78	3	640	213
32	man	10th grade	400	100	65	2	350	175
33	man	10	310	150	18	2	60	30
34	man	whole life	220	100	27	2	155	78
35	man	whole life	160	80	33	3	85	28
36	women	whole life	150	200	39	5	50	10
37	women	whole life	40	10	44	5	10	2
38	man	whole life	20	20	65	3	46	15
39	man	whole life	300	150	72	5	315	63
40	man	whole life	210	100	26	2	130	65
41	man	20 yr	600	300	30	3	412	137
42	man	30 yr	110	50	52	5	30	6

Appendix 5 Questionnaire used in the field work. Bulgan soum, Mongolia, 2005.

1. Date:
2. Location:
   Latitude: Longitude: Altitude:
3. What settlement is that?
   Winter autumn spring summer
4. Name of head of the household:
   Age: man or women:
5. Number of family members: children number:
6. When did you become a herder?
7. Are your family a
   Herder agriculturalist absentee herder herder-agriculturalist
   in pension?
8. What is your main source of income?
   Livestock cashmere pension vegetables else?.....

9. Where have you been 15 and 5 yeas ago (1990 & 2000)?:
   Same place
   Different
10. Number of livestock at present:
    Camel cattle sheep goats' horse
11. How many animals have you owned 15 and 5 years before?:
    1990: total goats
    2000: total goats
12. If livestock has not increased, why?
13. How much is your animal reproduction rate per year:
14. What properties do you have?:
    Tent Winter house Car Truck Wind generator Other

Movements

15. Movement (how many times per year or seasonal)?:
16. How many times used to move in former times (10 years ago)?:

Environmental degradation

17. How long and often do you use this seasonal pasture land?:
    Winter: Spring: Autumn: Summer:
18. Approximately how much area do you graze, grazing radius?:
19. Do you solely make the pasture land decision (grazing, movement) or together with someone else?:
20. Do you have any difficulty to access pasture?:
21. Do you involved any 'hot ail' arrangement, if not would you like to be involved in it?:
22. Do you think your pasture land is degrading?:
    Without change…….1
    Changed a lot……2
    Recovered……...3
23. In your opinion which of the following do you think is the most important factor of desertification?:
    Decreased movement …1
    Less rainfall ……...2
    Water resource scarcity..3
    Wind……4
    Other.. ……5
24. Do you think the dust storms have been increasing, please recall any impacts of it?
25. Do you think grassland is converting to shrubland or grassland to sand dunes?. What grass species invaded by what bushy species?:
    Grassland to shrubland …..1
    Grassland to sand dunes….2
    From what species…….to what species……..

26. If the land is degrading, how do you react to it (do you mostly move)?:
27. Have you expanded your grazing area for the last 10 years?:
    No yes? How many kms?
28. Do you have a private well?:
    yes no it's location:
29. What do you mostly use for fire?:
    Saxual… 1
    Bushes....2
    Dung.. .. 3
    Coal…… 4
30. Do you expand into distant area fuel wood collection?:

ACKNOWLEDGEMENTS

I thank God, Lord Almighty for the successful completion of this work. With his grace blessing, this work has been completed and achieved. I also thank my supervisor, Prof. Dr. Paul Vlek and Armin Skowronek and my tutor Dr. Manfred Denich for their advice, support, and guidance at all stages of this work. I have benefited immensely from their proficiency. My sincere gratitude also goes to Dr. M. Braun at ZFL and Randy Boone, my remote sensing tutor at Natural Resource Laboratory in USA for his constant, detailed, and comprehensive support at the times of difficulty. I thank the DAAD for supporting me with funds for the PhD program and international workshop on Deserts and Desertification: Challenges and Opportunities International Conference in Israel.

Special thanks to Dr. Günther Manske and Rosemarie Zabel for help with many administrative matters. I thank M. Jend for translating and proofreading this thesis. I thank my colleagues at ZEF namely Kofi Nyarko, Aleksander Stein and Dylis Kpongor for the helps, in particular my roommates Lazare Tia and Rene Capote Fuentes.

I'm grateful for my Mongolian colloquies from the Hydrometeorology Institute such as Erdenetuya and Baysgalan for the immense remote sensing and data mining concern and scientists at Geo-ecology institute for laboratory analysis of plant and soil samples. I also thank my university classmates, Ganbat and Ch.Gantigmaa for obtaining valuable information to me. I also thank my field trip scientist, Tsanjid, who gave me great guidance on the field on plant taxonomy and characteristics of the field.

The most acknowledgements should go to my mom and dad for their love, patience, inspiration and discipline to complete this program. Especially for my mom, for her gracious love, care, and patience for my degree program in Germany even though she was suffering severe brain cancer in Mongolia. I always think the spirits of my parents were always with me and even exist in the future to guide and protect me. I miss you a lot. Finally, I thank Pötter for his support and encouragement in every respect.